

UCLA

UCLA Electronic Theses and Dissertations

Title

Characterization of Trichomonas vaginalis Survival Factor under Nutrient Starvation and A Protein That Mediates Parasite Host Cell Binding and Killing

Permalink

<https://escholarship.org/uc/item/9qp0s24n>

Author

Chen, Yi-Pei

Publication Date

2018

Peer reviewed|Thesis/dissertation

UNIVERSITY OF CALIFORNIA

Los Angeles

Characterization of *Trichomonas vaginalis* Survival Factor under Nutrient Starvation and
A Protein That Mediates Parasite Host Cell Binding and Killing

A dissertation submitted in partial satisfaction of the requirements for the degree Doctor
of Philosophy in Molecular Biology

by

Yi-Pei Chen

2018

© Copyright by

Yi-Pei Chen

2018

ABSTRACT OF THE DISSERTATION

Characterization of *Trichomonas vaginalis* Survival Factor under Nutrient Starvation and
A Protein That Mediates Parasite Host Cell Binding and Killing

by

Yi-Pei Chen

Doctor of Philosophy in Molecular Biology

University of California, Los Angeles, 2018

Professor Patricia J. Johnson, Chair

Trichomonas vaginalis is a unicellular extracellular sexually transmitted parasite. While the infection may be cleared by nitroimidazole drugs, in cases where re-infection occurs or the treatment fails, the infected individual may live with inflammation, soreness, pain or itch surrounding urogenital areas without an alternative solution. To establish an infection, *T. vaginalis* attaches to the host and acquires nutrients from the host. Several parasite surface molecules and its secreted exosomes have been shown to be important for the parasite attachment to the host. However, none of the factors identified is solely responsible for host cell binding. In this study, we characterize a parasite surface protein TVAG_393390 (or cadherin-like protein) that significantly increases host binding and killing when it is overexpressed. In addition, to also understand how the parasite survives in the host under nutrient-deficient

conditions, we unravel the role of a survival protein in the parasite (TvMIF) that is homologous to human macrophage migration inhibitory factor (huMIF). We found that TvMIF-overexpressing parasites gain a strong survival advantage under nutrient stress. To obtain further insights into functions of parasite proteins, we adapted gene knockout method CRISPR (cluster regularly interspaced palindromic repeat)-Cas9 (CRISPR-associated protein 9) in *T. vaginalis* to efficiently knock out genes of interest. We then successfully knocked out TvMIF gene using CRISPR-Cas9 and observed a significant reduction in the survival of TvMIF knockout cells compared to the wild-type when these parasites were serum-starved. Last, we examine the human innate immune responses to *T. vaginalis* encounter. Human macrophages and dendritic cells produce strong inflammatory responses when *T. vaginalis* and *Mycoplasma hominis* are both present but remarkably less when *M. hominis* is absent. Together, these data reveal several independent mechanisms which allow *T. vaginalis* to successfully establish infection in human bodies and provide a framework for future studies on the “trichy” parasite.

The dissertation of Yi-Pei Chen is approved.

Peter John Bradley

David A. Campbell

Kent L. Hill

Matteo Pellegrini

Patricia J. Johnson, Committee Chair

University of California, Los Angeles

2018

Table of Contents

Abstract	ii - iii
Committee Page	iv
Acknowledgements	vi - vii
Vita	viii - ix
Chapter 1: Introduction	1
References	10
Chapter 2: <i>Trichomonas vaginalis</i> macrophage migration inhibitory factor mediates parasite survival during nutrient stress	18
References	30
Chapter 3: A <i>Trichomonas vaginalis</i> cadherin-like protein mediates adherence to and killing of host cells	33
References	61
Chapter 4: CRISPR/Cas9-mediated gene modification and gene knock out in the human-infective parasite <i>Trichomonas vaginalis</i>	67
References	79
Chapter 5: Examination of cytokine induction from human innate immune cells by <i>Trichomonas vaginalis</i> co-infected with <i>Mycoplasma hominis</i> and by the presence of <i>Tv</i> protein TvMIF	82
References	99
Chapter 6: Summary and Discussion	104
References	110

Acknowledgements

I would like to thank my advisor, Dr. Patricia Johnson, for supporting my projects, decisions, and career opportunities along the way as I pursue my graduate degree. Patricia's extensive knowledge in the field and contribution to science have given me a once in a lifetime opportunity to grow as a learning scientist. I also greatly appreciate my committee members for providing useful scientific and career advice at various meetings. I would also like to say thank you to all of the former, current and honorary Johnson lab members for technical and spiritual support. I especially want to thank Angelica Riestra for endless support. I want to thank Emma Goodwin, Brenda Molgora and Stephanie DeMarco for being silly so I am not silly alone and all the necessary boba and coffee trips we took together. I am really thankful for my roommates, Courtney Young and Christina Van, for taking out trash constantly, carpooling with me even though I am chatty, and maintaining my apartment as a welcoming place and also tolerating my insanity and providing me food when I am hungry.

The work in Chapter 2 was done with the following people's help. Dr. Feng Guo kindly provided us the pET SUMO plasmid and helped me with protein purification. Dr. Natalia de Miguel provided us an anti-TvMIF antibody. Dr. Mark Arbing provided advice on protein expression and purification. Drs. Olivia Twu and Frances Mercer have always been helping me with my projects generously. I also would like to thank my undergraduate student Emily Xu for working diligently during her time in lab.

In Chapter 3, the project involves an important *T. vaginalis* protein selected by Dr. Angelica Riestra from her former studies. She identified the key sites for the protein function and established its importance in parasite binding and host killing. Without her, the project would not have developed.

Throughout my PhD career, Dr. Brian Janssen has given countless ideas and suggestions that guided me through obstacles in my projects. Furthermore, his dedication to CRISPR-Cas9 development significantly advanced the knockout method in the *T. vaginalis* field which is described in Chapter 4. In Chapter 5, Dr. Frances Mercer has offered her expertise for working with immune cells and examining cytokine production.

I would also like to thank Drs. Taro Amagata, Zheng-Hui He and Colin Leasure as my advisors and mentors when I was at San Francisco State University. Their kindness to have me work and learn research in their laboratories and encouragement to pursue graduate research were the determining factor for me to choose this career path.

Finally, I would like to thank our funding sources, NIH Ruth L. Kirschstein National Research Service Award AI007323 and R01 AI103182-A1 & R21 AI105779 (PJJ).

Vita/Biographical Sketch

Education

San Francisco State University, B.S. in Cell and Molecular Biology 2008 – 2012
summa cum laude

Experience

University of California, Los Angeles 2013 – present

Graduate research with Dr. Patricia Johnson in the Department of Microbiology, Immunology & Molecular Genetics on *Trichomonas vaginalis* survival factors and host-binding proteins

University of California, Los Angeles 2014 – 2015

Teaching Assistant of “Molecular Parasitology”

San Francisco State University

Undergraduate research with Dr. Zheng-Hui He in the Department of Biology on the wild-type versus UV-sensitive mutant *Arabidopsis thaliana* 2012 – 2013

Undergraduate research with Dr. Robert Ramirez (In collaboration with Amagata Lab) in the Department of Biology on creation of *Saccharomyces cerevisiae* deletion strains for identification of anti-malarial drugs. 2012

Undergraduate research with Dr. Taro Amagata in the Department of Chemistry and Biochemistry on identification and characterization of histone deacetylase inhibitors from actinomycete bacteria. 2011 – 2013

Publications

1. **CHEN, YP**, Twu, O, and Johnson, PJ (2018) *Trichomonas vaginalis* macrophage migration inhibitory factor mediates parasite survival during nutrient stress. mBio. 9 (3): e00910-18.

2. Janssen, BD, **CHEN, YP**, Molgora, B, Wang, SE, Simoes-Barbosa, A, and Johnson, PJ (2018) CRISPR/Cas9-mediated gene modification and gene knock out in the human-infective parasite *Trichomonas vaginalis*. *Sci. Rep.* 8 (1):270.
3. Mercer, F, Diala, FG, **CHEN, YP**, Molgora, BM, Ng, SH, and Johnson, PJ (2016) Leukocyte lysis and cytokine induction by the human sexually-transmitted parasite *Trichomonas vaginalis*. *PLoS Negl. Trop. Dis.* 10(8): e0004913.
4. **CHEN, YP**, Catbagan, CC, Bowler, JT, Gokey, T, Goodwin, ND, Guliaev, AB, Wu, W and Amagata, T (2014) Evaluation of benzoic acid derivatives as sirtuin inhibitors. *Bioorg. Med. Chem. Lett.* 24 (1): 349-352.
5. Amagata, T, Tanaka, M, Yamada, T, **CHEN, YP**, Minoura, K and Numata, A (2013) Additional cytotoxic substances isolated from the sponge-derived *Gymnascella dankaliensis*. *Tetrahedron Letters.* 54 (45): 5960-5962.
6. Leasure, CD, **CHEN, YP** and He, ZH (2013) Enhancement of indole-3-acetic acid photodegradation by vitamin B6. *Mol. Plant.* 6 (6): 1992-1995.
7. Amagata, T, Xiao, J, **CHEN, YP**, Holsopple, N, Oliver, AG, Gokey, T, Guliaev, AB and Minoura, K (2012) Creation of an HDAC-based yeast screening method for evaluation of marine-derived actinomycetes: discovery of streptosetin A. *J. Nat. Prod.* 75 (12): 2193-2199.

Awards and Honors:

UCLA Microbial Pathogenesis Training Grant	2015 – 2018
Best Talk, Annual Molecular Parasitology Meeting	2017
Best Talk, Southern California Eukaryotic Pathogen Symposium	2017

Chapter 1:

Introduction

Trichomonas vaginalis is the causative agent of the most common non-viral sexually transmitted infection, trichomoniasis, both in the United States and the world [1]. Trichomoniasis has been classified as a neglected parasitic infection for being underestimated for its public health impact and disproportionate effects on minorities [2]. In fact, *T. vaginalis* infection outnumbers the total infection numbers of *Neisseria gonorrhoeae*, *Chlamydia trachomatis* and syphilis combined [1]. Poor recognition of the disease has been contributed to 70-85% asymptomatic nature of the infection [3]. However, in the symptomatic cases, mild to moderate levels of inflammation in the men and women's urogenital tracts is observed [2][4]. The symptoms include pain during sex and urination, lesions of urogenital epithelium, vaginal discharge, unpleasant smell, itching and irritation [2][3]. In worse scenarios, preterm labor [5], increased risks of other sexually transmitted diseases including human immunodeficiency virus (HIV) [6], and higher risks of cervical cancer [7] and extraprostatic cancer development have also been reported [8].

The current treatments for trichomoniasis are two different nitroimidazole drugs, metronidazole and tinidazole. Metronidazole is prescribed first and if the treatment fails, tinidazole with longer half-life is then prescribed [9][10]. Clinical data have recorded failed treatment using both nitroimidazole drugs [11]. In addition, drug-resistant parasites are reported to be on the rise [12]. The mode of actions of both drugs are not fully understood but evidence suggests that the nitroimidazoles form adducts with proteins and damage of the proteins induced by drug toxicity results in *T. vaginalis* killing [13]. The nitro functional group for drug activation of the two 5-nitroimidazoles is identical so it is likely that the parasite strains resistant to metronidazole are also resistant to tinidazole. Successful treatment in patients does not prevent

them from being re-infected. As a result, there is a need to develop novel treatments for trichomoniasis.

Biology of *T. vaginalis* survival mechanisms under stress

Understanding the parasite biology is crucial to drug development. For example, how the parasite survives in the constantly changing vaginal environment is poorly understood [10]. Targeting parasite survival factors can be used to prevent trichomoniasis. As an obligatory human parasite, *T. vaginalis* acquires nutrients from human host in order to survive and grow [10]. For example, *T. vaginalis* has high demand for iron uptake [14]. Iron-containing proteins from humans such as hemoglobin provide an iron source for *T. vaginalis* growth and its iron-containing enzymes [15][16]. Under iron-deficient condition, *T. vaginalis* accumulates nitric oxide to maintain its survival [17]. Glucose levels of vaginal secretions from *T. vaginalis*-infected patients reveal that the glucose concentrations can vary between 0.3 and 36.65 mM [18]. Under glucose restriction, *T. vaginalis* displays autophagic behavior and increases expressions of anti-oxidant genes which result in induced resistance to hydrogen peroxide [19]. Programmed cell death (apoptosis) in a protozoan parasite such as *T. vaginalis* has been speculated to be a mechanism to enhance population fitness under these stressful conditions [20] or reduce a potential risk of causing fatal effects on the host if the parasites overgrow [21]. Regulated death may prevent release of toxic elements from dying parasites [20] as we know in mammalian systems, necrosis releases a protein that can trigger inflammation [22]. Apoptosis has been described in *T. vaginalis* when treated with apoptotic inducers [23]. Drugs-induced apoptosis shows DNA condensation and fragmentation, externalization of phosphatidylserine on cell surface, and dissipation of hydrogenosomal (mitochondria-related organelle) membrane potential [23]. A closely related species *Tritrichomonas foetus* also demonstrates DNA condensation and

fragmentation when treated with hydrogen peroxide [24]. In addition, *T. foetus* exhibits vesicular formation and reaction with anti-human/mouse-caspase-3 antibody with immunocytochemical staining [24]. However, there is no homologous caspase 3 present in *T. foetus* or *T. vaginalis* [24]. This could mean the active sites of the caspase are conserved in *T. vaginalis* and can be recognized by the human/mouse antibody but the rest of the protein is too dissimilar to be identified by analyzing the primary sequence with BLAST. It is notable that metacaspases which are believed to have the same role as mammalian caspases in yeast are also present in protozoan parasites but their specific roles in parasites are not entirely understood [25][26]. Other conserved apoptotic players such as endonuclease G, caspase-activated DNase or inhibitors of caspase-activated DNase in other eukaryotic systems are not identifiable by searching the *T. vaginalis* genome [21]. Apoptosis in *T. vaginalis* presents some similar features as in multicellular eukaryotes but the mechanism and the players involved are likely to have diverged.

Biology of *T. vaginalis* adherence mechanisms

T. vaginalis is an extracellular parasite. The biology of *T. vaginalis* factors involved in parasite binding to its host is critical for understanding how the parasite establishes the infection. Killing of host epithelial cells by *T. vaginalis* is contact-dependent [27]. The differences between 26 examined *T. vaginalis* strains in host cell adherence and killing are up to 45-fold and 96-fold, respectively [27]. The drastic differences between *T. vaginalis* strains allow us to study the parasite factors involved in host binding and killing. A *T. vaginalis* surface proteome comparing 3 adherent strains and 3 less adherent strains revealed proteins that are more abundant in the adherent strains relative to the less adherent strains that may be involved in attachment [28]. The main polysaccharide lipoglycan (LG) found on *T. vaginalis* surface was found to be involved in host binding [29][30]. LG mutant parasites created by chemical mutagenesis significantly

reduced adherence to host and LG isolated from the parasites competes with wild-type parasite binding to host [30]. Other *T. vaginalis* factors such as laminin-binding proteins [31], adhesins [32][33][34] and cysteine and serine proteinases [35][36][37][38] have also been found to play a role in host binding. Recently, our laboratory demonstrated that parasite-derived small, secreted vesicles called exosomes mediate host attachment via both host:host and host:parasite interactions [39][40][41]. By pre-incubating either the parasites or the host, or both with exosomes from a highly adherent strain increases parasite adherence to host in less adherent strain [39]. In this dissertation, another *T. vaginalis* surface protein that plays an important role in adherence and host killing will be described in Chapter 3.

Host immune responses to *T. vaginalis*

Immune responses from human cells to *T. vaginalis* have been characterized to understand why chronic infection and re-infection can occur. Antibodies against *T. vaginalis* have been reported to be present in infected patients [42][43]. Our laboratory has found that primary human T cells and B cells are killed by a clinical *T. vaginalis* strain but much less so by a laboratory adapted strain and *T. vaginalis* [44]. Phagocytosis of leukocytes by *T. vaginalis* [45] and cysteine proteinases that can degrade host antibodies have been described [46]. Killing of leukocytes by *T. vaginalis* could be one of the reasons why the parasite is able to maintain a chronic infection. We and others found that only low levels of IL-8 are secreted by human monocytes by *T. vaginalis* alone, either laboratory adapted or clinical strain, but the presence of *T. vaginalis* with its symbiotic bacteria *Mycoplasma hominis* results in significant increase in IL-8 production and induction of IL-6 and IL-1 β that are not detectable in *M. hominis*-free samples [44][47]. *T. vaginalis* and *M. hominis* co-infection occurs at 5-90% rates. The dramatic differences in co-infection rate depends largely on the sources of the samples [48] and the

dissimilarity between *M. hominis*-free and *hominis*-containing cytokine responses could be responsible, at least in part, for the diverse infection outcomes.

T. vaginalis exosomes also induce IL-6 and IL-8 responses from host ectocervical cells (Ects) [39]. In addition, IL-8 cytokine induction is lessened when Ects are pre-incubated with *T. vaginalis* exosomes, a potential mechanism that the parasite employs to minimize the host immune response by priming the host with the parasite exosomes [39]. Olmos-Ortiz et al examined other immunomodulatory roles of *T. vaginalis* exosomes [49]. They found that *T. vaginalis* exosomes induced IL-10, IL-6 and TNF- α from mouse macrophages and in their mouse model, pretreatment with the exosomes significantly reduced the inflammatory responses [49], reminiscent of our in vitro study [39]. Identification of a homologue of human cytokine macrophage migration inhibitory factor in *T. vaginalis* (TvMIF) reveals a secretory factor which induces IL-8 production from human monocytes [50]. Isolated LG from the parasite surface is also found to induce a large amount of IL-8 and macrophage inflammatory protein 3 α , and mild IL-6 responses from Ects [51]. However, whether *M. hominis* is present or not in the LG preparation was not addressed. Revisiting the story with the *M. hominis*-containing and *M. hominis*-free controls may be necessary to parse the true immunomodulatory roles of LG. Additionally, *T. vaginalis* contains endosymbionts that are double-stranded RNA (dsRNA) viruses called *T. vaginalis* viruses (TVVs) [52]. A TVVs-containing strain upregulates Toll-like receptor 3, and also induces IL-8, IFN β , Regulated upon Activation, Normal T-cell Expressed, and Secreted (RANTES), IL-1 and MIP-3 α production in host cells while a TVVs-free strain does not [53]. *T. vaginalis* and its symbionts have multiple factors that could elicit host immune responses and more may yet to be discovered.

Lacking genetic tools to study *T. vaginalis* biology

Despite the interesting findings revealed previously by using molecular biology, biochemical and other tools, there are numerous technical limitations that restrict researchers in the field from better understanding *T. vaginalis* biology. Introducing DNA to *T. vaginalis* using electroporation was demonstrated more than two decades ago [54] but only ~3% of the parasites obtain the plasmids using this method and thus, selection with a drug-resistant marker is required [55]. In addition, using immunofluorescent assays to detect multiple overexpressed proteins in the parasites in separate experiments in our laboratory suggests that the existing transfection method results in highly variable protein expression levels within a population (Fig. 1-1). This renders characterization of protein function ambiguous. Large gene family amplification, abundant repetitive elements in the genome [56] and low transfection efficiency has impeded the development of gene knockout tools in *T. vaginalis*. Prior to the development of CRISPR (cluster regularly interspaced palindromic repeat)-Cas9 (CRISPR-associated protein 9) in *T. vaginalis*, only two separate knockouts have been accomplished using traditional homologous recombination method [57][58]. In this dissertation, adaptation and employment of CRISPR-Cas9 in our laboratory to knock out *T. vaginalis* genes will be described as a much more efficient method than traditional homologous recombination [55].

Due to low success rate of gene depletion in *T. vaginalis*, knockdown of transcripts of gene in the parasites was used as an imperfect alternative. MicroRNAs (miRNAs) and its machinery have been identified in *T. vaginalis* [59]. An endogenous miRNA and introduction of its mimics reduced *T. vaginalis* malate dehydrogenase protein expression by 60% [60]. Use of synthetic small interfering RNAs (siRNAs) reduced the transcripts of two genes by 48-67% and 33-72% [61]. Antisense targeting a transcription factor Myb3 [62], a metabolic enzyme glyceraldehyde-3-phosphate (GAPDH) [63], and two surface proteins involved in parasite

adherence, AP33 [33] and AP65 [34], and a major serine/threonine protein phosphatase called protein phosphatase 1 gamma [64] have been reported separately. Despite multiple attempts on knocking down genes in *T. vaginalis* were described, experiences in our laboratory revealed that knocking down genes is unreliable and the results are inconsistent (unpublished data). The presence of residual gene expression in knockdown parasites also prevents full characterization of a protein. Hence, efforts towards development of a reliable knockout system in *T. vaginalis* became essential.

The goals of my dissertation are to focus on understanding *T. vaginalis* proteins and host responses in shaping how the parasite becomes a “successful” parasite. First, a *T. vaginalis* protein called TvMIF is a survival factor for the parasite to survive in the constantly changing host environment [10]. How TvMIF enhances the parasite survival is described in Chapter 2. Chapter 3 focuses on a different protein called TVAG_393390 (or cadherin-like protein) which plays a critical role in parasite binding to and killing of host cells. To better understand parasite proteins and their function, we adapted CRISPR-Cas9 for knocking out genes in *T. vaginalis*, as discussed in Chapter 4. In Chapter 5, we shifted our focus from parasite factors to host immune responses to the infection to understand the other side of the story in this host:pathogen relationship.

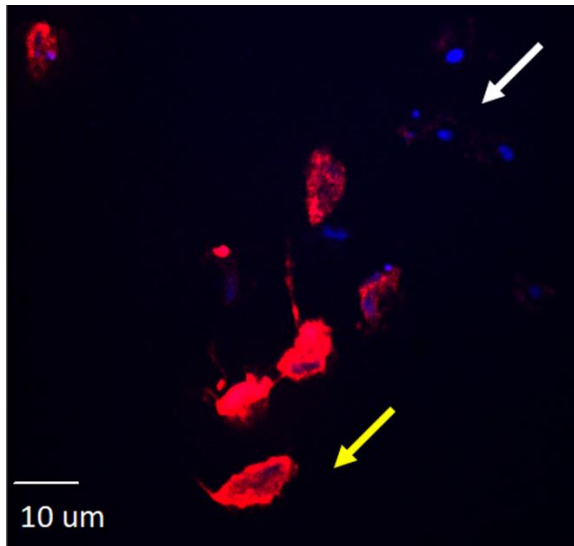


Figure 1-1: Immunofluorescent assay on TvMIF-overexpressing cells with anti-HA and DAPI staining to show variations of exogenous protein levels between cells. Standard transfection of *T. vaginalis* using G418-selection to exogenously express an epitope-tagged protein shows expressions of the protein are highly variable. Parasites shown here are expressing TvMIF with HA tags. The white arrow denotes an example of a parasite nucleus stained with DAPI (blue) but has almost no exogenous expression of the TvMIF protein (red) within a transfection population. The yellow arrow denotes a parasite with high expression of exogenous TvMIF protein. Red: anti-HA. Blue: DAPI.

References

- [1] World Health Organization. (2012). Global incidence and prevalence of selected curable sexually transmitted infections-2008. *Who* 1–28 doi:10.1016/S0968-8080(12)40660-7.
- [2] Secor, W. E., Meites, E., Starr, M. C. & Workowski, K. a. (2014). Neglected parasitic infections in the United States: trichomoniasis. *Am. J. Trop. Med. Hyg.* (90) 800–804.
- [3] Meites, E. (2013). Trichomoniasis: The ‘neglected’ sexually transmitted disease. *Infectious Disease Clinics of North America* (27) 755–764.
- [4] Swygard, H., Seña, A. C., Hobbs, M. M. & Cohen, M. S. (2004). Trichomoniasis: Clinical manifestations, diagnosis and management. *Sexually Transmitted Infections* (80) 91–95.
- [5] Cotch, M. F. *et al.* (1997). Trichomonas vaginalis associated with low birth weight and preterm delivery. The vaginal infections and prematurity study group. *Sexually transmitted diseases* (24) 353–360.
- [6] Mavedzenge, S. N. *et al.* (2010). Epidemiological synergy of trichomonas vaginalis and HIV in Zimbabwean and South African women. *Sex. Transm. Dis.* (37) 460–466.
- [7] Zhang, Z. F. *et al.* (1995). Trichomonas vaginalis and cervical cancer. A prospective study in China. *Ann. Epidemiol.* (5) 325–32.
- [8] Stark, J. R. *et al.* (2009). Prospective study of trichomonas vaginalis infection and prostate cancer incidence and mortality: Physicians’ health study. *J. Natl. Cancer Inst.* (101) 1406–1411.
- [9] Wood, B. A. & Monro, A. M. (1975). Pharmacokinetics of tinidazole and metronidazole in women after single large oral doses. *Br. J. Vener. Dis.* (51) 51–53.
- [10] Petrin, D., Delgaty, K., Bhatt, R. & Garber, G. (1998). Clinical and microbiological aspects of Trichomonas vaginalis. *Clin. Microbiol. Rev.* (11) 300–17.

- [11] Sobel, J. D., Nyirjesy, P. & Brown, W. (2001). Tinidazole Therapy for Metronidazole-Resistant Vaginal Trichomoniasis. *Clin. Infect. Dis.* (33) 1341–1346.
- [12] Cudmore, S. L., Delgaty, K. L., Hayward-McClelland, S. F., Petrin, D. P. & Garber, G. E. (2004). Treatment of infections caused by metronidazole-resistant *Trichomonas vaginalis*. *Clinical Microbiology Reviews* (17) 783–793.
- [13] Leitsch, D. *et al.* (2009). *Trichomonas vaginalis*: Metronidazole and other nitroimidazole drugs are reduced by the flavin enzyme thioredoxin reductase and disrupt the cellular redox system. Implications for nitroimidazole toxicity and resistance. *Mol. Microbiol.* (72) 518–536.
- [14] Arroyo, R. *et al.* (2015). *Trichomonas vaginalis* cysteine proteinases: Iron response in gene expression and proteolytic activity. *Biomed Res. Int.* (2015) 946787.
- [15] Lehker, M. W. & Alderete, J. F. (1992). Iron regulates growth of *Trichomonas vaginalis* and the expression of immunogenic trichomonad proteins. *Mol. Microbiol.* (6) 123–132.
- [16] Figueroa-Angulo, E. E. *et al.* (2012). The effects of environmental factors on the virulence of *Trichomonas vaginalis*. *Microbes Infect.* (14) 1411–27.
- [17] Cheng, W. H. *et al.* (2015). Nitric oxide maintains cell survival of *Trichomonas vaginalis* upon iron depletion. *Parasites and Vectors* (8) 393–404.
- [18] Miranda-Ozuna, J. F. T. *et al.* (2016). The glycolytic enzyme triosephosphate isomerase of *Trichomonas vaginalis* is a surface-associated protein induced by glucose that functions as a laminin- and fibronectin-binding protein. *Infect. Immun.* (84) 2878–2894.
- [19] Huang, K. Y. *et al.* (2014). Adaptive responses to glucose restriction enhance cell survival, antioxidant capability, and autophagy of the protozoan parasite *Trichomonas vaginalis*. *Biochim. Biophys. Acta - Gen. Subj.* (1840) 53–64.

- [20] Durand, P. M., Sym, S. & Michod, R. E. (2016). Programmed Cell Death and Complexity in Microbial Systems. *Current Biology* (26) R587–R593.
- [21] Kaczanowski, S., Sajid, M. & Reece, S. E. (2011). Evolution of apoptosis-like programmed cell death in unicellular protozoan parasites. *Parasites and Vectors* (4).
- [22] Scaffidi, P., Misteli, T. & Bianchi, M. E. (2002). Release of chromatin protein HMGB1 by necrotic cells triggers inflammation. *Nature* (418) 191–195.
- [23] Chose, O. *et al.* (2002). A form of cell death with some features resembling apoptosis in the amitochondrial unicellular organism *Trichomonas vaginalis*. *Exp. Cell Res.* (276) 32–39.
- [24] Mariante, R. M., Guimarães, C. A., Linden, R. & Benchimol, M. (2003). Hydrogen peroxide induces caspase activation and programmed cell death in the amitochondrial *Tritrichomonas foetus*. *Histochem. Cell Biol.* (120) 129–141.
- [25] Carmona-Gutierrez, D., Fröhlich, K. U., Kroemer, G. & Madeo, F. (2010). Editorial: Metacaspases are caspases. Doubt no more. *Cell Death and Differentiation* (17) 377–378.
- [26] Meslin, B., Zalila, H., Fasel, N., Picot, S. & Bienvenu, A. L. (2011). Are protozoan metacaspases potential parasite killers? *Parasites and Vectors* (4) doi: 10.1186/1756-3305-4-26.
- [27] Lustig, G., Ryan, C. M., Secor, W. E. & Johnson, P. J. (2013). *Trichomonas vaginalis* contact-dependent cytolysis of epithelial cells. *Infect. Immun.* (81) 1411–1419.
- [28] de Miguel, N. *et al.* (2010). Proteome analysis of the surface of *Trichomonas vaginalis* reveals novel proteins and strain-dependent differential expression. *Mol. Cell. Proteomics* (9) 1554–1566.
- [29] Singh, B. N. (1993). Lipophosphoglycan-like glycoconjugate of *Tritrichomonas foetus* and

- Trichomonas vaginalis. *Mol. Biochem. Parasitol.* (57) 281–294.
- [30] Bastida-Corcuera, F. D., Okumura, C. Y., Colocoussi, A. & Johnson, P. J. (2005). Trichomonas vaginalis lipophosphoglycan mutants have reduced adherence and cytotoxicity to human ectocervical cells. *Eukaryot. Cell* (4) 1951–1958.
- [31] Casta e Silva Filho, F., de Souza, W. & Lopes, J. D. (1988). Presence of laminin-binding proteins in trichomonads and their role in adhesion. *Proc. Natl. Acad. Sci. U. S. A.* (85) 8042–8046.
- [32] Alderete, J. F., Nguyen, J., Mundodi, V. & Lecker, M. W. (2004). Heme-iron increases levels of AP65-mediated adherence by Trichomonas vaginalis. *Microb. Pathog.* (36) 263–271.
- [33] Mundodi, V., Kucknoor, A. S. & Alderete, J. F. (2007). Antisense RNA decreases AP33 gene expression and cytoadherence by T. vaginalis. *BMC Microbiol.* (7) 64.
- [34] Mundodi, V., Kucknoor, A. S., Klumpp, D. J., Chang, T. H. & Alderete, J. F. (2004). Silencing the ap65 gene reduces adherence to vaginal epithelial cells by Trichomonas vaginalis. *Mol. Microbiol.* (53) 1099–1108.
- [35] Mendoza-Lopez, M. R. *et al.* (2000). CP30, a cysteine proteinase involved in Trichomonas vaginalis cytoadherence. *Infect. Immun.* (68) 4907–4912.
- [36] Rendón-Gandarilla, F. J. *et al.* (2013). The TvLEGU-1, a legumain-like cysteine proteinase, plays a key role in Trichomonas vaginalis cytoadherence. *Biomed Res. Int.* (2013) 561979.
- [37] Hernández, H. *et al.* (2004). Monoclonal antibodies against a 62 kDa proteinase of Trichomonas vaginalis decrease parasite cytoadherence to epithelial cells and confer protection in mice. *Parasite Immunol.* (26) 119–125.

- [38] Riestra, A. (University of California, Los Angeles, 2015). Characterization of rhomboid proteases and surface proteins of *Trichomonas vaginalis*. PhD [Dissertation].
- [39] Twu, O. *et al.* (2013). *Trichomonas vaginalis* Exosomes Deliver Cargo to Host Cells and Mediate Host:Parasite Interactions. *PLoS Pathog.* (9) e1003482.
- [40] Twu, O. & Johnson, P. J. (2014). Parasite Extracellular Vesicles: Mediators of Intercellular Communication. *PLoS Pathog.* (10) e1004289.
- [41] Marti, M. & Johnson, P. J. (2016). Emerging roles for extracellular vesicles in parasitic infections. *Current Opinion in Microbiology* (32) 66–70.
- [42] Kaur, S., Khurana, S., Bagga, R., Wanchu, A. & Malla, N. (2008). Antitrichomonas IgG, IgM, IgA, and IgG subclass responses in human intravaginal trichomoniasis. *Parasitol. Res.* (103) 305–312.
- [43] Nu, P. A. T., Rappelli, P., Dessì, D., Nguyen, V. Q. H. & Fiori, P. L. (2015). Kinetics of circulating antibody response to *Trichomonas vaginalis*: Clinical and diagnostic implications. *Sex. Transm. Infect.* (91) 561–563.
- [44] Mercer, F. *et al.* (2016). Leukocyte Lysis and Cytokine Induction by the Human Sexually Transmitted Parasite *Trichomonas vaginalis*. *PLoS Negl. Trop. Dis.* (10) e0004913.
- [45] Rendón-Maldonado, J. G., Espinosa-Cantellano, M., González-Robles, A. & Martínez-Palomo, A. (1998). *Trichomonas vaginalis*: In vitro phagocytosis of lactobacilli, vaginal epithelial cells, leukocytes, and erythrocytes. *Exp. Parasitol.* (89) 241–250.
- [46] Provenzano, D. & Alderete, J. F. (1995). Analysis of human immunoglobulin-degrading cysteine proteinases of *Trichomonas vaginalis*. *Infect. Immun.* (63) 3388–3395.
- [47] Fiori, P. L., Diaz, N., Cocco, A. R., Rappelli, P. & Dessi, D. (2013). Association of *Trichomonas vaginalis* with its symbiont *Mycoplasma hominis* synergistically upregulates

- the in vitro proinflammatory response of human monocytes. *Sex. Transm. Infect.* (89) 449–454.
- [48] Fichorova, R., Fraga, J., Rappelli, P. & Fiori, P. L. (2017). *Trichomonas vaginalis* infection in symbiosis with *Trichomonasvirus* and *Mycoplasma*. *Res. Microbiol.* (168) 882–891.
- [49] Olmos-Ortiz, L. M. *et al.* (2017). *Trichomonas vaginalis* exosome-like vesicles modify the cytokine profile and reduce inflammation in parasite-infected mice. *Parasite Immunol.* (39) doi: 10.1111/pim.12426.
- [50] Twu, O. *et al.* (2014). *Trichomonas vaginalis* homolog of macrophage migration inhibitory factor induces prostate cell growth, invasiveness, and inflammatory responses. *Proc. Natl. Acad. Sci.* (111) 8179–8184.
- [51] Fichorova, R. N. *et al.* (2006). *Trichomonas vaginalis* lipophosphoglycan triggers a selective upregulation of cytokines by human female reproductive tract epithelial cells. *Infect. Immun.* (74) 5773–5779.
- [52] Wang, A. L. & Wang, C. C. (1986). The double-stranded RNA in *Trichomonas vaginalis* may originate from virus-like particles. *Proc. Natl. Acad. Sci. U. S. A.* (83) 7956–7960.
- [53] Fichorova, R. N. *et al.* (2012). Endobiont Viruses Sensed by the Human Host - Beyond Conventional Antiparasitic Therapy. *PLoS One* (7) e48418.
- [54] Delgadillo, M. G., Liston, D. R., Niazi, K. & Johnson, P. J. (1997). Transient and selectable transformation of the parasitic protist *Trichomonas vaginalis*. *Proc. Natl. Acad. Sci.* (94) 4716–4720.
- [55] Janssen, B. D. *et al.* (2018). CRISPR/Cas9-mediated gene modification and gene knock out in the human-infective parasite *Trichomonas vaginalis*. *Sci. Rep.* (8) doi:

10.1038/s41598-017-18442-3.

- [56] Carlton, J. M. *et al.* (2007). Draft genome sequence of the sexually transmitted pathogen *Trichomonas vaginalis*. *Science* (315) 207–12.
- [57] Land, K. M. *et al.* (2004). Targeted gene replacement of a ferredoxin gene in *Trichomonas vaginalis* does not lead to metronidazole resistance. *Molecular Microbiology* (51) 115–122.
- [58] Brás, X. P. *et al.* (2013). Knockout of the abundant *Trichomonas vaginalis* hydrogenosomal membrane protein TvHMP23 increases hydrogenosome size but induces no compensatory up-regulation of paralogous copies. *FEBS Lett.* (587) 1333–1339.
- [59] Lin, W. C. *et al.* (2009). Identification of microRNA in the protist *Trichomonas vaginalis*. *Genomics* (93) 487–493.
- [60] Lin, W. C. *et al.* (2009). Malate dehydrogenase is negatively regulated by miR-1 in *Trichomonas vaginalis*. *Parasitol. Res.* (105) 1683–1689.
- [61] Ravae, R., Ebadi, P., Hatam, G., Vafafar, A. & Ghahramani Seno, M. M. (2015). Synthetic siRNAs effectively target cystein protease 12 and α -actinin transcripts in *Trichomonas vaginalis*. *Exp. Parasitol.* (157) 30–34.
- [62] Hsu, H. M., Ong, S. J., Lee, M. C. & Tai, J. H. (2009). Transcriptional regulation of an iron-inducible gene by differential and alternate promoter entries of multiple Myb proteins in the protozoan parasite *Trichomonas vaginalis*. *Eukaryot. Cell* (8) 362–372.
- [63] Lama, A., Kucknoor, A., Mundodi, V. & Alderete, J. F. (2009). Glyceraldehyde-3-phosphate dehydrogenase is a surface-associated, fibronectin-binding protein of *Trichomonas vaginalis*. *Infect. Immun.* (77) 2703–2711.
- [64] Munoz, C. *et al.* (2012). A protein phosphatase 1 gamma (PP1gamma) of the human

protozoan parasite *Trichomonas vaginalis* is involved in proliferation and cell attachment to the host cell. *Int J Parasitol* (42) 715–727.

Chapter 2:

Trichomonas vaginalis macrophage migration inhibitory factor mediates parasite survival
during nutrient stress

Trichomonas vaginalis Macrophage Migration Inhibitory Factor Mediates Parasite Survival during Nutrient Stress

Yi-Pei Chen,^{a,b} Olivia Twu,^{a,b*} Patricia J. Johnson^{a,b}

^aMolecular Biology Institute, University of California, Los Angeles, Los Angeles, California, USA

^bDepartment of Microbiology, Immunology & Molecular Genetics, University of California, Los Angeles, Los Angeles, California, USA

ABSTRACT *Trichomonas vaginalis* is responsible for the most prevalent non-viral sexually transmitted disease worldwide, and yet the mechanisms used by this parasite to establish and maintain infection are poorly understood. We previously identified a *T. vaginalis* homologue (TvMIF) of a human cytokine, human macrophage migration inhibitory factor (huMIF). TvMIF mimics huMIF's role in increasing cell growth and inhibiting apoptosis in human host cells. To interrogate a role of TvMIF in parasite survival during infection, we asked whether overexpression of TvMIF (TvMIF-OE) confers an advantage to the parasite under nutrient stress conditions by comparing the survival of TvMIF-OE parasites to that of empty vector (EV) parasites. We found that under conditions of serum starvation, overexpression of TvMIF resulted in increased parasite survival. Serum-starved parasites secrete 2.5-fold more intrinsic TvMIF than unstarved parasites, stimulating autocrine and paracrine signaling. Similarly, we observed that addition of recombinant TvMIF increased the survival of the parasites in the absence of serum. Recombinant huMIF likewise increased the parasite survival in the absence of serum, indicating that the parasite may use this host survival factor to resist its own death. Moreover, TvMIF-OE parasites were found to undergo significantly less apoptosis and reactive oxygen species (ROS) generation under conditions of serum starvation, consistent with increased survival being the result of blocking ROS-induced apoptosis. These studies demonstrated that a parasitic MIF enhances survival under adverse conditions and defined TvMIF and huMIF as conserved survival factors that exhibit cross talk in host-pathogen interactions.

IMPORTANCE Macrophage migration inhibitory factor (MIF) is a conserved protein found in most eukaryotes which has been well characterized in mammals but poorly studied in other eukaryotes. The limited analyses of MIF proteins found in unicellular eukaryotes have focused exclusively on the effect of parasitic MIF on the mammalian host. This was the first study to assess the function of a parasite MIF in parasite biology. We demonstrate that the *Trichomonas vaginalis* MIF functions to suppress cell death induced by apoptosis, thereby enhancing parasite survival under adverse conditions. Our research reveals a conserved survival mechanism, shared by a parasite and its host, and indicates a role for a conserved protein in mediating cross talk in host-pathogen interactions.

KEYWORDS *Trichomonas vaginalis*, apoptosis, macrophage migration inhibitory factor, nutrient starvation

Trichomonas vaginalis, an extracellular unicellular parasite, causes the most common non-viral sexually transmitted infection in the world (1) but has been long neglected. Thus, the mechanisms that drive parasite pathogenesis and the disease epidemiology are poorly understood (2). However, this is changing as more molecular and genetic tools for analyses are developed (3, 4). The majority of *T. vaginalis*

infections are asymptomatic. When they are symptomatic, the manifestations of infection vary greatly and may include inflammation of the urogenital tract, preterm delivery, and increased chances of HIV co-infection (5, 6). The factors that determine how the parasite maintains the infection in the vaginal microenvironment, where the nutrients, hormones, and pH are constantly changing, remain largely unknown (7–9).

Macrophage migration inhibitory factor (MIF) is a highly conserved eukaryotic protein found across unicellular protists, plants, arthropods, and mammals (10–13). Human MIF (huMIF) has been widely studied and is known to play essential roles in cell growth, survival and in cancer growth in humans (14–16). In our previous study, we reported that *T. vaginalis* shares a homologous protein (TvMIF) with the human host and that TvMIF can activate the same survival pathways as huMIF in human cells (17). MIF homologues found in other eukaryotic parasites are known to modulate the host immune system and to activate huMIF pathways (10, 18–21). Although the effects of parasite-derived MIFs from parasites on host cells have been studied, the role of MIF in parasites and non-mammalian systems is poorly understood.

T. vaginalis and other parasitic protists share certain apoptotic phenotypes with mammalian systems such as DNA fragmentation and phosphatidylserine exposure (22–25). However, no factor that either stimulates or suppresses apoptosis in these divergent, unicellular eukaryotes has yet been identified. In this report, we describe the anti-apoptotic effect caused by TvMIF, a conserved eukaryotic protein, and reveal similarities between this protein and its mammalian homologue. We also provide evidence that *T. vaginalis* is able to exploit huMIF to enhance its survival during nutrient starvation. These studies uncovered a highly conserved eukaryotic protein used by a parasite and its host to enhance survival.

RESULTS

***T. vaginalis* MIF (TvMIF) enhances survival of the parasites under conditions of nutrient stress.** We have previously shown that the homologue of huMIF in the parasite *T. vaginalis* (TvMIF) can induce the growth and activation of anti-apoptotic pathways in human host cells (17). To investigate whether TvMIF can perform a similar function and hence enhance the survival of the parasite under adverse conditions, we have studied the role of TvMIF in parasite survival under conditions of nutrient and density stress. *T. vaginalis* is typically grown in Diamond's media supplemented with serum (26). The parasite will not grow in the absence of serum as it provides lipids, precursors of nucleotides, and amino acids required for parasite survival (26, 27). Parasites also cease to swim and die within hours after reaching a density of 5×10^6 cells/ml in Diamond's media supplemented with serum (27). As a first step toward determining whether TvMIF plays a role in parasite survival, we compared the survival rates of parasites transfected with (28) and overexpressing TvMIF (TvMIF-OE) with those transfected with an empty vector (EV). Immunoblotting confirmed that expression of TvMIF in TvMIF-OE parasites is approximately 17-fold greater than in EV control parasites (see Fig. S1 in the supplemental material).

Fluorescence-activated cell sorter (FACS) analyses of living cells assessed using Zombie Red viability dye to compare TvMIF-OE and EV parasites were conducted using parasites grown in serum-free media or at a high density. We found that TvMIF-OE parasites survived significantly better than EV parasites in serum-free media after 8 h of incubation and that this survival phenotype became more pronounced after 24 to 32 h of starvation (Fig. 1A; see also Fig. S2). Comparison of the survival rates of TvMIF-OE and EV parasites at densities as high as 10^7 cells/ml or 2×10^7 cells/ml also revealed the death of a significantly higher proportion of EV parasites than of TvMIF-OE parasites at 4 and 8 h after they were subjected to density stress (Fig. 1B). When grown in regular media supplemented with serum, EV and TvMIF-OE had similar growth rates (Fig. S3), demonstrating that TvMIF promotes parasite survival under adverse conditions.

TvMIF is secreted as both a free soluble protein and an exosomal protein. We have previously demonstrated that *T. vaginalis* secretes small vesicles called exosomes (29, 30) and that TvMIF is found in the exosomal proteome (31). As the survival

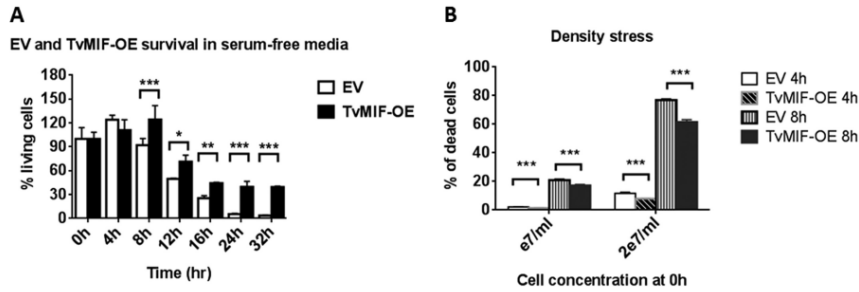


FIG 1 TvMIF increases parasite survival under conditions of nutrient stress. (A) Overexpression of TvMIF in the parasite enhances the survival of the parasite under conditions of serum starvation significantly after 8 h. All time points are normalized to time point 0 h for each parasite. Data are means \pm standard errors of results from triplicates, and data from 1 of 3 independent experiments are shown. (B) Overexpression of TvMIF enhances parasite resistance to density stress. The cultures started at a $1 \times e7/ml$ or $2 \times e7/ml$ concentration and were incubated for 4 and 8 h. Data shown are means \pm standard errors of results from triplicates, and data representative of 1 of 3 independent experiments are shown. *, P value ≤ 0.05 ; **, P value ≤ 0.01 ; ***, P value ≤ 0.001 .

pathways activated by huMIF require a secreted soluble form of the protein (16, 32), we examined both the exosomal fractions (Exo) and the non-exosomal soluble fractions (NESF) secreted by the parasite for TvMIF using a Vivaflow crossflow cassette and an ultracentrifugation-based method (Fig. 2A). Parasites grown overnight were collected and then incubated in phosphate-buffered saline (PBS)–5% sucrose at either 16°C (negative control for secretion) or 37°C. After 2 h of incubation, the cells were pelleted and lysed to make whole-cell lysates (Wcl). The supernatant was passed through a Vivaflow crossflow cassette using a 100-kDa molecular weight cutoff (MWCO) to separate the heavier exosomes (Exo > 100 kDa) from the lighter non-exosomal secreted fraction (NESF < 100 kDa). The level of NESF TvMIF was found to be 1.4-fold higher than that of Exo TvMIF by immunoblotting using an anti-TvMIF antibody (4) (Fig. 2B). As the Exo fraction had much less protein than the Wcl fraction and NESF from equal numbers of cells, equal (20 μ g) amounts of protein were loaded in each fraction. At 37°C, 20 μ g of protein is equal to 2.87% of the total NESF and 17.2% of the Exo fraction. As a result, we can reason that approximately 8.4-fold-more TvMIF is secreted in the NESF than in the Exo (17.2% divided by 2.87% and then multiplied by 1.4-fold).

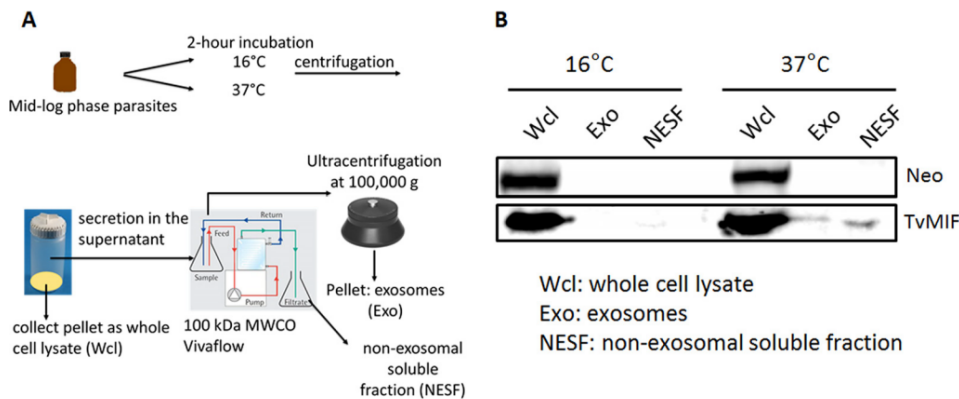


FIG 2 TvMIF is present in the exosome and the non-exosomal secreted fractions. (A) A secretion assay used to determine proportions of TvMIF in the exosome (Exo) and non-exosomal soluble fraction (NESF) is illustrated. Parasites were incubated at either 16°C or 37°C. Incubation at 16°C is a negative control for secretion. After the incubation, the cells were pelleted and lysed to become whole-cell lysates (Wcl) and the secreted supernatant fraction was passed through a Vivaflow crossflow cassette to separate Exo from NESF. Then, the Exo was collected by ultracentrifugation. (B) At 16°C, no detectable TvMIF was present in Exo and NESF. At 37°C, 1.4-fold more TvMIF was detected in the NESF than in the Exo fraction using immunoblotting and a TvMIF antibody. Neomycin phosphotransferase (Neo) was used to detect cellular lysis.

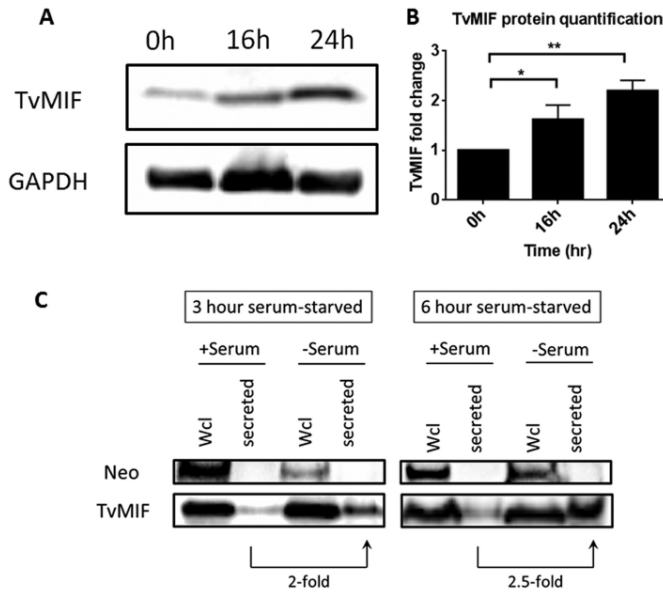


FIG 3 Endogenous TvMIF protein is induced under conditions of serum starvation. (A) Anti-TvMIF immunoblot showing that the TvMIF level was induced during serum starvation. Detection of GAPDH served as the loading control. One representative immunoblot of three independent experiments is shown. (B) Quantification of TvMIF was determined by normalizing the TvMIF signal to GAPDH for each sample; the data were compared to the 0-h time point value (set at 1) in each experiment, so no error bar was made for 0 h. Data are means \pm standard errors. (C) TvMIF secretion was induced in the absence of serum. +Serum, cells grown in complete media; -Serum, cells grown without serum. Secreted TvMIF was induced \sim 2-fold at 3 h and \sim 2.5-fold at 6 h after serum starvation comparing -serum and +serum signals. Neo was used as a negative control for cell lysis.

These data show that the majority of total secreted TvMIF is present as a soluble protein.

Both intracellular TvMIF and secreted TvMIF are induced during serum starvation. As shown in Fig. 1, overexpression of TvMIF increased the survival of the parasites during nutrient stress. Thus, we asked if induction of TvMIF expression and its secretion play a role in the enhanced survival. First, to test if intracellular TvMIF expression is induced under conditions of serum starvation, we collected the whole-cell lysates (Wcl) from cells starved for 16 or 24 h and TvMIF levels were quantified by immunoblotting. Intracellular TvMIF was found to be induced 1.6-fold at 16 h and 2.2-fold at 24 h after starvation (Fig. 3A and B). For determining TvMIF secretion levels under conditions of serum starvation, parasites grown overnight in complete Diamond's media were collected, resuspended, and incubated in serum-free media for 3 h or 6 h at 37°C. Cells were then spun, resuspended in PBS-5% sucrose, and incubated for an additional 2 h at 37°C. Cells were then pelleted and lysed to make Wcl, and the supernatant was collected to assess secretion. Immunoblot analyses showed that the secreted TvMIF were induced \sim 2-fold and 2.5-fold higher from cells incubated in serum-free media for 3 and 6 h, respectively, than from parasites grown in serum-containing media (Fig. 3C). Neomycin phosphotransferase (Neo), a non-secreted protein, was used as a control to monitor cell lysis. The presence of Neo signal only in the Wcl confirms that the TvMIF signal detected was the result of secretion and not cell lysis.

Addition of recombinant MIFs increases survival of the parasite during serum starvation. As survival and anti-apoptotic pathways are activated by huMIF in an autocrine manner (15, 33, 34) and TvMIF secretion is induced during serum starvation (Fig. 3), we generated recombinant MIF and added it to parasites to directly test whether soluble TvMIF plays a role in enhancing parasite survival during serum starvation. As shown in Fig. 4A, 50 ng/ml of recombinant TvMIF (rTvMIF) increased

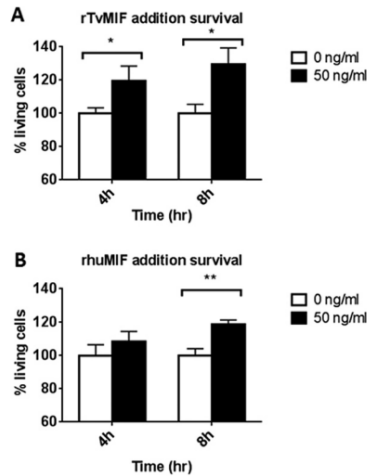


FIG 4 Both recombinant TvMIF and recombinant huMIF increase the survival of the parasite under conditions of serum starvation. (A) rTvMIF (50 ng/ml) or PBS (indicated as 0 ng/ml) was added to parasites grown without serum at time point 0 h. rTvMIF at 50 ng/ml increased the parasite survival at both 4 h and 8 h after serum starvation. (B) rhuMIF (50 ng/ml) or PBS (indicated as 0 ng/ml) was added to parasites grown without serum at time point 0 h. rhuMIF at 50 ng/ml increased the parasite survival at 8 h after starvation. Results of 3 independent experiments, each done in quadruplet, are represented by the data shown here. Error bars represent means \pm standard errors. *, P value \leq 0.05; **, P value \leq 0.01.

parasite survival 1.2-fold at 4 h and 1.3-fold at 8 h after serum starvation. Human MIF has been reported to be secreted during parasitic infection (35, 36). Thus, we tested whether recombinant huMIF (rhuMIF) can also increase parasite survival. We found that 50 ng/ml of rhuMIF induced parasite survival 1.2-fold at 8 h (Fig. 4B). These results support the idea of ability of the parasite to respond to both TvMIF and huMIF, increasing parasite survival, and indicate that *T. vaginalis* can hijack huMIF to enhance its survival.

Parasites overexpressing TvMIF can enhance survival of neighboring parasites in co-cultures. Having established that secreted TvMIF is involved in signaling to parasites, we next tested whether this occurs in an autocrine manner only or can operate in *trans*. To test if secreted TvMIF can enhance the survival of neighboring parasites, we set up a co-culture of EV and TvMIF-OE parasites in a transwell apparatus using complete Diamond's media. The bottom wells contained EV, and the top wells, separated from the bottom wells by membranes with 0.4- μ m pores, contained either EV or TvMIF-OE. Parasites in both the top and bottom wells were passaged into new media daily for 7, 14, and 21 days (Fig. 5A) to maximize exposure of EV to abundant TvMIF secreted from TvMIF-OE. Then, the cultures were switched to serum-free media to induce nutrient stress and we measured the survival of the EV parasites in the bottom wells under conditions of co-culture with either EV or TvMIF-OE parasites. We found that EV parasites co-cultured with TvMIF-OE parasites for 7 days had a 1.4-fold-higher survival rate than those co-cultured with EV control parasites, that those co-cultured for 14 days had a 1.7-fold-higher survival rate, and that those co-cultured for 21 days had a 2.3-fold-higher survival rate and that the survival advantage became more dramatic with increasing numbers of days of co-culturing (Fig. 5B). These data indicate that the abundance of TvMIF secretion from TvMIF-OE parasites enhanced the survival of neighboring EV parasites, possibly exerting this effect via a positive-feedback loop.

TvMIF inhibits parasite apoptosis. HuMIF is known to activate anti-apoptotic pathways in human cells (14, 15, 37–39). To test whether TvMIF inhibits the apoptosis of the parasites during serum starvation, we employed a double-staining method similar to the commonly used annexin V and propidium iodide (PI) method (40) except that we replaced PI with Zombie Red as the viability dye to exclude dead cells in the

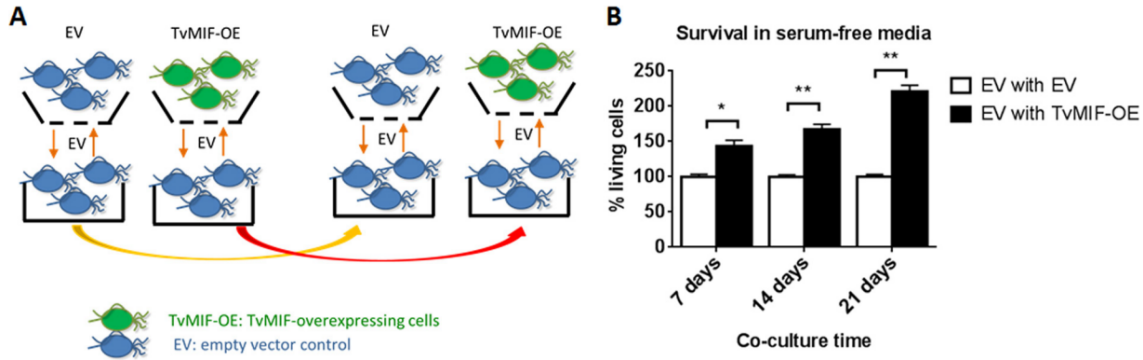


FIG 5 Increased secretion of TvMIF by TvMIF-OE parasites increases survival of EV parasites after co-culture with TvMIF-OE parasites. (A) Scheme of co-culture transwell assay. EV parasites in the wells indicated at the bottom were separated from EV or TvMIF-OE in the wells indicated at the top by a membrane with 0.4- μm pores. (B) Co-culturing EV parasites with TvMIF-OE parasites confers a survival advantage. EV parasites (bottom well in Fig. 5A) were co-cultured with TvMIF-OE parasites (black bars) or EV parasites (white bars) for the number of days indicated on the x axis. The EV parasites in the bottom well were then transferred to serum-free media for 24 h, and survival was measured. Error bars represent means \pm standard errors. *, P value \leq 0.05; **, P value \leq 0.01. The data represent results from 3 independent experiments, each done in triplicate.

population. Annexin V, which labels externalized phosphatidylserine, is used as an indicator of the number of parasites undergoing apoptosis (40). Using this assay, we observed that EV parasites had slightly more apoptosis than TvMIF-OE parasites at 16 h (P value = 0.07). Moreover, after 24 h of serum starvation, EV parasites were significantly more apoptotic than TvMIF-OE parasites (P value = 0.01) (Fig. 6A). To further

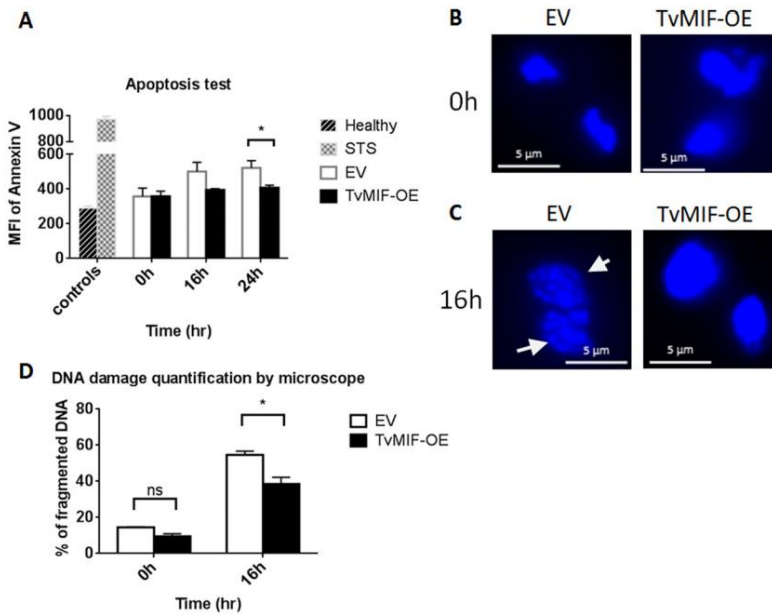


FIG 6 TvMIF inhibits parasite apoptosis. (A) Double staining with annexin V and Zombie Red was used to assess apoptosis. TvMIF-OE parasites (black bars) underwent less apoptosis at 16 h and 24 h after serum starvation than EV parasites (white bars). MFI, mean fluorescence intensity; Healthy, DMSO-treated control; STS, staurosporine (apoptosis inducer positive control). Error bars represent standard errors. *, P value \leq 0.05. (B) At 0 h, both EV and TvMIF-OE nuclei were intact with little damage. (C) Nuclei were stained with DAPI. At 16 h after serum starvation, DNA damage in EV parasites was clearly visible. White arrows indicate examples of DNA fragmentation. (D) DNA damage in EV parasites was significantly greater than that observed in TvMIF-OE parasites after 16 h of serum starvation. The imaging data shown in panels B and C were quantified by counting the number of fragmented DNA in a total of 300 nuclei from both EV and TvMIF-OE parasites. *, P value \leq 0.05. Error bars represent means \pm standard errors. All data represent results from 3 independent triplicated experiments.

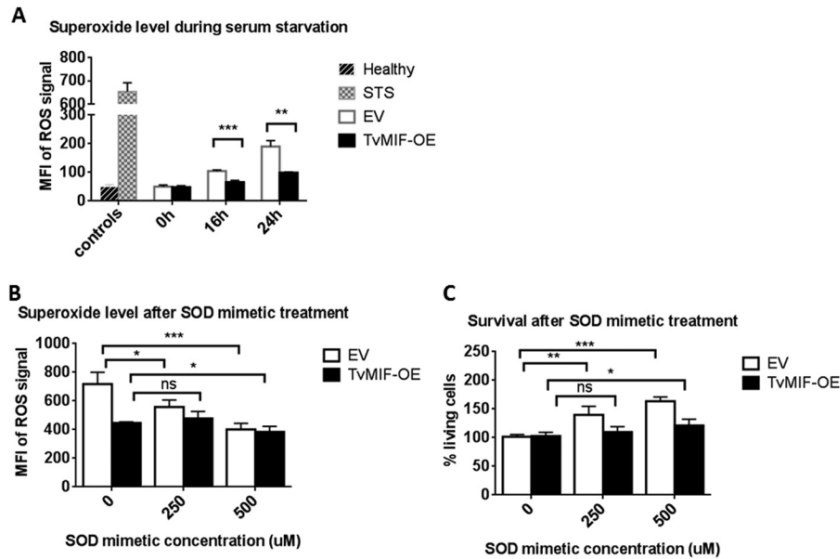


FIG 7 TvMIF inhibits parasite apoptosis under conditions of serum starvation via ROS suppression. (A) The superoxide level detected by using dihydroethidium (DHE) was significantly higher at both 16 h and 24 h in EV parasites than in TvMIF-OE parasites after serum starvation. MFI, mean fluorescence intensity. (B) Superoxide dismutase (SOD) mimetic treatment at time point 0 h decreased the superoxide level in EV at both 250 μM and 500 μM and in TvMIF-OE at 500 μM . (C) SOD mimetic treatment increased EV parasite survival at both 250 μM and 500 μM and TvMIF-OE parasite survival at 500 μM . Ns, non-significant; *, P value ≤ 0.05 ; **, P value ≤ 0.01 ; ***, P value ≤ 0.001 . All data represent results from 3 independent experiments, performed in triplicate.

validate the apoptotic phenotypes of the serum-starved parasites, we examined the nuclei of EV and TvMIF-OE parasites grown in serum-free media for 16 h, as the nuclei of *T. vaginalis* are reported to become condensed and fragmented when treated with apoptosis inducers (24, 25). As shown in Fig. 6B and quantified in Fig. 6D, both EV and TvMIF-OE parasites had low levels of DNA fragmentation at 0 h. In contrast, 16 h after serum starvation, ~55% of EV parasites exhibited apoptotic-like DNA fragmentation, whereas only ~38% of TvMIF-OE parasites displayed this phenotype (Fig. 6B to D). These data demonstrate that TvMIF enhancement of parasite survival is associated with a decrease in apoptosis. It is notable that the observed difference between TvMIF-OE and EV parasites with respect to the anti-apoptotic phenotypes seen at 16 and 24 h is not as dramatic as that observed for the survival phenotype (Fig. 1A), indicating that other mechanisms may contribute to survival during serum starvation.

TvMIF inhibits parasite apoptosis during serum starvation via ROS suppression. Reactive oxygen species (ROS) activate apoptosis signaling in mammalian systems (41), and huMIF is known to inhibit apoptosis by suppressing ROS production (42, 43). To test whether TvMIF-induced survival under conditions of serum starvation is dependent on ROS inhibition, we measured levels of superoxide, a known by-product of ROS signaling, by staining EV and TvMIF-OE parasites with dihydroethidium (DHE). Upon oxidization by superoxide, DHE is converted to fluorescent 2-hydroxyethidium (44) and the intensity can then be used as a measure of ROS levels. We found that TvMIF-OE parasites produced significantly less superoxide than EV parasites when grown without serum for 16 or 24 h (Fig. 7A). To validate the specificity of the DHE signal, we treated EV and TvMIF-OE parasites with the superoxide dismutase (SOD) mimetic manganese(III) tetrakis(1-methyl-4-pyridyl)porphyrin (MnTmPyP) during serum starvation. MnTmPyP significantly decreased the superoxide signal in EV parasites at both 250 μM and 500 μM and in TvMIF-OE parasites at 500 μM (Fig. 7B). The less dramatic effect that MnTmPyP had on TvMIF-OE parasites is consistent with the ability of TvMIF-OE parasites to suppress ROS production prior to the treatment. In addition, the survival of EV parasites

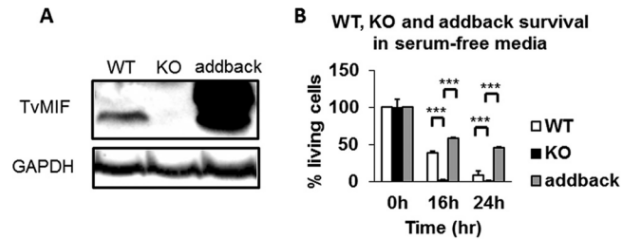


FIG 8 Parasites with the TvMIF gene knocked out have significantly less survival than the wild-type (WT) parasites. (A) Immunoblot using anti-TvMIF antibody to confirm the loss of TvMIF in knockout (KO) parasites and its presence in addback parasites. GAPDH is the loading control. (B) Knockout of TvMIF in the parasite severely reduces the survival of the parasite under conditions of serum starvation. Adding back of TvMIF in knockout parasites that exogenously overexpress the protein restores and enhances the survival phenotype, reminiscent of the increased survival seen with TvMIF-OE. All time points are normalized to time point 0 h for each parasite. Data are means \pm standard errors of results from triplicates, and data from 1 of 3 independent experiments are shown. *, P value \leq 0.05; **, P value \leq 0.01; ***, P value \leq 0.001.

was strongly enhanced by MnTmPyP treatment, whereas TvMIF-OE parasite survival was increased only slightly by the addition of 500 μ M MnTmPyP (Fig. 7C). The low increase in survival of TvMIF-OE parasites resulted from normalizing the percentages of living cells of treated TvMIF-OE and untreated TvMIF-OE parasites (Fig. 7C) as the untreated TvMIF-OE parasites had higher survival rates than EV. Together, these data indicate that inhibition of superoxide by TvMIF contributes to parasite survival under conditions of serum starvation.

Gene knockout (KO) of TvMIF severely reduced parasite survival in serum-free media. After completing the work described above, using TvMIF-OE and EV parasites to study the role of TvMIF in parasite survival under nutrient stress, we succeeded in developing CRISPR-Cas9 methods to knock out (KO) genes in *T. vaginalis* (4). These methods allowed us to KO TvMIF in the parasite (4). As shown in Fig. 8A, immunoblot analyses using the anti-TvMIF antibody confirmed that TvMIF was depleted in the TvMIF KO parasites. To test whether the effects observed in comparisons of wild-type and KO parasites were specific to the loss of TvMIF, we restored TvMIF to the KO parasites (referred to here as “addback parasites”) to test whether this rescued the KO phenotype and caused reversion to that of the wild-type parasites. Immunoblot analysis of addback parasites where TvMIF was overexpressed on a plasmid showed that this resulted in greater expression of TvMIF than was observed in the wild-type parasites (Fig. 8A). Testing the wild-type, TvMIF KO, and addback parasites for survival under conditions of serum starvation, we found that TvMIF KO parasites had 16-fold less and 9-fold less survival than the wild-type parasites and 23.7-fold and 27.7-fold less survival than the addback parasites after 16 h and 24 h under conditions of serum starvation, respectively (Fig. 8B). The increase in survival of addback parasites relative to wild-type parasites is consistent with the higher levels of TvMIF expressed in addback parasites, due to the gene’s presence on a multicopy plasmid. To further validate the survival effect of TvMIF, we added rTvMIF to TvMIF KO parasites in serum-free media and found that 100 ng/ml rTvMIF increased the survival 1.7-fold after 24 h, compared to vehicle control (Fig. S4). Together, these results provide definitive evidence that TvMIF plays a crucial role in resistance to death of the parasite under conditions of nutrient stress.

DISCUSSION

We have established a role for TvMIF in the survival of the parasite under adverse conditions. Although MIF has been widely studied in mammals, the function of this conserved protein in other eukaryotes is largely unknown. We demonstrated that overexpression of TvMIF increases parasite survival under conditions of nutrient starvation, which may be important for the parasite to maintain chronic infection in the constantly changing vaginal environment (5). Nutrient starvation was also shown to

induce the expression and secretion of TvMIF by the parasite. By co-culturing parasites that overexpress TvMIF (TvMIF-OE) with empty vector (EV) parasites that do not, secreted TvMIF was shown to enhance the survival of EV parasites upon prolonged co-culturing, suggesting the presence of an intracellular positive-feedback pathway by which uptake of TvMIF triggers an increase in TvMIF expression and secretion. We were ultimately able to knock out (KO) TvMIF and to show definitively that the loss of TvMIF severely altered the ability of *T. vaginalis* to survive under conditions of nutrient stress.

We found that TvMIF inhibits parasite apoptosis during serum starvation, consistent with the increased survival phenotype conferred on TvMIF-OE parasites. These data imply that nutrient deprivation during infection induces parasite apoptotic pathways and that increased production of TvMIF may allow the parasite to survive, awaiting more favorable conditions within the urogenital tract. The ability of huMIF to inhibit apoptosis and to contribute to oncogenesis is well established (15, 38, 45–48). This functional conservation between huMIF and TvMIF is remarkable given their evolutionary divergence. Our findings are consistent with host-parasite interactions providing an environment that allowed co-evolution of the two proteins.

Previous studies indicated that *T. vaginalis* undergoes apoptosis when treated with drugs known to induce apoptosis in mammalian cells. Treatment with staurosporine (STS) led to DNA condensation and staining with annexin V, both indicators of apoptosis (24). The survival of *T. vaginalis* under conditions of iron depletion, glucose restriction, or serum starvation has also been described, followed by examination of the resulting differential gene expression (49–51). Re-evaluation of these data revealed that under conditions of glucose restriction, TvMIF mRNA is upregulated by 3.8-fold at 12 h and 1.3-fold at 24 h, indicating that TvMIF may be involved in enhancing parasite survival under conditions of glucose starvation (50). In contrast, RNA analyses of parasites grown under conditions of iron depletion revealed that TvMIF mRNA levels were 2.5 times lower under iron-deficient conditions than under iron-rich conditions (49). However, the time point used to extract RNA for the transcriptome sequencing (RNA-seq) analysis was not stated. Therefore, it is possible that TvMIF was upregulated to exert its survival effect at a different time during the analyses.

Although the studies on RNA regulation under glucose-deficient and iron-deficient conditions (49, 50) provide insights into potential pathways that induce parasite survival, prior to this study, no survival factor had been characterized or manipulated by genetic approaches to directly address mechanisms underlying the survival phenotype. Our study results show that the induction of parasite survival by TvMIF via the inhibition of apoptosis is accompanied by reactive oxygen species (ROS) suppression. These data confirm the evolutionary conservation of apoptosis inhibition pathways, as ROS has been shown to activate apoptosis signaling in mammalian systems (41) and huMIF is known to inhibit apoptosis by suppressing ROS production (42, 43).

Induction of apoptosis in the parasitic protists *Leishmania* spp., *Trypanosoma cruzi*, and *Trypanosoma brucei* is accompanied by an increase in ROS (52–57). However, whether the modulation of apoptosis by MIF has been generally conserved between protists and mammals, as appears to be the case for ROS, is yet to be determined. In this regard, it is notable that the known roles of MIF in *Xenopus laevis* and *Caenorhabditis elegans* are not directly related to survival under conditions of stress (58, 59). The main functions of other parasite MIFs have been shown to be focused on their effects on hosts. *Leishmania major* MIF (LmMIF), *Plasmodium* species MIF, *Toxoplasma gondii* MIF, and *Entamoeba histolytica* MIF can bind huMIF receptor CD74 and modulate host immune responses, activate huMIF pathways such as the extracellular signal-regulated kinase/mitogen-activated protein kinase (ERK/MAPK) pathways, and affect the infection outcome (10, 18, 20, 60, 61). LmMIF and *Plasmodium yoelii* MIF also inhibit apoptosis of host macrophages by activating mammalian survival pathways (10, 61, 62). However, the possible anti-apoptotic effect of parasite MIFs on these parasites is yet to be examined.

We found that both TvMIF and huMIF confer cell survival, which may be the result of host-parasite co-evolution. This notion is supported by our previous studies showing

that TvMIF and huMIF induce the same signaling pathways in human cells, conferring an anti-apoptotic and increased-growth phenotype (17), as well as by the data reported here indicating that addition of rhuMIF induces parasite survival under conditions of serum starvation. The latter observation implies that secreted huMIF could also directly affect parasite survival under adverse conditions during infection.

TvMIF was originally identified in the *T. vaginalis* exosomal proteome (31). HuMIF is also present in the exosomal proteome derived from a variety of human cell types (63–71). The effect of huMIF on cell survival has been shown to be mostly focused on soluble huMIF (14, 72, 73). However, Costa-Silva et al. showed that pancreatic ductal adenocarcinoma-derived exosomes with abundant huMIF play a role in inducing liver metastasis, although they did not test whether exosomal huMIF directly triggers anti-apoptotic pathways (71). Further analyses will be required to determine whether exosomal huMIF or TvMIF is capable of triggering anti-apoptotic pathways when exosomes fuse and deliver their protein cargo into human and/or trichomonad cells. Likewise, future transcriptomic and/or proteomic analyses should assist in identifying the anti-apoptotic pathway(s) triggered by TvMIF.

MATERIALS AND METHODS

***T. vaginalis* cell culture and transfection.** *T. vaginalis* strain B7RC2 (ATCC 50167) was cultured in Diamond's medium supplemented with 100 U/ml penicillin and 100 μ g/ml streptomycin (Thermo Fisher Scientific), 180 μ M ferrous ammonium sulfate (Fisher), 28 μ M sulfosalicylic acid (Fisher), and 10% horse serum (Sigma) (complete Diamond's media) (26). TVAG_219770 (TvMIF) was overexpressed in Master-Neo-(HA [hemagglutinin])₂ plasmid and transfected as previously described (17). The plasmid was maintained with 100 μ g/ml of G418 (Gibco) for selection. Parasites were cultured at 37°C and passaged daily for 2 weeks or less.

Serum starvation assay. *T. vaginalis* was cultured overnight in complete Diamond's media (26). The parasites were then pelleted by centrifugation and resuspended at 10⁶ cells/ml in the same media, with the exception that no horse serum was added (serum-free Diamond's media), and incubated at 37°C at the time points indicated. At each time point, 500 μ l of culture was taken from each sample and read on a FACS instrument. The survival rates of the parasites were determined by excluding dead cells using Zombie Red viability dye at a 1:1,000 dilution in PBS (BioLegend) and quantitated using CountBright Absolute Counting Beads (Thermo Fisher Scientific) with a BD LSRFortessa cell analyzer (see Fig. S2 in the supplemental material). The percentages of living cells at all of the time points were normalized to the level at time point 0 h, which was set as 100%.

Density stress assay. EV and TvMIF-OE parasites were grown to mid-log phase (10⁶ cells/ml) overnight and concentrated to 10⁷ cells/ml or 2 \times 10⁷ cells/ml in complete Diamond's media. These parasites were then incubated for 4 h or 8 h. The cells were subjected to FACS analyses using a BD LSRFortessa cell analyzer. The percentages of dead cells were determined by gating the Zombie Red-positive population and determining its percentage relative to the total cell population.

Growth assay. EV and TvMIF-OE parasites (4 \times 10⁴ cells/ml) were cultured in complete Diamond's media. At 12 h and 24 h, 500 μ l of each sample was taken for FACS analyses to determine the numbers of living cells. Numbers of living cells were determined as described for the serum starvation assay.

Secretion assay. The parasites were grown to mid-log phase overnight in complete Diamond's media, collected, and resuspended in PBS–5% sucrose at 10⁶ cells/ml. The parasites (5 \times 10⁸) were incubated at either 16°C or 37°C for 2 h. The 16°C condition was used for the secretion inhibition control. After the incubation, the parasites were spun at 3,200 rpm for 10 min and the cell pellets were collected and lysed in lysis buffer containing 50 mM Tris-HCl (pH 7.5), 2% SDS, and 1 \times Halt protease inhibitor cocktail (Thermo Fisher Scientific) to make whole-cell lysates (Wcl). The supernatant was passed through a PES Vivaflow crossflow cassette (Sartorius) (MWCO, 100 kDa) to separate the exosomes (Exo) from the non-exosomal soluble fraction (NESF). The NESF was concentrated by using Amicon Ultra Centrifugal filters (EMD Millipore) (MWCO, 10 K). The Exo were pelleted at 100,000 \times g for 70 min. Anti-neomycin phosphotransferase (Neo) (Jackson Laboratory) (1:2,500) and anti-TvMIF antibodies (polyclonal rabbit antisera raised against TvMIF) (1:500) (4) were used as the primary antibodies and anti-rabbit antibody (Jackson Laboratory) (1:25,000) was used as the secondary antibody for both Neo and TvMIF probing.

Intracellular and secreted TvMIF quantitation. Anti-TvMIF polyclonal antibody, anti-glyceraldehyde 3-phosphate dehydrogenase (anti-GAPDH) antibody (Cocalico Biologicals) (1:10,000), and anti-Neo antibody (Jackson Laboratory) (1:2,500) were used as the primary antibodies, and anti-rabbit (Jackson Laboratory) was used as the secondary antibody. For intracellular TvMIF quantitation, mid-log-phase parasites were spun down and washed with PBS–5% sucrose–1 \times Halt protease inhibitor cocktail (Thermo Fisher Scientific). The cells were then lysed in 50 mM Tris-HCl (pH 7.5)–2% SDS–1 \times Halt protease inhibitor cocktail lysis buffer. Equal total proteins were loaded from whole-cell lysates from 0 h, 16 h, and 24 h. For secreted TvMIF quantitation, *T. vaginalis* parasites cultured overnight in complete Diamond's media were collected and resuspended in serum-free or complete Diamond's media for 3 h or 6 h of incubation. After the incubation, the parasites were resuspended in PBS–5% sucrose for 2 h of incubation for secretion collection. The cells were spun down and collected using the method described for intracellular TvMIF quantitation as the whole-cell lysate (Wcl) control. The supernatant was then concentrated with

Amicon Ultra Centrifugal Filters (MWCO = 10 K). Equal total protein amounts were loaded for the Wcl control and secreted fractions for all samples.

Production and purification of rTvMIF and rhuMIF. TvMIF and huMIF was cloned into the pET SUMO expression vector with an N-terminal SUMO domain with 6×His tag separately. Both constructs were transformed into BL21(DE3) *E. coli* (Thermo Fisher Scientific) for protein expression (74). rTvMIF and rhuMIF were purified using a HisPur nickel-nitrilotriacetic acid (Ni-NTA) Spin column (Thermo Fisher Scientific) and dialyzed into 20 mM Tris-HCl (pH 8.0)–150 mM NaCl–1 mM dithiothreitol (DTT). His-tagged SUMO protease (mclab) in combination with SUMO protease buffer (50 mM Tris (pH 8.0), 1 mM DTT) was used to cleave off N-terminal SUMO and the 6×His tag to produce rTvMIF and rhuMIF with their native sequences. SUMO protease and the SUMO domain with the His tag were removed by the use of a HisPur Ni-NTA Spin column. rTvMIF and rhuMIF were then purified by the use of Econo-Pac 10DG desalting prepacked gravity flow columns (Bio-Rad).

Exogenous rTvMIF and rhuMIF addition and survival assay. A 50 ng/ml volume of rTvMIF or rhuMIF or PBS vehicle control was added to TvMIF-OE grown in serum-free Diamond's media. The survival rates were determined 4 h and 8 h after starvation. rTvMIF (100 ng/ml) or PBS vehicle was added to TvMIF KO parasites in serum-free Diamond's media. The survival rates were determined 24 h after starvation.

Co-culture in transwell. Transwell (Corning) with a 0.4- μ m-pore-size polycarbonate membrane insert was used. EV or TvMIF-OE (1.8×10^5) was plated in 300 μ l of complete Diamond's media in each individual top insert, and EV (2×10^5) was plated in 1 ml of media in each individual bottom well. The top and bottom cells were passaged and rediluted daily to the concentrations described above in complete Diamond's media. Every 7 days, the cells were resuspended in serum-free Diamond's media at the concentration described above and incubated for 24 h for survival tests. The survival rates were determined as described for the serum starvation assays.

Apoptosis assays. Zombie Red (1:1,000) and 4.5 μ g/ml of fluorescein isothiocyanate (FITC)-annexin V (BioLegend) in annexin V binding buffer (BioLegend) were used to stain parasites grown without serum at 0 h, 16 h, and 24 h, and the cells were subjected to FACS analysis using a BD LSRFortessa cell analyzer. The live parasites were gated by excluding positive Zombie Red signal. Apoptotic levels were determined by analysis of the mean fluorescence intensity (MFI) of annexin V of live parasites. Parasites treated with dimethyl sulfoxide (DMSO) were used as the healthy control, and parasites treated with 4 μ M staurosporine (STS) for 16 h composed the apoptotic control.

DNA fragmentation was done by incubating EV and TvMIF-OE in serum-free Diamond's media and fixing parasites in 4% formaldehyde–PBS. Parasite nuclei were stained with ProLong Gold antifade mountant with 4',6-diamidino-2-phenylindole (DAPI) (Thermo Fisher Scientific). The slides were then imaged using an Axioskop 2 epifluorescence microscope (Zeiss). The percentage of fragmented DNA was determined by the number of fragmented DNA in a total of 300 nuclei counted in each sample by using ZEN lite software.

Reactive oxygen species (ROS) detection and superoxide dismutase (SOD) mimetic treatment. EV and TvMIF-OE parasites were grown in serum-free Diamond's media as previously described. At 0 h, 16 h, and 24 h, cells were stained with 2 μ M dihydroethidium (DHE) (Thermo Fisher Scientific) mixed with PBS at 37°C for 30 min in the dark. The MFI of ROS signal was determined by the MFI of phycoerythrin-Texas Red (PE-Texas Red)-treated live cells gated by the use of a flow cytometer.

For SOD mimetic treatment, a 250 μ M or 500 μ M concentration of manganese(III) tetrakis(1-methyl-4-pyridyl)porphyrin (MnTmPyP) (Sigma) or DMSO was used to treat parasites grown in serum-free Diamond's media at time point 0 h. At 16 h, parasites were stained with DHE and CountBright absolute counting beads (Thermo Fisher Scientific) were added to determine the number of live cells. The ROS signal and the percentage of living cells were measured by the use of a flow cytometer.

Gene knockout and adding back of TvMIF in *T. vaginalis* B7RC2. The constructs and reagents used to create the TvMIF knockout were as described by Janssen et al. (4). Adding back of TvMIF to TvMIF KO cells was done by transfection of TVAG_219770 (TvMIF) in Master-Neo-(HA)₂ plasmid with selection of G418 at the concentration of 900 μ g/ml in order to select for the plasmid in the presence of a neomycin phosphotransferase (Neo) gene knock-in at the TvMIF gene locus, replacing the TvMIF gene.

SUPPLEMENTAL MATERIAL

Supplemental material for this article may be found at <https://doi.org/10.1128/mBio.00910-18>.

FIG S1, TIF file, 2.3 MB.

FIG S2, TIF file, 2.2 MB.

FIG S3, TIF file, 1.8 MB.

FIG S4, TIF file, 1.3 MB.

ACKNOWLEDGMENTS

We thank Natalia de Miguel and Feng Guo for providing the TvMIF antibody and the pET SUMO plasmid, respectively. We thank members of the Johnson laboratory for intellectual discussion and David Campbell, Azeez Aranmolate, Brian Janssen and Frances Mercer, and Brenda Molgora for helpful comments on the manuscript.

This work was supported by NIH grants R01 AI103182 and R21 AI105779 (P.J.J.) and NIH grant T32 AI007323 (Y.-P.C.).

Y.-P.C. and P.J.J. designed the research; Y.-P.C. and O.T. performed the research; Y.-P.C. and P.J.J. analyzed the data; and Y.-P.C. and P.J.J. wrote the paper.

REFERENCES

1. World Health Organization. 2008. Global incidence and prevalence of selected curable sexually transmitted infections. World Health Organization, Geneva, Switzerland.
2. Secor WE, Meites E, Starr MC, Workowski KA. 2014. Neglected parasitic infections in the United States: trichomoniasis. *Am J Trop Med Hyg* 90:800–804. <https://doi.org/10.4269/ajtmh.13-0723>.
3. Conrad MD, Bradic M, Warring SD, Gorman AW, Carlton JM. 2013. Getting Trichy: tools and approaches to interrogating *Trichomonas vaginalis* in a post-genome world. *Trends Parasitol* 29:17–25. <https://doi.org/10.1016/j.pt.2012.10.004>.
4. Janssen BD, Chen YP, Molgora BM, Wang SE, Simoes-Barbosa A, Johnson PJ. 2018. CRISPR/Cas9-mediated gene modification and gene knock out in the human-infective parasite *Trichomonas vaginalis*. *Sci Rep* 8:270. <https://doi.org/10.1038/s41598-017-18442-3>.
5. Petrin D, Delgaty K, Bhatt R, Garber G. 1998. Clinical and microbiological aspects of *Trichomonas vaginalis*. *Clin Microbiol Rev* 11:300–317.
6. McClelland RS, Sangare L, Hassan WM, Lavreys L, Mandaliya K, Kiarie J, Ndinya-Achola J, Jaoko W, Baeten JM. 2007. Infection with *Trichomonas vaginalis* increases the risk of HIV-1 acquisition. *J Infect Dis* 195:698–702. <https://doi.org/10.1086/511278>.
7. Ryan CM, de Miguel N, Johnson PJ. 2011. *Trichomonas vaginalis*: current understanding of host-parasite interactions. *Essays Biochem* 51:161–175. <https://doi.org/10.1042/bse0510161>.
8. Hirt RP. 2013. *Trichomonas vaginalis* virulence factors: an integrative overview. *Sex Transm Infect* 89:439–443. <https://doi.org/10.1136/sextrans-2013-051105>.
9. Leitsch D. 2016. Recent advances in the *Trichomonas vaginalis* field. *F1000Res* 5:162. <https://doi.org/10.12688/f1000research.7594.1>.
10. Kamir D, Zierow S, Leng L, Cho Y, Diaz Y, Griffith J, McDonald C, Merk M, Mitchell RA, Trent J, Chen Y, Kwong YK, Xiong H, Vermeire J, Cappello M, McMahon-Pratt D, Walker J, Bernhagen J, Lolis E, Bucala R. 2008. A *Leishmania* ortholog of macrophage migration inhibitory factor modulates host macrophage responses. *J Immunol* 180:8250–8261. <https://doi.org/10.4049/jimmunol.180.12.8250>.
11. Wasala NB, Jaworski DC. 2012. *Dermacentor variabilis*: characterization and modeling of macrophage migration inhibitory factor with phylogenetic comparisons to other ticks, insects and parasitic nematodes. *Exp Parasitol* 130:232–238. <https://doi.org/10.1016/j.exppara.2011.12.010>.
12. Panstruga R, Baumgarten K, Bernhagen J. 2015. Phylogeny and evolution of plant macrophage migration inhibitory factor/D-dopachrome tautomerase-like proteins. *BMC Evol Biol* 15:64. <https://doi.org/10.1186/s12862-015-0337-x>.
13. Sparkes A, De Baetselier P, Roelants K, De Trez C, Magez S, Van Ginderachter JA, Raes G, Bucala R, Stijlemans B. 2017. The non-mammalian MIF superfamily. *Immunobiology* 222:473–482. <https://doi.org/10.1016/j.imbio.2016.10.006>.
14. Calandra T, Roger T. 2003. Macrophage migration inhibitory factor: a regulator of innate immunity. *Nat Rev Immunol* 3:791–800. <https://doi.org/10.1038/nri1200>.
15. Lue H, Thiele M, Franz J, Dahl E, Speckgens S, Leng L, Fingerle-Rowson G, Bucala R, Lüscher B, Bernhagen J. 2007. Macrophage migration inhibitory factor (MIF) promotes cell survival by activation of the Akt pathway and role for CSN5/JAB1 in the control of autocrine MIF activity. *Oncogene* 26:5046–5059. <https://doi.org/10.1038/sj.onc.1210318>.
16. Lue H, Kleemann R, Calandra T, Roger T, Bernhagen J. 2002. Macrophage migration inhibitory factor (MIF): mechanisms of action and role in disease. *Microbes Infect* 4:449–460. [https://doi.org/10.1016/S1286-4579\(02\)01560-5](https://doi.org/10.1016/S1286-4579(02)01560-5).
17. Twu O, Dessí D, Vu A, Mercer F, Stevens GC, de Miguel N, Rappelli P, Cocco AR, Clubb RT, Fiori PL, Johnson PJ. 2014. *Trichomonas vaginalis* homolog of macrophage migration inhibitory factor induces prostate cell growth, invasiveness, and inflammatory responses. *Proc Natl Acad Sci U S A* 111:8179–8184. <https://doi.org/10.1073/pnas.1321884111>.
18. Augustijn KD, Kleemann R, Thompson J, Kooistra T, Crawford CE, Reece SE, Pain A, Siebum AH, Janse CJ, Waters AP. 2007. Functional characterization of the *Plasmodium falciparum* and *P. berghei* homologues of macrophage migration inhibitory factor. *Infect Immun* 75:1116–1128. <https://doi.org/10.1128/IAI.00902-06>.
19. Cho Y, Jones BF, Vermeire JJ, Leng L, DiFedele L, Harrison LM, Xiong H, Kwong YK, Chen Y, Bucala R, Lolis E, Cappello M. 2007. Structural and functional characterization of a secreted hookworm macrophage migration inhibitory factor (MIF) that interacts with the human MIF receptor CD74. *J Biol Chem* 282:23447–23456. <https://doi.org/10.1074/jbc.M702950200>.
20. Sommerville C, Richardson JM, Williams RA, Mottram JC, Roberts CW, Alexander J, Henriquez FL. 2013. Biochemical and immunological characterization of *Toxoplasma gondii* macrophage migration inhibitory factor. *J Biol Chem* 288:12733–12741. <https://doi.org/10.1074/jbc.M112.419911>.
21. Tan TH, Edgerton SA, Kumari R, McAlister MS, Roe SM, Nagl S, Pearl LH, Selkirk ME, Bianco AE, Totty NF, Engwerda C, Gray CA, Meyer DJ. 2001. Macrophage migration inhibitory factor of the parasitic nematode *Trichinella spiralis*. *Biochem J* 357:373–383. <https://doi.org/10.1042/bj3570373>.
22. Deponte M. 2008. Programmed cell death in protists. *Biochim Biophys Acta* 1783:1396–1405. <https://doi.org/10.1016/j.bbamcr.2008.01.018>.
23. Kaczanowski S, Sajid M, Reece SE. 2011. Evolution of apoptosis-like programmed cell death in unicellular protozoan parasites. *Parasit Vectors* 4:44. <https://doi.org/10.1186/1756-3305-4-44>.
24. Chose O, Noël C, Gerbod D, Brenner C, Viscogliosi E, Roseto A. 2002. A form of cell death with some features resembling apoptosis in the mitochondrial unicellular organism *Trichomonas vaginalis*. *Exp Cell Res* 276:32–39. <https://doi.org/10.1006/excr.2002.5496>.
25. Ofer K, Gold D, Flescher E. 2008. Methyl jasmonate induces cell cycle block and cell death in the amitochondriate parasite *Trichomonas vaginalis*. *Int J Parasitol* 38:959–968. <https://doi.org/10.1016/j.ijpara.2007.12.008>.
26. Clark CG, Diamond LS. 2002. Methods for cultivation of luminal parasitic protists of clinical importance. *Clin Microbiol Rev* 15:329–341. <https://doi.org/10.1128/CMR.15.3.329-341.2002>.
27. Gelbart SM, Thomason JL, Osypowski PJ, Kellett AV, James JA, Broekhuizen FF. 1990. Growth of *Trichomonas vaginalis* in commercial culture media. *J Clin Microbiol* 28:962–964.
28. Delgadillo MG, Liston DR, Niazi K, Johnson PJ. 1997. Transient and selectable transformation of the parasitic protist *Trichomonas vaginalis*. *Proc Natl Acad Sci U S A* 94:4716–4720. <https://doi.org/10.1073/pnas.94.9.4716>.
29. Twu O, Johnson PJ. 2014. Parasite extracellular vesicles: mediators of intercellular communication. *PLoS Pathog* 10:e1004289. <https://doi.org/10.1371/journal.ppat.1004289>.
30. Marti M, Johnson PJ. 2016. Emerging roles for extracellular vesicles in parasitic infections. *Curr Opin Microbiol* 32:66–70. <https://doi.org/10.1016/j.mib.2016.04.008>.
31. Twu O, de Miguel N, Lustig G, Stevens GC, Vashisht AA, Wohlschlegel JA, Johnson PJ. 2013. *Trichomonas vaginalis* exosomes deliver cargo to host cells and mediate host-parasite interactions. *PLoS Pathog* 9:e1003482. <https://doi.org/10.1371/journal.ppat.1003482>.
32. Flieger O, Engling A, Bucala R, Lue H, Nickel W, Bernhagen J. 2003. Regulated secretion of macrophage migration inhibitory factor is mediated by a non-classical pathway involving an ABC transporter. *FEBS Lett* 551:78–86. [https://doi.org/10.1016/S0014-5793\(03\)00900-1](https://doi.org/10.1016/S0014-5793(03)00900-1).
33. Mitchell RA, Metz CN, Peng T, Bucala R. 1999. Sustained mitogen-activated protein kinase (MAPK) and cytoplasmic phospholipase A2 activation by macrophage migration inhibitory factor (MIF). Regulatory role in cell proliferation and glucocorticoid action. *J Biol Chem* 274:18100–18106. <https://doi.org/10.1074/jbc.274.25.18100>.
34. Du W, Wright BM, Li X, Finke J, Rini BI, Zhou M, He H, Lal P, Welford SM. 2013. Tumor-derived macrophage migration inhibitory factor promotes an autocrine loop that enhances renal cell carcinoma. *Oncogene* 32:1469–1474. <https://doi.org/10.1038/ncr.2012.143>.

35. Bozza MT, Martins YC, Carneiro LAM, Paiva CN. 2012. Macrophage migration inhibitory factor in protozoan infections. *J Parasitol Res* 2012: 413052. <https://doi.org/10.1155/2012/413052>.
36. Rosado JDD, Rodriguez-Sosa M. 2011. Macrophage migration inhibitory factor (MIF): a key player in protozoan infections. *Int J Biol Sci* 7:1239–1256. <https://doi.org/10.7150/ijbs.7.1239>.
37. Hudson JD, Shoaibi MA, Maestro R, Carnero A, Hannon GJ, Beach DH. 1999. A proinflammatory cytokine inhibits p53 tumor suppressor activity. *J Exp Med* 190:1375–1382. <https://doi.org/10.1084/jem.190.10.1375>.
38. Mitchell RA, Liao H, Chesney J, Fingerle-Rowson G, Baugh J, David J, Bucala R. 2002. Macrophage migration inhibitory factor (MIF) sustains macrophage proinflammatory function by inhibiting p53: regulatory role in the innate immune response. *Proc Natl Acad Sci U S A* 99:345–350. <https://doi.org/10.1073/pnas.012511599>.
39. Mitchell RA, Bucala R. 2000. Tumor growth-promoting properties of macrophage migration inhibitory factor (MIF). *Semin Cancer Biol* 10: 359–366. <https://doi.org/10.1006/scbi.2000.0328>.
40. Vermes I, Haanen C, Steffens-Nakken H, Reutelingsperger C. 1995. A novel assay for apoptosis. Flow cytometric detection of phosphatidylserine expression on early apoptotic cells using fluorescein labelled annexin V. *J Immunol Methods* 184:39–51. [https://doi.org/10.1016/0022-1759\(95\)00072-1](https://doi.org/10.1016/0022-1759(95)00072-1).
41. Simon HU, Haj-Yehia A, Levi-Schaffer F. 2000. Role of reactive oxygen species (ROS) in apoptosis induction. *Apoptosis* 5:415–418. <https://doi.org/10.1023/A:1009616228304>.
42. Koga K, Kenessey A, Ojamaa K. 2013. Macrophage migration inhibitory factor antagonizes pressure overload-induced cardiac hypertrophy. *Am J Physiol Heart Circ Physiol* 304:H282–H293. <https://doi.org/10.1152/ajpheart.00595.2012>.
43. Sobierajski J, Hendgen-Cotta U, Lüdtke P, Rammos C, Bernhagen J, Kelm M, Rassaf T. 2013. Time dependent regulation of MIF by S-nitrosylation reduces apoptosis in myocardial I/R-injury. *Eur Heart J* 34:P4990. <https://doi.org/10.1093/eurheartj/eh310.P4990>.
44. Zhao H, Joseph J, Fales HM, Sokoloski EA, Levine RL, Vasquez-Vivar J, Kalyanaraman B. 2005. Detection and characterization of the product of hydroethidine and intracellular superoxide by HPLC and limitations of fluorescence. *Proc Natl Acad Sci U S A* 102:5727–5732. <https://doi.org/10.1073/pnas.0501719102>.
45. Nguyen MT, Lue H, Kleemann R, Thiele M, Tolle G, Finkelmeier D, Wagner E, Braun A, Bernhagen J. 2003. The cytokine macrophage migration inhibitory factor reduces pro-oxidative stress-induced apoptosis. *J Immunol* 170:3337–3347. <https://doi.org/10.4049/jimmunol.170.6.3337>.
46. Wilson JM, Coletta PL, Cuthbert RJ, Scott N, MacLennan K, Hawcroft G, Leng L, Lubetsky JB, Jin KK, Lolis E, Medina F, Brieva JA, Poulson R, Markham AF, Bucala R, Hull MA. 2005. Macrophage migration inhibitory factor promotes intestinal tumorigenesis. *Gastroenterology* 129: 1485–1503. <https://doi.org/10.1053/j.gastro.2005.07.061>.
47. Conroy H, Mawhinney L, Donnelly SC. 2010. Inflammation and cancer: macrophage migration inhibitory factor (MIF)—the potential missing link. *QJM* 103:831–836. <https://doi.org/10.1093/qjmed/hcq148>.
48. Denz A, Pilarsky C, Muth D, Rückert F, Saeger HD, Grützmann R. 2010. Inhibition of MIF leads to cell cycle arrest and apoptosis in pancreatic cancer cells. *J Surg Res* 160:29–34. <https://doi.org/10.1016/j.jss.2009.03.048>.
49. Cheng WH, Huang KY, Huang PJ, Hsu JH, Fang YK, Chiu CH, Tang P. 2015. Nitric oxide maintains cell survival of *Trichomonas vaginalis* upon iron depletion. *Parasit Vectors* 8:393. <https://doi.org/10.1186/s13071-015-1000-5>.
50. Huang KY, Chen YY, Fang YK, Cheng WH, Cheng CC, Chen YC, Wu TE, Ku FM, Chen SC, Lin R, Tang P. 2014. Adaptive responses to glucose restriction enhance cell survival, antioxidant capability, and autophagy of the protozoan parasite *Trichomonas vaginalis*. *Biochim Biophys Acta* 1840:53–64. <https://doi.org/10.1016/j.bbagen.2013.08.008>.
51. Frasson AP, Charão MF, Rosemberg DB, de Souza AP, Garcia SC, Bororino C, Bogo MR, De Carli GA, Tasca T. 2012. Analysis of the NTPDase and ecto-5'-nucleotidase profiles in serum-limited *Trichomonas vaginalis*. *Mem Inst Oswaldo Cruz* 107:170–177. <https://doi.org/10.1590/S0074-02762012000200004>.
52. Mukherjee SB, Das M, Sudhandiran G, Saha C. 2002. Increase in cytosolic Ca²⁺ levels through the activation of non-selective cation channels induced by oxidative stress causes mitochondrial depolarization leading to apoptosis-like death in *Leishmania donovani* promastigotes. *J Biol Chem* 277:24717–24727. <https://doi.org/10.1074/jbc.M201961200>.
53. Sen N, Das BB, Ganguly A, Mukherjee T, Tripathi G, Bandyopadhyay S, Rakshit S, Sen T, Majumder HK. 2004. Camptothecin induced mitochondrial dysfunction leading to programmed cell death in unicellular hemoflagellate *Leishmania donovani*. *Cell Death Differ* 11:924–936. <https://doi.org/10.1038/sj.cdd.4401435>.
54. Sen N, Das BB, Ganguly A, Mukherjee T, Bandyopadhyay S, Majumder HK. 2004. Camptothecin-induced imbalance in intracellular cation homeostasis regulates programmed cell death in unicellular hemoflagellate *Leishmania donovani*. *J Biol Chem* 279:52366–52375. <https://doi.org/10.1074/jbc.M406705200>.
55. Alzate JF, Arias AA, Moreno-Mateos D, Alvarez-Barrientos A, Jiménez-Ruiz A. 2007. Mitochondrial superoxide mediates heat-induced apoptotic-like death in *Leishmania infantum*. *Mol Biochem Parasitol* 152:192–202. <https://doi.org/10.1016/j.molbiopara.2007.01.006>.
56. Piacenza L, Irigoín F, Alvarez MN, Peluffo G, Taylor MC, Kelly JM, Wilkinson SR, Radi R. 2007. Mitochondrial superoxide mediates heat-induced programmed cell death in *Trypanosoma cruzi*: cytoprotective action of mitochondrial iron superoxide dismutase overexpression. *Biochem J* 403:323–334. <https://doi.org/10.1042/BJ20061281>.
57. Figarella K, Uzcategui NL, Beck A, Schoenfeld C, Kubata BK, Lang F, Duzsenko M. 2006. Prostaglandin-induced programmed cell death in *Trypanosoma brucei* involves oxidative stress. *Cell Death Differ* 13: 1802–1814. <https://doi.org/10.1038/sj.cdd.4401862>.
58. Suzuki M, Takamura Y, Maéno M, Tochinali S, Iyaguchi D, Tanaka I, Nishihira J, Ishibashi T. 2004. *Xenopus laevis* macrophage migration inhibitory factor is essential for axis formation and neural development. *J Biol Chem* 279:21406–21414. <https://doi.org/10.1074/jbc.M311416200>.
59. Marson AL, Tarr DE, Scott AL. 2001. Macrophage migration inhibitory factor (mif) transcription is significantly elevated in *Caenorhabditis elegans* dauer larvae. *Gene* 278:53–62. [https://doi.org/10.1016/S0378-1119\(01\)00706-5](https://doi.org/10.1016/S0378-1119(01)00706-5).
60. Moonah SN, Abhyankar MM, Haque R, Petri WA, Jr. 2014. The macrophage migration inhibitory factor homolog of *Entamoeba histolytica* binds to and immunomodulates host macrophages. *Infect Immun* 82: 3523–3530. <https://doi.org/10.1128/IAI.01812-14>.
61. Shao D, Zhong X, Zhou YF, Han Z, Lin Y, Wang Z, Bu L, Zhang L, Su XD, Wang H. 2010. Structural and functional comparison of MIF ortholog from *Plasmodium yoelii* with MIF from its rodent host. *Mol Immunol* 47:726–737. <https://doi.org/10.1016/j.molimm.2009.10.037>.
62. Holowka T, Castilho TM, Garcia AB, Sun T, McMahon-Pratt D, Bucala R. 2016. *Leishmania*-encoded orthologs of macrophage migration inhibitory factor regulate host immunity to promote parasite persistence. *FASEB J* 30:2249–2265. <https://doi.org/10.1096/fj.201500189R>.
63. Buschow SI, van Balkom BW, Aalberts M, Heck AJ, Wauben M, Stoorvogel W. 2010. MHC class II-associated proteins in B-cell exosomes and potential functional implications for exosome biogenesis. *Immunol Cell Biol* 88:851–856. <https://doi.org/10.1038/icb.2010.64>.
64. Welton JL, Khanna S, Giles PJ, Brennan P, Brewis IA, Staffurth J, Mason MD, Clayton A. 2010. Proteomics analysis of bladder cancer exosomes. *Mol Cell Proteomics* 9:1324–1338. <https://doi.org/10.1074/mcp.M000063-MCP201>.
65. Admyre C, Johansson SM, Qazi KR, Filén JJ, Lahesmaa R, Norman M, Neve EP, Schevnius A, Gabrielsson S. 2007. Exosomes with immune modulatory features are present in human breast milk. *J Immunol* 179: 1969–1978. <https://doi.org/10.4049/jimmunol.179.3.1969>.
66. Choi DS, Lee JM, Park GW, Lim HW, Bang JY, Kim YK, Kwon KH, Kwon HJ, Kim KP, Gho YS. 2007. Proteomic analysis of microvesicles derived from human colorectal cancer cells. *J Proteome Res* 6:4646–4655. <https://doi.org/10.1021/pr070192y>.
67. He M, Qin H, Poon TC, Sze SC, Ding X, Co NN, Ngai SM, Chan TF, Wong N. 2015. Hepatocellular carcinoma-derived exosomes promote motility of immortalized hepatocyte through transfer of oncogenic proteins and RNAs. *Carcinogenesis* 36:1008–1018. <https://doi.org/10.1093/carcin/bgv081>.
68. Lazar I, Clement E, Ducoux-Petit M, Denat L, Soldan V, Dauvillier S, Balor S, Burret-Schiltz O, Larue L, Muller C, Nieto L. 2015. Proteome characterization of melanoma exosomes reveals a specific signature for metastatic cell lines. *Pigment Cell Melanoma Res* 28:464–475. <https://doi.org/10.1111/pcmr.12380>.
69. Hosseini-Beheshti E, Pham S, Adomat H, Li N, Tomlinson Guns ES. 2012. Exosomes as biomarker enriched microvesicles: characterization of exosomal proteins derived from a panel of prostate cell lines with distinct AR phenotypes. *Mol Cell Proteomics* 11:863–885. <https://doi.org/10.1074/mcp.M111.014845>.
70. Park JE, Tan HS, Datta A, Lai RC, Zhang H, Meng W, Lim SK, Sze SK. 2010. Hypoxic tumor cell modulates its microenvironment to enhance angiogenic and metastatic potential by secretion of proteins and exosomes.

- Mol Cell Proteomics 9:1085–1099. <https://doi.org/10.1074/mcp.M900381-MCP200>.
71. Costa-Silva B, Aiello NM, Ocean AJ, Singh S, Zhang H, Thakur BK, Becker A, Hoshino A, Mark MT, Molina H, Xiang J, Zhang T, Theilen TM, Garcia-Santos G, Williams C, Ararso Y, Huang Y, Rodrigues G, Shen TL, Labori KJ, Lothe IM, Kure EH, Hernandez J, Dousset A, Ebbesen SH, Grandgenett PM, Hollingsworth MA, Jain M, Mallya K, Batra SK, Jarnagin WR, Schwartz RE, Matei I, Peinado H, Stanger BZ, Bromberg J, Lyden D. 2015. Pancreatic cancer exosomes initiate pre-metastatic niche formation in the liver. *Nat Cell Biol* 17:816–826. <https://doi.org/10.1038/ncb3169>.
 72. Donn RP, Ray DW. 2004. Macrophage migration inhibitory factor: molecular, cellular and genetic aspects of a key neuroendocrine molecule. *J Endocrinol* 182:1–9. <https://doi.org/10.1677/joe.0.1820001>.
 73. Fingerle-Rowson GR, Bucala R. 2001. Neuroendocrine properties of macrophage migration inhibitory factor (MIF). *Immunol Cell Biol* 79:368–375. <https://doi.org/10.1046/j.1440-1711.2001.01024.x>.
 74. Malakhov MP, Mattern MR, Malakhova OA, Drinker M, Weeks SD, Butt TR. 2004. SUMO fusions and SUMO-specific protease for efficient expression and purification of proteins. *J Struct Funct Genomics* 5:75–86. <https://doi.org/10.1023/B:JSFG.0000029237.70316.52>.

Chapter 3:

A Trichomonas vaginalis cadherin-like protein mediates adherence to and killing of host cells

Abstract

Trichomonas vaginalis, a worldwide prevalent sexually-transmitted parasite, adheres to and induces cytolysis of human mucosal epithelial cells. We have functionally characterized a hypothetical protein, TVAG_393390, whose tertiary structure modeling using Phyre2 revealed similarity to cadherin proteins. TVAG_393390 contains four predicted calcium-binding sites at structurally similar locations to cadherin proteins; thus we renamed it cadherin-like protein (CLP). CLP was found to be surface localized and CLP mRNA was significantly up-regulated when parasites contacted host cells. To test the roles of CLP and its calcium-binding domains in host cell adherence, wild-type CLP (CLP) and a calcium-binding site mutant (CLP-mut) were overexpressed in *T. vaginalis*. We found that CLP parasites have ~3.5-fold greater adherence to host cells relative to the empty vector control (EV), and this increased adherence is ablated by mutating the 4th calcium-binding domain. Additionally, competition with recombinant CLP decreased parasite binding to host cells. As cadherin proteins help mediate cell-cell interactions and adherent *T. vaginalis* strains also display parasite-parasite interactions, we tested the contribution of CLP and CLP-mut on parasite aggregation in the presence and absence of both calcium and host cells. Overexpression of CLP induced parasite aggregation whereas CLP-mut overexpression did not, and CLP-induced parasite aggregation was significantly increased in the presence of calcium, further establishing a Ca²⁺-binding dependency for CLP's function. Lastly, parasites overexpressing wild-type CLP increases killing of host cells by ~3.3 and ~2.35-fold, compared to parasites overexpressing EV and CLP-mut, respectively. Our data identify the first CLP characterized in a unicellular eukaryote that contributes to both parasite-parasite and host-parasite interactions. CLP may represent convergent evolution of a parasite cadherin protein that

is structurally similar to the mammalian cell adhesion protein cadherin and whose function also contributes to pathogenesis.

Introduction

Trichomonas vaginalis is an extracellular eukaryotic parasite that causes trichomoniasis, the most common non-viral sexually transmitted infection, which affects more than 275 million people worldwide annually [1]. In the United States, trichomoniasis is classified as a neglected disease due to limited knowledge of the consequence of infection and its disproportionate affliction of low-income populations and minorities [2][3]. Although the majority of *T. vaginalis* infections are asymptomatic, trichomoniasis can result in inflammation of the urogenital tract of both men and women, resulting in vaginitis, prostatitis, pruritus, dysuria and discharge [4]. Furthermore, *T. vaginalis* is also associated with adverse pregnancy outcomes and HIV co-infection [5][6][7].

As a parasite that does not invade host cells, it is critical for *T. vaginalis* to attach to urogenital epithelial cells in order to establish an infection and acquire nutrients from host cells. *T. vaginalis* can also attach to, lyse, and phagocytose leukocytes and red blood cells [8][9]. *T. vaginalis* strains display different abilities to bind host cells in vitro, with up to a 45-fold difference in attachment observed between different strains [10]. Therefore, understanding the molecular mechanisms of how *T. vaginalis* attaches to host cells is the key to understanding how the parasite establishes infection. In an attempt to determine what factors play a role in adherence, we previously compared the plasma membrane surface proteome of 3 adherent and 3 less adherent *T. vaginalis* strains, identifying proteins that are significantly more abundant in the adherent strains relative to the less adherent strains [11]. Mining this surface proteomics data

revealed a hypothetical protein, TVAG_393390, that is more abundant in 2 out of 3 adherent strains relative to less adherent strains by 1.7 to 3.4-fold [11]. TVAG_393390 was also identified as a putative substrate of the *T. vaginalis* rhomboid protease 1, TvROM1, a membrane serine protease that we have shown is involved in parasite attachment and host cytolysis [12]. Together, these findings highlight a potential role of the TVAG_393390 protein contributing to *T. vaginalis*-host cell interactions.

T. vaginalis cell-cell interactions may also be an important phenotype contributing to pathogenesis. Groups of parasites are readily visible when attached to ectocervical cells and prostate cells [13][14]. The ability of *T. vaginalis* to aggregate also correlates with a strain having higher host cell adherence and cytolytic properties [15]. In metazoans, the strongest forms of cell-cell attachment are mediated by cadherin proteins that bind to each other on apposing cells forming adherens junctions [16]. While single-celled eukaryotes, such as *T. vaginalis*, do not contain cell junctions, it has been hypothesized that protein precursors found in protozoans may have given rise to the complexes that allowed cell-cell interactions leading to multicellularity [17][18]. Bioinformatic analysis revealed that TVAG_393390 is predicted to be structurally similar to metazoan cadherin proteins, indicating its potential role in mediating cell-cell adhesion in the protozoan *T. vaginalis*.

Classic cadherin proteins are large single-pass, transmembrane proteins with extracellular cadherin (EC) repeats, calcium-binding sites, and a cytosolic tail that is involved in intracellular signaling and interactions with p120 catenin, β -catenin, α -catenin and, indirectly, with f-actin [19][20]. Cadherin proteins are involved in both homophilic and heterophilic interactions [21]. Homophilic interactions occur when cadherin protein binds to the same type of cadherin protein *in trans* on another cell. A classic example is the mouse epithelial cadherin (E-cadherin), which

mediates cell-cell interactions in epithelial cells [22][23][24]. Heterophilic interaction involves cadherin proteins binding to a different type of cadherin protein on a different cell type [25]. An example of a heterophilic interaction that has a role in pathogenesis, is the binding of the human E-cadherin protein to a bacterial *Listeria monocytogenes* surface protein, an interaction which helps to mediate invasion of the bacteria [25].

Here we characterize TVAG_393390 and show that it is structurally and functionally similar to cadherin proteins. This cadherin-like protein (CLP) was also found to play significant roles in parasite attachment to and lysis of host cells, as well as parasite aggregation. CLP may thus represent an evolutionary relic of cadherin-like proteins. To our knowledge, this is the first report of a cadherin-like protein in protozoans contributing to host-pathogen and parasite-parasite interactions.

Results

Bioinformatic analysis reveals that TVAG_393390 is structurally similar to cadherin proteins

The *T. vaginalis* protein encoded by TVAG_393390 is listed as a conserved hypothetical protein in the genome sequence database for *T. vaginalis* (trichdb.org/trichdb). This protein was found to be more abundant in the surface proteome of adherent *T. vaginalis* strains relative to less adherent strains by 1.7 to 3.4-fold [11]. We also identified TVAG_393390 as a putative substrate of a *T. vaginalis* rhomboid protease demonstrated to be involved in parasite attachment and host cytolysis [12]. To further investigate a potential role of TVAG_393390 in the *T. vaginalis* adherence, we searched both the gene sequence and the protein sequence using National Center for Biotechnology Information (NCBI) Basic Local Alignment Search Tool

(BLAST) and found no homologues in other organisms. We also used InterPro [26] and Pfam [27] analyses to identify functional domains and none was identified. Next, we employed a secondary structure prediction program called Phyre2 which predicts protein structure by comparing a large database of known protein secondary structures and building three-dimensional models based on the identified homology [28]. Using this approach, we found that the most common modeling for TVAG_393390 to a particular type of protein was to cadherin proteins, with each model having at least 97.9% confidence scores (probability that a template is homologous to our sequence) and 7% identity (Fig. 3-1A). Fig. 3-1B shows a TVAG_393390 model derived using one of the highest ranking tertiary structures, mouse E-cadherin protein. Similar to cadherin proteins, TVAG_393390 is predicted to have 5 extracellular domains with the classical β -sandwich domains and Greek-key folding of cadherin proteins [29][30] (Fig. 3-1B).

Another defining characteristic of cadherin proteins is their binding to extracellular Ca^{2+} via calcium-binding pockets located in between the extracellular domains [31]. Visual inspection of the TVAG_393390 protein sequence for the highly conserved Ca^{2+} -binding sites LDRE, DXD, DXXD, x = any amino acid [29], located at the interfaces of the extracellular domains predicted by Phyre2, identified four candidate Ca^{2+} -binding sites (Fig. 3-1C). TVAG_393390 is also predicted to have one transmembrane domain, near the C-terminus of the protein, based on the transmembrane protein topology prediction software TMHMM [32]. Thus, the predicted orientation of TVAG_393390 would result in the cadherin-like modeled region being exposed to the outside of the cell with a small C-terminal tail located intracellularly (Fig. 3-1B). Due to TVAG_393390's high confidence modeling to cadherin proteins and the presence of key cadherin-like features, we renamed TVAG_393390 as cadherin-like protein (CLP).

CLP is expressed on the surface of the parasite

To determine whether CLP was surface-localized and displays the predicted orientation, we cloned the gene in our standard *T. vaginalis* expression vector, MasterNeo [33] under the control of *T. vaginalis* α -succinyl Co-A synthetase promoter and fused with two C-terminal hemagglutinin (HA) tags. The construct was then introduced into *T. vaginalis* by transfection and parasites were selected with G418 as previously described [34]. Using indirect immunofluorescence assay with an anti-HA antibody, exogenously overexpressed CLP was shown to localize to the surface of the parasite (Fig. 3-2A & B). Since it is also predicted that the C-terminal tail of the protein with the fused HA tags will be located inside the cell, to further probe the orientation of CLP, we performed indirect immunofluorescence with and without permeabilization. We found that the fluorescent signal from CLP is significantly stronger when the parasites are treated with a permeabilizing agent (Fig. S3-1A & C) as permeabilization allows anti-HA antibody access to the intracellular HA tags. These results provided additional support that the C-terminal domain of CLP is located inside the cells. The data are consistent with the predicted CLP structure generated with the Phyre2 analysis (Fig. 3-1B) and demonstrated that overexpression of the protein resulted in the predicted membrane localization with the cadherin-like domains being exposed on the outer surface of the parasite. Therefore, the predicted CLP protein topology is graphically depicted in Fig 3-2C.

CLP mRNA is up-regulated during host contact

Upon parasite contact with human ectocervical cells (Ects), *T. vaginalis* up-regulates expression of a variety of proteins including actin, actin-binding proteins [35] and tetraspanin proteins (TvTSP3, TvTSP5, TvTSP6, and TvTSP8), the latter of which are transmembrane proteins that modulate their own expression and subcellular localizations during host contact

[15][36]. Thus, we hypothesized that surface localized CLP might be up-regulated upon interaction of *T. vaginalis* with host cells. To test this, wild-type parasites were incubated with human Ects for 30 min, 1 h, 2 h or 6 h, followed by removal of unbound parasites in suspension and extraction of RNA from only the parasites adhered to Ects. We found that CLP mRNA is up-regulated by ~5-fold, 19- and 20-fold at 1h, 2h and 6h, respectively, relative to 30 min after host contact (Fig. 3-3). As reduced temperature might affect the ability of the parasites to sense the environment initially and modulate surface protein expression, we used 30 min instead of 0 min for baseline comparison because immediately before co-culturing the parasite with Ects, the parasites are exposed to 4°C to collect and concentrate them. These data support a role for CLP in host cell sensing and/or binding.

Calcium binding is predicted to be important for the function of CLP

Calcium binding plays a critical role in the adhesive role of cadherin proteins by rigidifying the extracellular domains and mediating binding between cadherin proteins on apposing cells [37][38]. Specifically, aspartate residues that help coordinate calcium ions at the base of the cadherin extracellular domains constitute one of the most conserved domains of cadherin proteins across different species [29]. Therefore, to understand how CLP functions, we used Phyre2 and SuSPect mutational analysis to help identify which aspartate residues of the 4 predicted Ca²⁺-binding domains [28][39] (shown in Fig. 3-1C) would lead to the strongest phenotypic effects if mutated (Fig. 3-4A and Fig. S3-2). The two aspartate residues D443 and D445 in the putative fourth Ca²⁺-binding domain are predicted to be the most sensitive to mutation (Fig. 3-4A and Fig. S3-2) so we proceeded to mutate both of these residues to alanine as this type of mutation is standardly performed to study the function of calcium-binding domains in cadherin proteins [40]. We then overexpressed both the wild-type CLP (CLP) and the

D443A D445A CLP mutant (CLP-mut) with an N-terminal GFP tag in *T. vaginalis* and an empty vector (EV) as a negative control. Next, we compared the expression of CLP and CLP-mut proteins in the selected transfectants and found that expression of the wild-type CLP and CLP-mut was similar as determined by immunoblotting using an anti-GFP antibody (Fig. 3-4B).

CLP protein contributes to increased host cell binding which is dependent on the CLP calcium-binding domain

To test whether CLP is important for host binding, we compared the ability of CLP vs CLP-mut overexpressing cells to bind host Ects. We found that CLP increases the host attachment by 3.5-fold compared to EV (Fig. 3-5A). In contrast, CLP-mut has a significantly decreased attachment phenotype that is similar to that of EV (Fig. 3-5A). This data strongly indicate a role for CLP in host cell binding.

To further support the role of CLP in host cell binding, we competed parasite binding to Ects with addition of recombinant CLP. The extracellular domain (EC) of CLP (rCLP EC) was used instead of the entire protein for the ease of expressing the protein in *E. coli* periplasm and since EC is predicted to be responsible for the cadherin protein-protein interactions [31]. We added rCLP EC to Ects for 30 min prior to the addition of parasites. We found that as the concentration of rCLP EC was increased, the percentage of parasite binding to the host cell decreased (Fig. 3-5B). These results further support a role of CLP in host binding.

CLP contributes to parasite-parasite clumping and the effect is abolished in CLP-mut parasites

We and others have observed that more adherent *T. vaginalis* strains appear to clump with each other more readily than poorly adherent strains. In addition, overexpression of the TvTSP8 surface protein which increases parasite adherence to host cells also increased parasite

clumping compared to the EV control parasites [15][10]. Furthermore, cadherin proteins are known to mediate homophilic interactions where cadherin proteins interact with the same type of cadherin on another cell [21][41][42]. We thus compared the clumping behavior of EV, CLP and CLP-mut parasites with or without Ca^{2+} and in the presence or absence of the host. CLP displayed a ~7.5-240 fold increase in parasite clumping compared to the EV control and CLP-mut had almost the same levels of clumping as EV under all conditions tested (Fig. 3-6A & B). Addition of Ca^{2+} but not the presence of host cells significantly increased the clumping of CLP parasites (Fig. 3-6A & B). These data together suggest that the CLP-mediated clumping phenotype is calcium-dependent and the ability does not necessitate a host signal.

CLP contributes to increased killing of host cells

Since CLP is involved in host cell binding and parasite clumping, we hypothesized that these properties could also contribute to increasing host cell death as epithelial host cell killing by *T. vaginalis* is contact-dependent [10] and the increased parasite-parasite association may further increase the number of parasites attacking the host. We found that CLP overexpression increased host death by 3.3-fold compared to EV (Fig. 3-7). In contrast, CLP-mut only displayed a 1.4-fold increase in host killing compared to EV (Fig. 3-7). The slight increase in cytotoxicity observed with the CLP-mut may be due to the fact that the CLP-mut has one of the four hypothesized Ca^{2+} -binding domains mutated so it may not completely abolish the enhanced killing effect of CLP.

Discussion

We have identified and characterized a surface protein of *T. vaginalis* called cadherin-like protein (CLP) and showed that it plays a significant role in host binding, parasite clumping

and host cell killing. This is the first functional analyses of a cadherin-like protein in a unicellular eukaryote. Mammalian cadherin proteins are known to be co-opted for pathogen invasion or colonization by several bacteria and the pathogenic yeast *Candida albicans* [43][44][45]. However, the identification of CLPs or a role for unicellular pathogen CLPs in the adherent to and killing of mammalian cells have not been previously described to our knowledge. We show that this *T. vaginalis* CLP mimics the structure and the function of host cadherin proteins, raising the possibility that other parasites may also use CLPs with low sequence identity but with structural similarity to mammalian cadherins to interact with host cells. The presence of a CLP in *T. vaginalis* that is structurally and functionally similar to mammalian cadherins is likely an example of convergence evolution of 3D structures with similar properties, in the absence of strong primary sequence homology.

Cadherin proteins are known to be involved in homophilic interactions that cause the same cell types to adhere to each other [25][41]. We observed that CLP-overexpressing parasites clump significantly more than empty vector control and the CLP mutant-overexpressing parasites, demonstrating a role for parasite CLP in homophilic adherence of parasites to one another. We also demonstrated that CLP-induced parasite clumping is significantly increased in the presence of calcium, consistent with the calcium-dependent homophilic interaction mediated by cadherin proteins [41]. Highly adherent strains of *T. vaginalis* have been observed to clump (i.e. adhere to each other) significantly more than poorly adherent strains [15]; however, the role of clumping in infection is unclear. To our knowledge, only another family of surface proteins, tetraspanins, have been have been found to help mediate parasite aggregation [15]. In mammalian cells, integrin proteins are one of the predominant protein groups complexed by tetraspanins [46]. However, the *T. vaginalis* genome does not contain any proteins annotated as

integrin-like. On the other hand, it has been reported that human E-cadherin protein interacts with its tetraspanin protein in colon carcinoma [47]. Therefore, future investigation into whether CLPs and TSPs functionally interact is merited. It should also be noted that this *T. vaginalis* CLP is predicted to have a small C-terminal tail with only 2 amino acid residues (Fig. 3-1B). In classical cadherin proteins, the C-terminal is important for cadherin-mediated signaling [48]. It is therefore possible that if CLP represents an early evolutionary form of cadherin-like proteins, part of its functions such as the role we observed in sensing the presence of host cells and increasing its expression in response, may in part be mediated by associating with other proteins that help recruit the signaling proteins. Overall, we speculate that parasites clumping increases the number of parasites attaching to host cells, which in turn, increases the likelihood of parasites successfully colonizing the host. Additionally, human neutrophils have been shown to kill *T. vaginalis* by taking bites from the parasites, in a process called trogocytosis [49]. Aggregation of the parasite could potentially protect parasites in the center of an aggregate from being attacked by neutrophils. Future analyses will better define the functional importance of parasites adhering to one another in parasite survival and infection.

Pre-incubation of host cells with recombinant CLP (rCLP) reduced parasite binding to host cells, confirming a role for parasite CLP in host cell binding. While *T. vaginalis* attachment to host cells likely depends on multiple factors which have been identified to date [11][12][50][51][52][53][54][55][56][57][58], the highest amounts of rCLP tested reduced parasite binding by a significant 21% (Fig. 3-7). Furthermore, the observed 3.3-fold increase in host cell killing is also, to our knowledge, one of the strongest phenotypic effects mediated by exogenous expression of a single protein factor. E-cadherin and N-cadherin are expressed in the human male and female urogenital and reproductive tracts [59][60]. E- and N-cadherin are also found on

spermatozoa [60] to which *T. vaginalis* can also attach and phagocytose [61]. It is therefore of interest to investigate in future studies whether CLP has a conserved role in attaching to and lysing multiple cell types and how it may structurally mediate molecular mimicry.

Previous functional studies on cadherin proteins have revealed that mutations at the first and second calcium-binding sites cause the strongest disruption in homophilic interactions of cadherin proteins that mediate cell-cell binding, whereas mutation at the latter two calcium-binding sites have a slight or almost no effect [40][62]. However, antibody blocking experiments and subsequent mapping of the epitope of the blocking antibody points to a direct interaction between the antibody and the fourth calcium-binding site in E-cadherin protein [63][64]. Here we show that mutating the 4th calcium-binding domain in CLP almost completely reverses the enhanced host attachment, parasite clumping and host cell killing observed with parasites overexpressing the wild-type CLP. It is possible that the overexpression of the *T. vaginalis* protein mutated in the 4th calcium-binding domain results in a dominant negative effect on the endogenous wild-type CLP. Alternatively, the low identity of *T. vaginalis* CLP to mammalian cadherins (10%) (Fig. 3-1A) could explain why the 4th calcium-binding domain of *T. vaginalis* plays a significant role in host cell interactions relative to the 1st or 2nd domain. Further analyses of the evolution and function of this, and perhaps other, CLPs in pathogens is warranted.

Although CLP surface expression levels are different in adherent vs less adherent *T. vaginalis* strains, the fact that CLP is expressed by all the six strains surveyed in our prior proteomics study [11] may indicate an important and conserved function. Our work has uncovered new roles for a family of previously undescribed proteins in *T. vaginalis*, helping us to further scratch the surface of the mechanistic interactions contributing to pathogenesis. Our

work also places *T. vaginalis* as a model organism for the broader study of cell-cell interactions and cell-cell adhesion.

Material and Methods

Bioinformatic analyses

To predict TVAG_393390 function, we used InterPro [26], Pfam [27] and Phyre2 [28] programs to analyze its protein sequence and BLAST with both the gene and protein sequences published on TrichDB [65]. For Phyre2 analysis, we chose the intensive modeling mode, then used the “Run Investigator” feature using the mouse E-cadherin template and performed SuSPect mutational analysis on the four calcium-binding domains/eight aspartate residues in TVAG_393390. The topology of TVAG_393390 was generated with the TOPO2 program [66].

***T. vaginalis* and ectocervical cell line Ect1 culture**

T. vaginalis strain RU393 (ATCC 50142) was grown as previously described [67]. Parasites were grown at 37°C and sub-cultured daily for up to 2 weeks. The human ectocervical cell line Ect1 E6/E7 (ATCC CRL-2614) (Ects) was grown and passaged as previously described [68].

CLP wild-type and mutant plasmid construction and *T. vaginalis* transfection

TVAG_393390 (CLP) wild-type sequence was cloned into the Master-Neo-(HA)₂ plasmid [33] or the N-terminal enhanced green fluorescent protein (eGFP)-Master-Neo plasmid [12]. Two rounds of site-directed mutagenesis were performed using QuikChange kit (Stratagene) in order to introduce the D443A and D445A mutations sequentially using the following primer sets. To introduce D443A mutation: D443A Fwd: CACAGCCGTAGTTGTTGcTCCAGATACTAACTTTG and D443A Rev:

CAAAGTTAGTATCTGGA_gCAACAACACTACGGCTGTG. To introduce the D445A mutation:
D445A Fwd: GTAGTTGTTG_cTCCAG_cTACTAACTTTGATTCC and D445A Rev:
GGAATCAAAGTTAGTA_gCTGGA_gCAACAACACTAC. Introduction of the desired mutations
was confirmed by sequencing (Genewiz). The constructs were transfected into *T. vaginalis* strain
RU393 and parasites containing the constructs were selected using G418 as previously described
[34].

Indirect immunofluorescence assays

Parasite transfectants overexpressing the wild-type (WT) CLP with C-terminal HAx2
were plated on glass coverslips coated with 100 µg/ml of poly-l-lysine (Sigma) and then fixed in
4% formaldehyde in phosphate-buffered saline (PBS) for 20 minutes. The cells were then
permeabilized in 0.2% Triton X-100 in PBS or just PBS for non-permeabilized control for 15
minutes and blocked in 3% BSA for 30 minutes. 1:1000 dilution of anti-HA mouse (BioLegend)
and 1:5000 goat anti-mouse Alexa Fluor488-conjugated secondary antibody (Molecular Probes)
were used for staining. The coverslips were then mounted using ProLong Gold Antifade
Mountant with 4',6-diamidino-2-phenylindole (DAPI) (Thermo Fisher Scientific). The images
were taken by a Zeiss confocal microscope with Yokogawa spinning disc and analyzed with
SlideBook 6 software.

Real-time reverse transcription PCR (qRT-PCR)

1 X 10⁷ of non-transfected RU393 parasites were incubated with 80% confluent Ects for
30 minutes, 1 hour, 2 hours or 6 hours. Unbound parasites were removed and RNA was collected
by adding TriZol to attached parasites on Ects. Total RNA was purified by phenol-chloroform
extraction and treated with TURBO DNase (Invitrogen). cDNA was prepared by using
SuperScript III with oligo dT primers (Thermo Fisher Scientific). Platinum SYBR Green qPCR

SuperMix-UDG and the manufacturer's protocol (Thermo Fisher Scientific) were used for real-time PCR. *T. vaginalis* beta-tubulin was used as the housekeeping gene control. The primer sequences for beta-tubulin are Tub-f: GGCTCGTAACACATCCTACTTC and Tub-r: CTGTTGTGTTGCCGATGAATG. The primer sequences for CLP are 393-f: GACGATGTTGTTAATTTACAGCC and 393-r: CCATCAGAGTTTGATCTTGAAATTGA.

Immunoblot Analyses

Mouse anti-GFP polyclonal antibody (1:1,000) (Clontech) and anti-glyceraldehyde 3-phosphate dehydrogenase (GAPDH) (1:10,000) (Cocalico Biologicals) were used as the primary antibodies and anti-mouse (1:25,000) and anti-rabbit (1:25,000) (Jackson Labs) were used as the secondary antibodies, respectively. 5×10^6 parasites were taken from *T. vaginalis* culture and washed with PBS + 5% sucrose + 1xHalt Protease Inhibitor Cocktail (Thermo Fisher Scientific). The cells were then lysed in lysis buffer (0.1% Nonidet P-40, 0.5% deoxycholate, 2% SDS, 50 mM Tris, pH 8, 5 mM EDTA, 150 mM NaCl) + 1xHalt Protease Inhibitor Cocktail (Thermo Fisher Scientific). Equal amounts of proteins were loaded from each sample.

Production and purification of rCLP ECD

Sequence encoding the CLP ECD was cloned into the pET22b(+) expression vector flanked by a N-terminal pelB periplasm signal sequence and C-terminal 6xHis tag. The primers for cloning were pET22b_393-f: TAATTCGGATCCGATGATTTGGACTTTTTTATTGCAGGATG and pET22b_393-r: ACTAAGCTCGAGCTTCTTTTGTTTTTGCTGCTTTCTTTG. The plasmid was transformed into C41(DE3) *E. coli* cells [69]. An overnight culture was inoculated into 1L LB medium and when this culture reached $OD_{600} = 0.5$ expression was induced with 1 mM isopropyl β -D-1-thiogalactopyranoside (IPTG) for 16h at 25°C. The culture was then spun at 5000 g for 10 min.

The cultured media was precipitated with 50% saturated ammonium sulfate at 4°C overnight and dialyzed against PBS overnight. Protein in the periplasm was extracted as previously described [70][71]. In brief, the cell pellet was washed with ice-cold 20% sucrose + 30 mM Tris pH8 + 1 mM EDTA and then the periplasm was extracted with ice-cold 5 mM MgSO₄. The periplasmic fraction was then dialyzed against PBS at 4°C overnight. A small-scale protein production was done initially to determine that rCLP ECD was abundant in both the culture media and periplasm. As a result, the medium fraction and the periplasmic fraction were combined and loaded onto HisPur Ni-NTA Spin column (Thermo Fisher Scientific). Purified rCLP ECD was dialyzed into PBS and the protein concentration was determined by Pierce BCA Protein Assay (Thermo Fisher Scientific).

***T. vaginalis* attachment to Ects and attachment with rCLP ECD competition**

Attachment of *T. vaginalis* to Ects was performed as described in [10]. Briefly, 5 X 10⁴ of CellTracker Blue CMAC (Thermo Fisher Scientific) labeled *T. vaginalis* were incubated with confluent Ects for 30 minutes and the coverslips were fixed in 4% formaldehyde in PBS and mounted on slides using Mowiol (Calbiochem). Fifteen images of each coverslip were acquired using an Axioscope 2 epifluorescence microscope (Zeiss) and cell counts were quantified using Zen lite and Image J software.

Attachment assays that included rCLP ECD to compete for Ect binding were performed using wild-type, non-transfected RU393 parasites and the difference in the procedure was addition of 0.25 µg, 1 µg or 4 µg of rCLP ECD or 4 µg of BSA as a negative control to Ects for 30 min. Media was then removed and replenished with new media containing CellTracker Blue labeled parasites.

Parasite clumping assay

The parasite clumping assay was done as described in [15] with modifications indicated below. CellTracker Blue CMAC (Thermo Fisher Scientific) pre-labeled *T. vaginalis* was plated at 1×10^6 /ml on glass coverslips covered with confluent Ects or coverslips alone and incubated in completed keratinocyte-SFM with no CaCl_2 or 1 mM of CaCl_2 for 30 minutes. Parasites were then fixed in 4% formaldehyde in PBS and mounted on slides using Mowiol (Calbiochem). Fifteen images of each coverslip were acquired using Axioscope 2 epifluorescence microscope (Zeiss) and analyzed by Zen lite software. A clump is defined as an aggregate of 10 or more parasites.

***T. vaginalis*-induced cytotoxicity of ectocervical cells**

Cytotoxicity of Ects was measured as described [10]. The only modification was 3×10^5 parasites was added to confluent Ects and incubated for 4 hours.

A

Template	Amino acid region aligned	% confidence	% identity
<i>Mus musculus</i> E-cadherin ectodomain	7-520	98.6	10
<i>Xenopus laevis</i> C-cadherin ectodomain	7-520	98.6	10
<i>Drosophila melanogaster</i> N-cadherin 1 ectodomain 1-3	225-515	98.3	7
<i>Mus musculus</i> N-cadherin ectodomain	8-514	98	12
<i>Drosophila melanogaster</i> N-cadherin ectodomain 1-4	170-515	97.9	10

B**C**

Predicted sequence of Ca ²⁺ binding site	Amino acid locations
DQD	112-114
DGED	171-174
DEYD	218-221
DPD	443-445

Figure 3-1: Tertiary structure modeling of TVAG_393390 predicts cadherin-like protein function. (A) The most common high-quality 3D models of CLP predicted by Phyre2 revealed homology modelling to cadherin proteins. Characteristics of the aligned regions of these models are shown. (B) The predicted structure of TVAG_393390 generated by Phyre2 using one of the highest confidence models, mouse E-cadherin, as the template. (C) Inspection of TVAG_393390 sequence for LDRE, DXD, DXXD, x = any amino acid revealed four predicted Ca²⁺-binding sites.

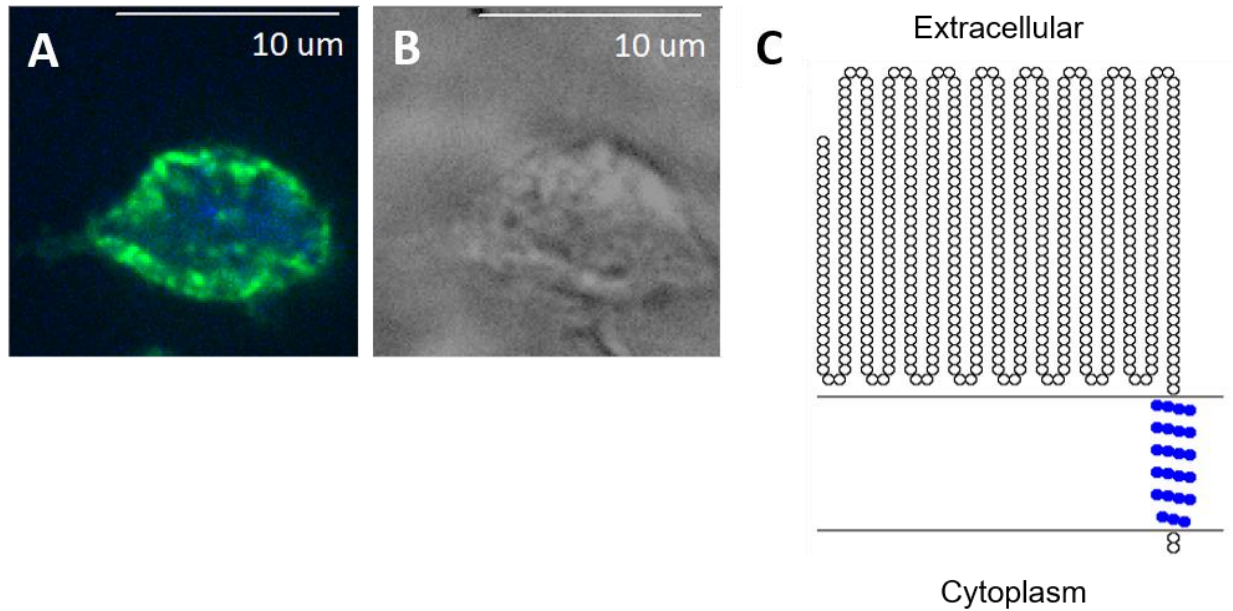


Figure 3-2 Cadherin-like protein (CLP) is localized to the surface of the parasites. (A) The parasite exogenously expressing CLP with two C-terminal HA tags (CLP-2X-HA) were stained for immunofluorescence microscopy using an anti-HA antibody (green) and 4'-6'-diamidino-2-phenylindole (DAPI) for nuclear staining (blue). This image is representative of 60 parasite viewed. (B) Brightfield image of (A). (C) The predicted topology of CLP generated with the TOPO2 program [66]. The predicted orientation is based on results from immunofluorescent assays performed in the absence or presence of a permeabilizing reagent (Fig. S3-1) as well as from the structural prediction from Fig. 3-1B. Predicted transmembrane residues are shown in blue.

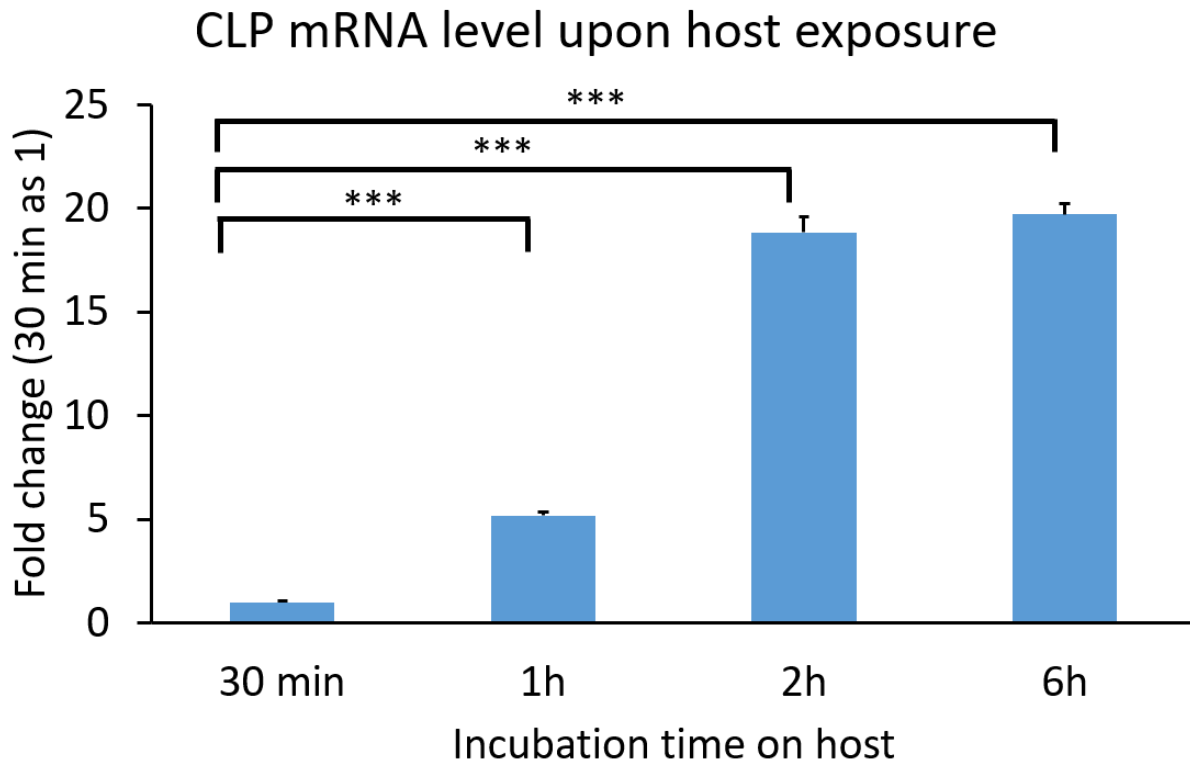


Figure 3-3 CLP mRNA is up-regulated during host contact. *T. vaginalis* was exposed to host ectocervical cells (Ects) for 1h, 2h and 6h and the amount of CLP mRNA was quantified by qRT-PCR. CLP mRNA levels relative to 30 min exposure time point are shown. CLP is up-regulated 5, 19, and 20-fold after contact with Ects for 1h, 2h and 6h, respectively. 1 representative experiment of 3 independent experiments is shown. Data shown are means of triplicates \pm standard deviations. *** = $p \leq 0.001$

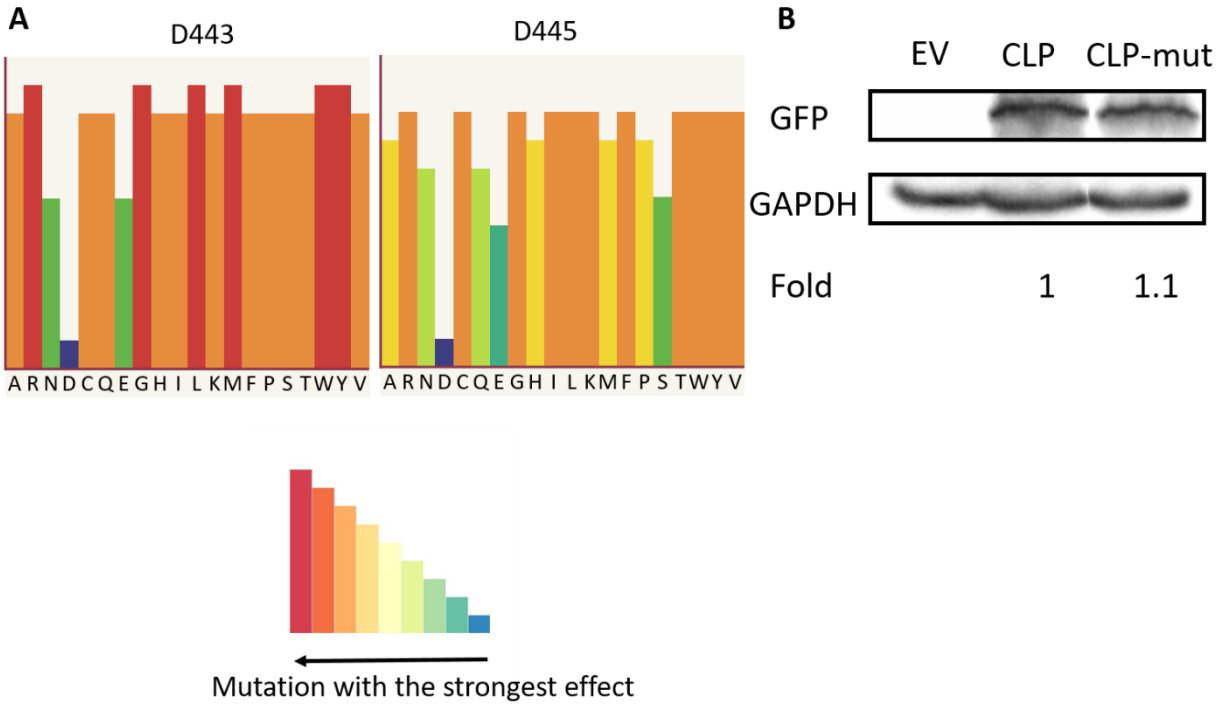


Figure 3-4 Generation of a CLP calcium-binding mutant. (A) Phyre2 and SusPect analyses identify the predicted calcium-binding site composed of D443 and D445 as the most sensitive to mutation (see Fig. S3-2 for analysis and comparison of other predicted calcium-binding sites in CLP). The height and color of the bars shown in the legend indicate the predicted functional impact of mutating the aspartate residue to the amino acids shown at the bottom of the histogram. Long and red bars in the histogram indicate that introduction of that particular amino acid would lead to the greatest phenotypic change while short blue bars have the smallest predicted phenotypic effect. (B) A CLP mutant that has D443 and D445 mutated to alanines (CLP-mut) was generated to investigate the functional effects of calcium-binding in CLP. Wild-type CLP and CLP-mut were exogenously expressed with an N-terminal GFP tag. As a negative control, parasites were transfected with an empty vector plasmid (EV). Immunoblot using an anti-GFP antibody confirmed that there are approximately equal amounts of CLP wild-type and CLP-mut overexpression. GAPDH is shown as a loading control. Fold represents the CLP expression levels between CLP and CLP-mut relative to CLP (=1).

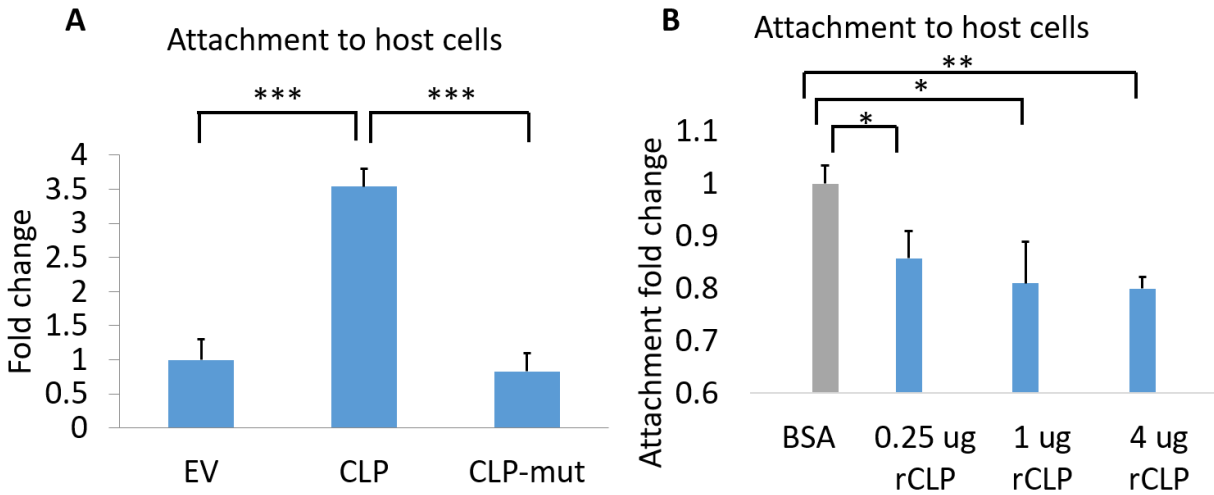
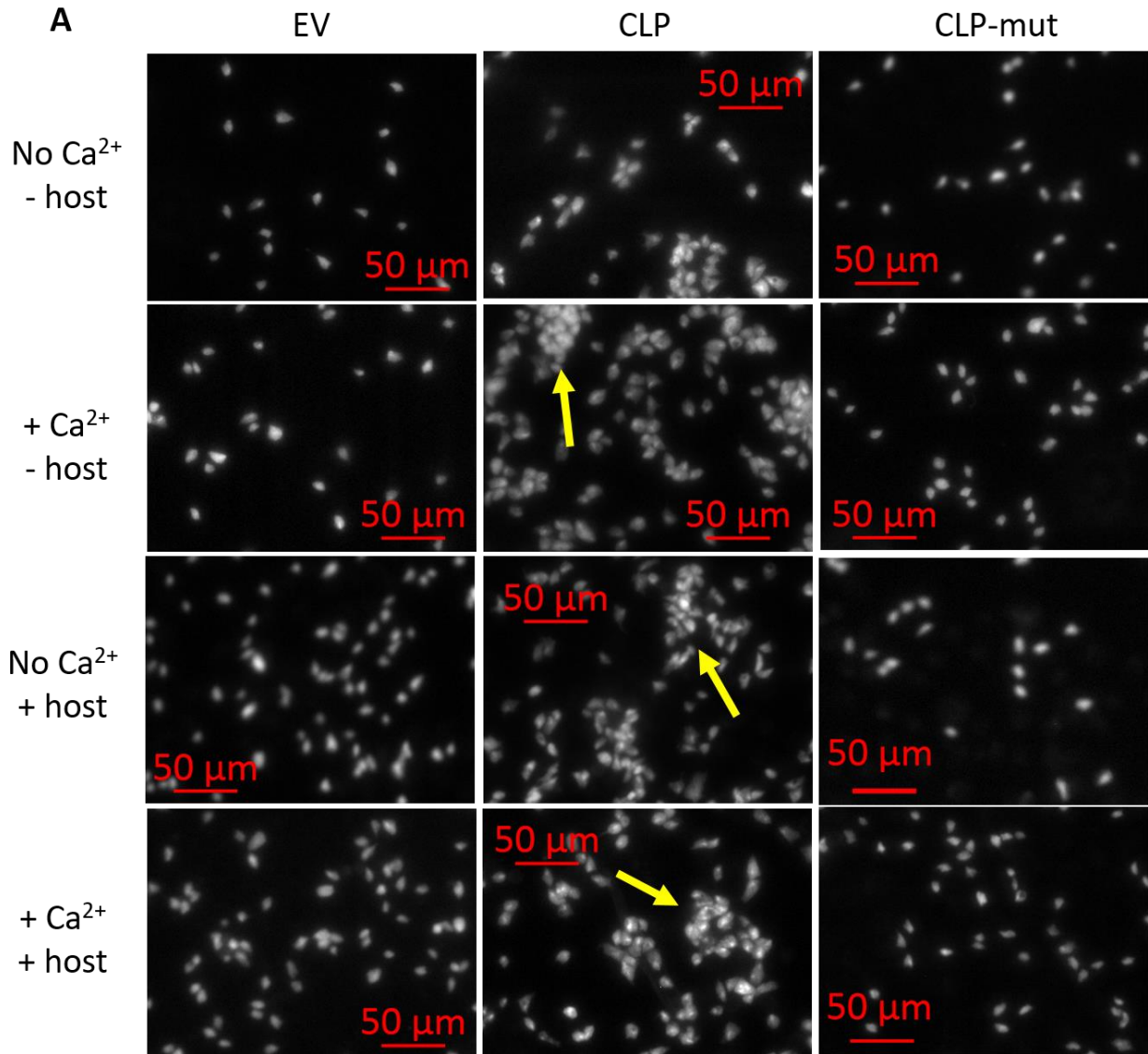


Figure 3-5 CLP contributes to *T. vaginalis* adherence to host cells Ects. (A) Empty vector (EV) and CLP or CLP-mut transfectants were fluorescently labeled and incubated with Ects for 30 min followed by quantification of adhered parasites. The average fold changes of CLP and CLP-mut relative to EV were 3.5- and 0.83-fold. (B) The ability of CLP's extracellular domain to compete with *T. vaginalis* binding to host cells was tested by the addition of 0.25 µg (7.7 nM), 1 µg (30.8 nM) or 4 µg (123.2 nM) of rCLP. Exogenous rCLP decreased host binding by 14%, 19% and 21% compared to bovine serum albumin (BSA)-treated control. Both data represent 3 independent experiments, each performed in triplicate. Error bars indicate \pm standard deviations. * = $p \leq 0.05$, ** = $p \leq 0.01$, *** $p \leq 0.001$



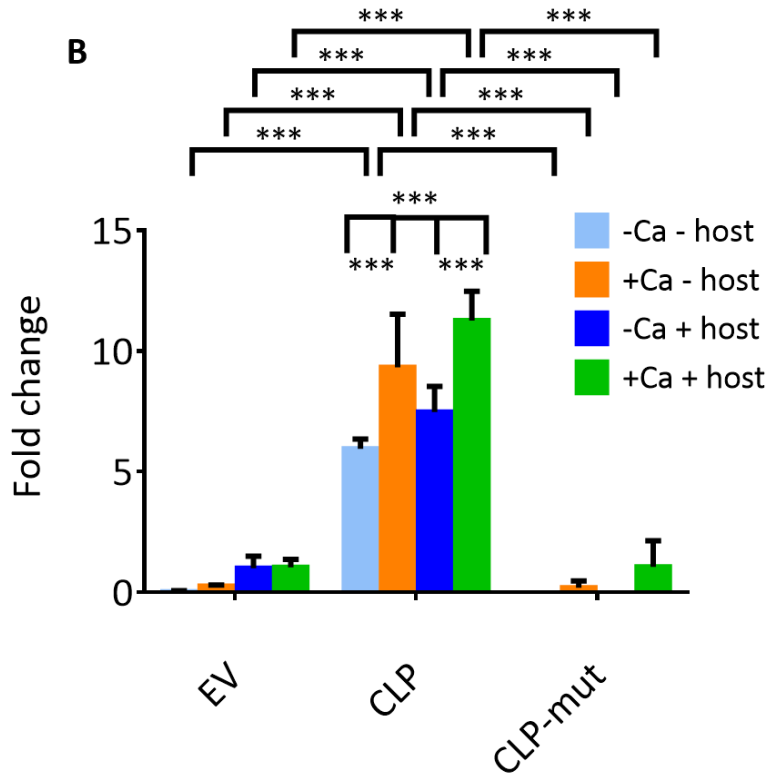


Figure 3-6 CLP increases parasite clumping and the CLP-mut reversed the enhanced clumping. (A) The clumping ability of the parasites was assessed by quantifying an aggregate of 10 or more parasites. The parasites were incubated in the absence or presence of the host and in the absence or presence of 1 mM CaCl₂. Images shown are with 100X magnification and each white dot is a single parasite. Yellow arrows denote clumps with 10 or more parasites. (B) Quantification of clumping behavior observed in (A). The fold changes shown are relative to the EV - Ca + host condition. The results represent 3 independent experiments, each performed in triplicate. Error bars indicate \pm standard deviations. *** = $p \leq 0.001$

Cytotoxicity of host cells

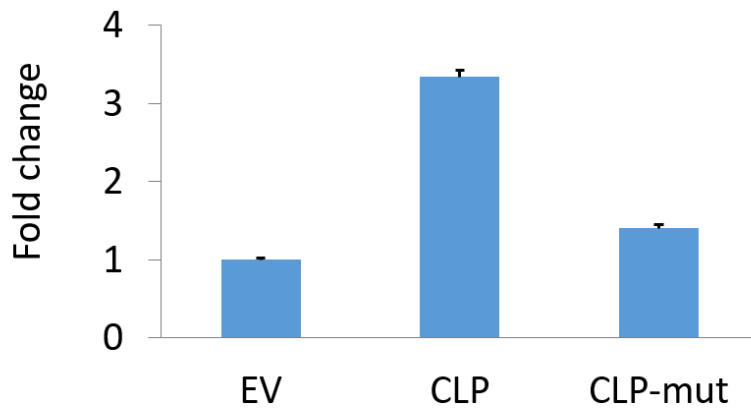
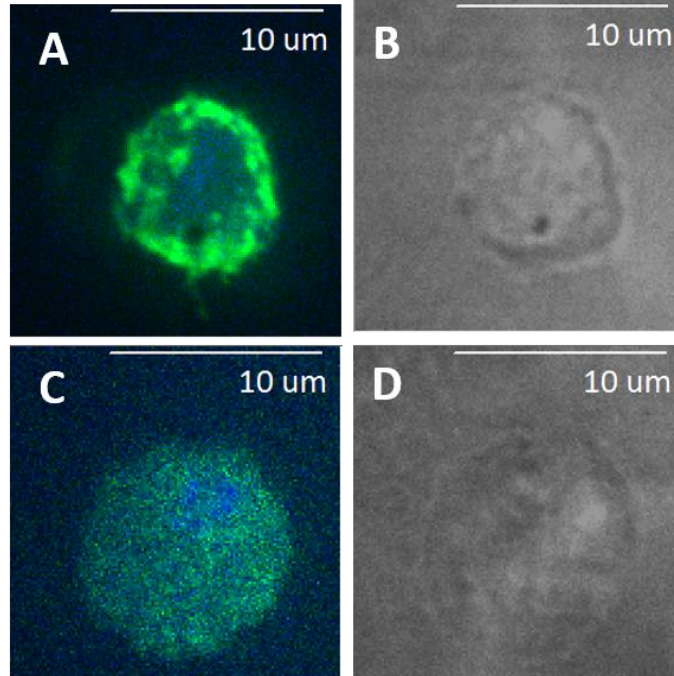


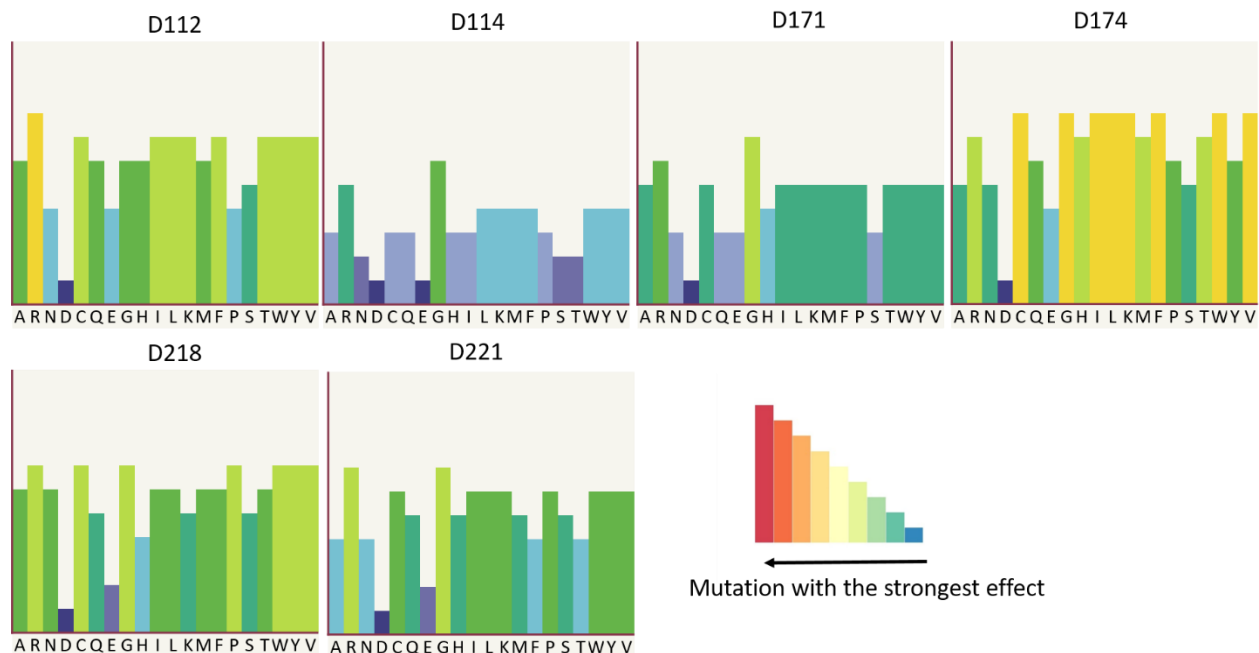
Figure 3-7 Death of Ects induced by *T. vaginalis* is increased by the wild-type CLP overexpression by 3.3-fold relative to the EV parasites and the CLP-mut parasites reduces the cytotoxicity level to 1.4-fold of the EV parasites. Data shown are means of triplicates \pm standard deviations and one representative set of 3 independent experiments. *** = $p \leq 0.001$

Permeabilized



Non-permeabilized

Supplemental Figure 3-1 To determine the topology of overexpressed CLP, indirect immunofluorescent assay in the presence or absence of a permeabilizing agent on C-terminally HA-tagged CLP was performed. (A) Bright green signal from anti-HA staining on permeabilized parasites versus faint green in non-permeabilized parasites (C) suggests that C-terminally tagged HA is on the intracellular side of the parasites. (B) and (D) are the brightfield images of (A) and (C), respectively. Green: HA. Blue: DAPI. These images are representative of ~30 parasites viewed under each condition.



Supplemental Figure 3-2 Mutational analysis of the rest of predicted Ca^{2+} -binding sites in CLP. Phyre2 and SuSPect analyses of the other 3 predicted Ca^{2+} -binding sites (from Fig. 3-1C). See Fig. 3-4A for the Ca^{2+} -binding sites which is the most sensitive to mutation. The height and color of the bars shown in the legend indicate the predicted functional impact of mutating the aspartate residue to the amino acids shown at the bottom of the histogram. Long and red bars in the histogram indicate that introduction of that particular amino acid would lead to the greatest phenotypic change while short blue bars have the smallest predicted phenotypic effect.

References

- [1] World Health Organization. (2012). Global incidence and prevalence of selected curable sexually transmitted infections-2008. *Who* 1–28 doi:10.1016/S0968-8080(12)40660-7.
- [2] Secor, W. E., Meites, E., Starr, M. C. & Workowski, K. a. (2014). Neglected parasitic infections in the United States: trichomoniasis. *Am. J. Trop. Med. Hyg.* (90) 800–804.
- [3] IOM (Institute of Medicine). (2011). *The Causes and Impacts of Neglected Tropical and Zoonotic Diseases : Opportunities for Integrated Intervention Strategies: Workshop Summary*. *Nature* doi:10.17226/13087.
- [4] Swygard, H., Seña, A. C., Hobbs, M. M. & Cohen, M. S. (2004). Trichomoniasis: Clinical manifestations, diagnosis and management. *Sexually Transmitted Infections* (80) 91–95.
- [5] Cotch, M. F. *et al.* (1997). Trichomonas vaginalis associated with low birth weight and preterm delivery. The vaginal infections and prematurity study group. *Sexually transmitted diseases* (24) 353–360.
- [6] Shafir, S. C., Sorvillo, F. J. & Smith, L. (2009). Current issues and considerations regarding Trichomoniasis and human immunodeficiency virus in African-Americans. *Clinical Microbiology Reviews* doi:10.1128/CMR.00002-08.
- [7] Mavedzenge, S. N. *et al.* (2010). Epidemiological synergy of trichomonas vaginalis and HIV in Zimbabwean and South African women. *Sex. Transm. Dis.* (37) 460–466.
- [8] Rendón-Maldonado, J. G., Espinosa-Cantellano, M., González-Robles, A. & Martínez-Palomo, A. (1998). Trichomonas vaginalis: In vitro phagocytosis of lactobacilli, vaginal epithelial cells, leukocytes, and erythrocytes. *Exp. Parasitol.* (89) 241–250.
- [9] Ryan, C. M., de Miguel, N. & Johnson, P. J. (2011). Trichomonas vaginalis : current understanding of host–parasite interactions. *Essays Biochem.* (51) 161–175.
- [10] Lustig, G., Ryan, C. M., Secor, W. E. & Johnson, P. J. (2013). Trichomonas vaginalis contact-dependent cytolysis of epithelial cells. *Infect. Immun.* (81) 1411–1419.
- [11] de Miguel, N. *et al.* (2010). Proteome analysis of the surface of Trichomonas vaginalis reveals novel proteins and strain-dependent differential expression. *Mol. Cell. Proteomics* (9) 1554–1566.
- [12] Riestra, A. (University of California, Los Angeles, 2015). Characterization of rhomboid proteases and surface proteins of Trichomonas vaginalis. PhD [Dissertation].
- [13] Kusdian, G., Woehle, C., Martin, W. F. & Gould, S. B. (2013). The actin-based machinery of Trichomonas vaginalis mediates flagellate-amoeboid transition and migration across host tissue. *Cell. Microbiol.* doi:10.1111/cmi.12144.
- [14] Vazquez-carrillo, L. I. *et al.* (2011). The effect of Zn 2 + on prostatic cell cytotoxicity caused by Trichomonas vaginalis. *J. Integr. OMICS* doi:10.5584/jiomics.v1i2.56.

- [15] Coceres, V. M. *et al.* (2015). The C-terminal tail of tetraspanin proteins regulates their intracellular distribution in the parasite *Trichomonas vaginalis*. *Cell. Microbiol.* (17) 1217–1229.
- [16] Miller, P. W., Clarke, D. N., Weis, W. I., Lowe, C. J. & Nelson, W. J. (2013). The evolutionary origin of epithelial cell-cell adhesion mechanisms. *Curr. Top. Membr.* doi:10.1016/B978-0-12-417027-8.00008-8.
- [17] King, N., Hittinger, C. T. & Carroll, S. B. (2003). Evolution of key cell signaling and adhesion protein families predates animal origins. *Science* (301) 361–363.
- [18] King, N. (2004). The unicellular ancestry of animal development. *Developmental Cell* doi:10.1016/j.devcel.2004.08.010.
- [19] Halbleib, J. M. & Nelson, W. J. (2006). Cadherins in development: Cell adhesion, sorting, and tissue morphogenesis. *Genes and Development* (20) 3199–3214.
- [20] Klezovitch, O. & Vasioukhin, V. (2015). Cadherin signaling: keeping cells in touch. *F1000Research* (4) 550.
- [21] Prakasam, A. K., Maruthamuthu, V. & Leckband, D. E. (2006). Similarities between heterophilic and homophilic cadherin adhesion. *Proc. Natl. Acad. Sci.* (103) 15434–15439.
- [22] Nagafuchi, A., Shirayoshi, Y., Okazaki, K., Yasuda, K. & Takeichi, M. (1987). Transformation of cell adhesion properties by exogenously introduced E-cadherin cDNA. *Nature* (329) 341–343.
- [23] Ringwald, M. *et al.* (1987). The structure of cell adhesion molecule uvomorulin. Insights into the molecular mechanism of Ca²⁺-dependent cell adhesion. *EMBO J* (6) 3647–3653.
- [24] Vestweber, D., Gossler, A., Boller, K. & Kemler, R. (1987). Expression and distribution of cell adhesion molecule uvomorulin in mouse preimplantation embryos. *Dev. Biol.* (124) 451–456.
- [25] Van Roy, F. & Berx, G. (2008). The cell-cell adhesion molecule E-cadherin. *Cellular and Molecular Life Sciences* (65) 3756–3788.
- [26] Finn, R. D. *et al.* (2017). InterPro in 2017-beyond protein family and domain annotations. *Nucleic Acids Res.* (45) D190–D199.
- [27] Finn, R. D. *et al.* (2014). Pfam: The protein families database. *Nucleic Acids Research* (42) D222–D230.
- [28] Kelly, L. A., Mezulis, S., Yates, C., Wass, M. & Sternberg, M. (2015). The Phyre2 web portal for protein modelling, prediction, and analysis. *Nat. Protoc.* (10) 845–858.
- [29] Nollet, F., Kools, P. & Van Roy, F. (2000). Phylogenetic analysis of the cadherin superfamily allows identification of six major subfamilies besides several solitary members. *Journal of Molecular Biology* doi:10.1006/jmbi.2000.3777.

- [30] Patel, S. D., Chen, C. P., Bahna, F., Honig, B. & Shapiro, L. (2003). Cadherin-mediated cell-cell adhesion: Sticking together as a family. *Current Opinion in Structural Biology* doi:10.1016/j.sbi.2003.10.007.
- [31] Shapiro, L. & Weis, W. I. (2009). Structure and biochemistry of cadherins and catenins. *Cold Spring Harbor perspectives in biology* (1) a003053.
- [32] Krogh, a, Larsson, B., von Heijne, G. & Sonnhammer, E. L. (2001). Predicting transmembrane protein topology with a hidden Markov model: application to complete genomes. *J. Mol. Biol.* (305) 567–580.
- [33] Dyall, S. D. *et al.* (2000). Presence of a member of the mitochondrial carrier family in hydrogenosomes: conservation of membrane-targeting pathways between hydrogenosomes and mitochondria. *Mol. Cell. Biol.* doi:10.1128/MCB.20.7.2488-2497.2000.
- [34] Delgadoillo, M. G., Liston, D. R., Niazi, K. & Johnson, P. J. (1997). Transient and selectable transformation of the parasitic protist *Trichomonas vaginalis*. *Proc. Natl. Acad. Sci.* (94) 4716–4720.
- [35] Gould, S. B. *et al.* (2013). Deep sequencing of *Trichomonas vaginalis* during the early infection of vaginal epithelial cells and amoeboid transition. *Int. J. Parasitol.* (43) 707–719.
- [36] de Miguel, N., Riestra, A. & Johnson, P. J. (2012). Reversible association of tetraspanin with *Trichomonas vaginalis* flagella upon adherence to host cells. *Cell. Microbiol.* (14) 1797–1807.
- [37] Nagar, B., Overduin, M., Ikura, M. & Rini, J. M. (1996). Structural basis of calcium-induced E-cadherin rigidification and dimerization. *Nature* (380) 360–364.
- [38] Boggon, T. J. *et al.* (2002). C-cadherin ectodomain structure and implications for cell adhesion mechanisms. *Science* (296) 1308–1313.
- [39] Yates, C. M., Filippis, I., Kelley, L. A. & Sternberg, M. J. E. (2014). SuSPect: Enhanced prediction of single amino acid variant (SAV) phenotype using network features. *J. Mol. Biol.* (426) 2692–2701.
- [40] Prakasam, A., Chien, Y. H., Maruthamuthu, V. & Leckband, D. E. (2006). Calcium site mutations in cadherin: Impact on adhesion and evidence of cooperativity. *Biochemistry* (45) 6930–6939.
- [41] Leckband, D. & Sivasankar, S. (2000). Mechanism of homophilic cadherin adhesion. *Current Opinion in Cell Biology* (12) 587–592.
- [42] Nose, A., Tsuji, K. & Takeichi, M. (1990). Localization of specificity determining sites in cadherin cell adhesion molecules. *Cell* (61) 147–155.
- [43] Mengaud, J., Ohayon, H., Gounon, P., Mege, R. M. & Cossart, P. (1996). E-cadherin is the receptor for internalin, a surface protein required for entry of *L. monocytogenes* into

- epithelial cells. *Cell* (84) 923–932.
- [44] Phan, Q. T. *et al.* (2007). Als3 is a *Candida albicans* invasin that binds to cadherins and induces endocytosis by host cells. *PLoS Biol.* (5) 0543–0557.
- [45] Anderton, J. M. *et al.* (2007). E-cadherin is a receptor for the common protein pneumococcal surface adhesin A (PsaA) of *Streptococcus pneumoniae*. *Microb. Pathog.* (42) 225–236.
- [46] Hemler, M. E. (2005). Tetraspanin functions and associated microdomains. *Nature Reviews Molecular Cell Biology* doi:10.1038/nrm1736.
- [47] Greco, C. *et al.* (2010). E-cadherin/p120-catenin and tetraspanin Co-029 cooperate for cell motility control in human colon carcinoma. *Cancer Res.* (70) 7674–7683.
- [48] Sotomayor, M., Gaudet, R. & Corey, D. P. (2014). Sorting out a promiscuous superfamily: Towards cadherin connectomics. *Trends in Cell Biology* doi:10.1016/j.tcb.2014.03.007.
- [49] Mercer, F., Ng, S. H., Brown, T. M., Boatman, G. & Johnson, P. J. (2018). Neutrophils kill the parasite *Trichomonas vaginalis* using trogocytosis. *PLoS Biol.* (16) e2003885.
- [50] Bastida-Corcuera, F. D., Okumura, C. Y., Colocoussi, A. & Johnson, P. J. (2005). *Trichomonas vaginalis* lipophosphoglycan mutants have reduced adherence and cytotoxicity to human ectocervical cells. *Eukaryot. Cell* (4) 1951–1958.
- [51] Casta e Silva Filho, F., de Souza, W. & Lopes, J. D. (1988). Presence of laminin-binding proteins in trichomonads and their role in adhesion. *Proc. Natl. Acad. Sci. U. S. A.* (85) 8042–8046.
- [52] Alderete, J. F., Nguyen, J., Mundodi, V. & Lecker, M. W. (2004). Heme-iron increases levels of AP65-mediated adherence by *Trichomonas vaginalis*. *Microb. Pathog.* (36) 263–271.
- [53] Mundodi, V., Kucknoor, A. S. & Alderete, J. F. (2007). Antisense RNA decreases AP33 gene expression and cytoadherence by *T. vaginalis*. *BMC Microbiol.* (7) 64.
- [54] Mundodi, V., Kucknoor, A. S., Klumpp, D. J., Chang, T. H. & Alderete, J. F. (2004). Silencing the ap65 gene reduces adherence to vaginal epithelial cells by *Trichomonas vaginalis*. *Mol. Microbiol.* (53) 1099–1108.
- [55] Mendoza-Lopez, M. R. *et al.* (2000). CP30, a cysteine proteinase involved in *Trichomonas vaginalis* cytoadherence. *Infect. Immun.* (68) 4907–4912.
- [56] Rendón-Gandarilla, F. J. *et al.* (2013). The TvLEGU-1, a legumain-like cysteine proteinase, plays a key role in *Trichomonas vaginalis* cytoadherence. *Biomed Res. Int.* (2013) 561979.
- [57] Twu, O. *et al.* (2013). *Trichomonas vaginalis* Exosomes Deliver Cargo to Host Cells and Mediate Host:Parasite Interactions. *PLoS Pathog.* (9) e1003482.
- [58] Hernández, H. *et al.* (2004). Monoclonal antibodies against a 62 kDa proteinase of


- Trichomonas vaginalis decrease parasite cytoadherence to epithelial cells and confer protection in mice. *Parasite Immunol.* (26) 119–125.
- [59] Blaskewicz, C. D., Pudney, J. & Anderson, D. J. (2011). Structure and Function of Intercellular Junctions in Human Cervical and Vaginal Mucosal Epithelia1. *Biol. Reprod.* doi:10.1095/biolreprod.110.090423.
- [60] Vazquez-Levin, M. H., Marín-Briggiler, C. I., Caballero, J. N. & Veiga, M. F. (2015). Epithelial and neural cadherin expression in the mammalian reproductive tract and gametes and their participation in fertilization-related events. *Dev. Biol.* doi:10.1016/j.ydbio.2014.12.029.
- [61] Benchimol, M., De Andrade Rosa, I., Da Silva Fontes, R. & Burla Dias, Â. J. (2008). Trichomonas adhere and phagocytose sperm cells: Adhesion seems to be a prominent stage during interaction. *Parasitol. Res.* (102) 597–604.
- [62] Handschuh, G., Lubber, B., Hutzler, P., Höfler, H. & Becker, K. F. (2001). Single amino acid substitutions in conserved extracellular domains of E-cadherin differ in their functional consequences. *J. Mol. Biol.* (314) 445–454.
- [63] Vestweber, D., Kemler, R. & Simons, K. (1985). Identification of a putative cell adhesion domain of uvomorulin. *EMBO J.* (4) 3393–3398.
- [64] Ozawa, M., Hoschützky, H., Herrenknecht, K. & Kemler, R. (1990). A possible new adhesive site in the cell-adhesion molecule uvomorulin. *Mech. Dev.* (33) 49–56.
- [65] Aurrecochea, C. *et al.* (2009). GiardiaDB and TrichDB: Integrated genomic resources for the eukaryotic protist pathogens Giardia lamblia and Trichomonas vaginalis. *Nucleic Acids Res.* doi:10.1093/nar/gkn631.
- [66] Johns, S. J. TOPO2, Transmembrane protein display software. www.sacs.ucsf.edu/TOPO2.
- [67] Clark, C. G. & Diamond, L. S. (2002). Methods for cultivation of luminal parasitic protists of clinical importance. *Clinical Microbiology Reviews* (15) 329–341.
- [68] Fichorova, R., Rheinwald, J. & Anderson, D. (1997). Generation of papillomavirus-immortalized cell lines from normal human ectocervical, endocervical, and vaginal epithelium that maintain expression of tissue-specific differentiation proteins. *Biol. Reprod.* (57) 847–855.
- [69] Miroux, B. & Walker, J. E. (1996). Over-production of proteins in Escherichia coli: Mutant hosts that allow synthesis of some membrane proteins and globular proteins at high levels. *J. Mol. Biol.* (260) 289–298.
- [70] Sockolosky, J. T. & Szoka, F. C. (2013). Periplasmic production via the pET expression system of soluble, bioactive human growth hormone. *Protein Expr. Purif.* (87) 129–135.
- [71] Nematollahi, L., Khalaj, V., Babazadeh, S. M. & Rahimpour, A. (2012). Periplasmic Expression of a Novel Human Bone Morphogenetic Protein-7 Mutant in Escherichia coli.

Avicenna J Med Biotech (4) 178–185.

Chapter 4:

CRISPR/Cas9-mediated gene modification and gene knock out in the human-infective
parasite *Trichomonas vaginalis*

CRISPR/Cas9-mediated gene modification and gene knock out in the human-infective parasite *Trichomonas vaginalis*

Brian D. Janssen¹, Yi-Pei Chen^{1,2}, Brenda M. Molgora^{1,2}, Shuqi E. Wang³ , Augusto Simoes-Barbosa³ & Patricia J. Johnson^{1,2}

The sexually-transmitted parasite *Trichomonas vaginalis* infects ~1/4 billion people worldwide. Despite its prevalence and myriad adverse outcomes of infection, the mechanisms underlying *T. vaginalis* pathogenesis are poorly understood. Genetic manipulation of this single-celled eukaryote has been hindered by challenges presented by its complex, repetitive genome and inefficient methods for introducing DNA (i.e. transfection) into the parasite. Here, we have developed methods to increase transfection efficiency using nucleofection, with the goal of efficiently introducing multiple DNA elements into a single *T. vaginalis* cell. We then created DNA constructs required to express several components essential to drive CRISPR/Cas9-mediated DNA modification: guide RNA (gRNA), the Cas9 endonuclease, short oligonucleotides and large, linearized DNA templates. Using these technical advances, we have established CRISPR/Cas9-mediated repair of mutations in genes contained on circular DNA plasmids harbored by the parasite. We also engineered CRISPR/Cas9 directed homologous recombination to delete (i.e. knock out) two non-essential genes within the *T. vaginalis* genome. This first report of the use of the CRISPR/Cas9 system in *T. vaginalis* greatly expands the ability to manipulate the genome of this pathogen and sets the stage for testing of the role of specific genes in many biological processes.

Trichomonas vaginalis is an obligate extracellular, unicellular flagellated protozoan parasite and the causative agent of trichomoniasis, an infection that afflicts ~1/4 billion people worldwide¹. Infection can be asymptomatic or result in a variety of negative outcomes in women and men including vaginitis, cervicitis, pelvic inflammatory disease, prostatitis and urethritis^{2,3}. Alarming, public health studies have reported an increased incidence of drug resistance to the drug used to treat infections, metronidazole⁴⁻⁷. Despite being a very common sexually transmitted infection, the basic mechanisms underlying pathogenesis and drug resistance are poorly understood. This is in part due to the slow adoption of molecular tools to study the genes and proteins involved in these processes^{8,9}. The development and application of cutting-edge gene technologies to manipulate this medically-important parasite are needed to further advance our knowledge of disease mechanisms.

Studies aimed to test the function of *T. vaginalis* genes have been limited by inefficient methods of genomic manipulation. Most reports have relied on isolates naturally lacking expression of particular genes¹⁰⁻²² or those directed by lab-acquired mutations²³⁻²⁷ that result in changes in gene expression. Only two studies have reported gene knockout of non-essential proteins by integrating a drug resistance selection cassette in the gene locus relying purely on homologous recombination^{28,29}. A few reports have also utilized knockdown-based strategies utilizing antisense RNA expression^{30,31} and modified oligonucleotides^{32,33}. Knockdown techniques do not result in elimination of gene expression, which is often required to effectively test gene function, limiting the usefulness of this technology.

Recent advances in *in vivo* gene modification techniques have increased the ability to test gene function in both model and non-model organisms. The CRISPR (clustered regularly interspaced short palindromic repeats) system has recently revolutionized the ability to specifically target genes for modification in many organisms³⁴⁻³⁷.

¹Department of Microbiology, Immunology & Molecular Genetics, University of California, Los Angeles, California, USA. ²Molecular Biology Institute, University of California, Los Angeles, California, USA. ³School of Biological Sciences, University of Auckland, Auckland, New Zealand. Correspondence and requests for materials should be addressed to P.J.J. (email: johnsonp@ucla.edu)

The CRISPR system is composed of two components, the Cas9 double stranded DNA nuclease of *Streptococcus pyogenes* and a user-customized version of its cofactor (guide RNA) to selectively target genes and induce double stranded DNA breaks. The double stranded breaks are repaired by non-homologous end joining (NHEJ), microhomology-mediated end joining (MMEJ) or homology-directed repair (HDR) pathways^{36,38}. In many organisms, Cas9-gRNA expression induces repair of the double stranded break by the NHEJ and MMEJ pathways, which can result in insertion (NHEJ) or deletions (NHEJ and MMEJ) of nucleotides that may cause gene disruption and loss-of-function mutations. A more directed approach utilizes Cas9-gRNA in combination with a provided DNA template containing homology to the repair site to direct specific user-defined gene modifications. This approach requires a small region of donor DNA homology around the site of modification. More recently, CRISPR-based techniques have been applied to modify genes in a variety of parasitic protozoa^{49–50} and have been proposed for multicellular parasites⁵¹.

Here we report the first application of CRISPR/Cas9 to alter genes in *T. vaginalis*. We demonstrate Cas9-gRNA directed modification of a nanoluciferase reporter gene using homology directed repair. Cas9-gRNA mediated knockout of two endogenous *T. vaginalis* genes by replacement with a drug resistance gene cassette were also achieved. This report lays the foundation for further development and utilization of this CRISPR/Cas9 to rigorously test gene function in this understudied parasite.

Results

Expression of Cas9 and gRNA in *Trichomonas vaginalis*. To date only two genes are reported^{28,29} to have been deleted (i.e. knocked out) from the haploid genome⁵² of the human parasite *T. vaginalis*. In order to improve the ability to modify *T. vaginalis* genes, we have developed the use of the CRISPR/Cas9 system as a means to directly modify genes in this parasite. One technical problem encountered when developing CRISPR/Cas9 in several systems is the toxicity associated with Cas9 expression *in vivo*⁴³. In initial experiments in which *cas9* was constitutively expressed using our standard *T. vaginalis* expression vector (pMasterNEO)⁵³ and selection with G418, we were unable to select viable parasites, consistent with possible Cas9 toxicity. To address whether Cas9 was toxic in *T. vaginalis* cells selected for stable expression, we cloned the *cas9* gene as a fusion protein with an N-terminal FKBP destabilization domain (FKBP-DD). The presence of this domain on a protein results in the degradation of the protein in the absence of the stabilizing ligand, Shield-1^{54,55}. We also added both a hemagglutinin (HA) tag and two SV40 C-terminal nuclear localization motifs⁵⁶ at the 3' end of Cas9, to allow detection of the protein by immunoblot and to direct it into the nucleus, respectively (pMN::kfbp-*cas9*; Fig. 1A). Using this construct, we were able to transfect and G418 select for parasites with the pMN::kfbp-Cas9 plasmid in the presence or absence of the stabilization ligand Shield-1. Regulating the expression of Cas9 using the FKBP-DD and Shield-1 greatly reduced, but did not eliminate, basal expression of the FKBP-Cas9 protein in the absence of Shield-1 (Fig. 1B). We found that a low concentration of Shield-1 (0.1 μ M) resulted in ~4-fold increased stabilization of the FKBP-Cas9 protein compared to cultures lacking Shield-1. A greater than 6.5-fold increase was observed using 1 μ M Shield-1 (Fig. 1B). Moreover, we noticed no growth difference in parasites containing the pMN::kfbp-*cas9* plasmid compared to parasites transfected with an empty vector (pMN::EV) when grown in the absence of Shield-1 (data not shown). Upon addition of Shield-1 parasite numbers were reduced in the pMN::kfbp-*cas9* transfectants compared to the pMN::EV parasites which did not exhibit growth rate reduction (data not shown), confirming the initial suspicion that Cas9 might exhibit toxicity in *T. vaginalis*.

We then made a construct that would allow the expression of gRNA(s) using the pMasterNEO plasmid backbone (Fig. 1C; see Methods for details). The gRNA construct (pMN::gRNA) contains the 360 bp sequence upstream of the U6 transcription start site (TSS), and is flanked at the 3' end by the original 37 bp downstream of the U6 transcription unit to ensure proper transcription termination⁵⁷. Between these 5' and 3' regulatory elements, we inserted the first 20 nt sequence of the U6 snRNA transcript (5'- AGCTGAGGATATGGCCTAGT)⁵⁷ followed by the conserved 76 bp scaffold sequence necessary for Cas9 targeting specificity and gRNA interaction, respectively (Fig. 1C). To evaluate whether transcription of this small RNA (a gRNA mimic) would be driven by the putative *T. vaginalis* U6 promoter, we performed RT-PCR on total RNA extracts from cells transfected with this construct (pMN::gRNA). Transcription was only detected from cells transfected with this construct (Fig. 1D) and was absent in negative control samples, transfected with an empty vector (pMN::EV). Next, sequential mutagenesis was done to replace the first 20 nt of *T. vaginalis* U6 snRNA, except for the first adenosine. None of the nt substitutions had an effect on transcription by end-point RT-PCR (data not shown). While the first transcribed nucleotide in the U6 transcript of metazoans and plants is typically a guanosine, *T. vaginalis* uses an adenosine⁵⁷. Since the first transcribed nucleotide is necessary for U6 transcription in other systems⁵⁸, but dispensable for the DNA target specificity of the Cas9 gRNA⁵⁹, we did not alter the +1 adenosine in our gRNA construct. The ability of the 360 nts upstream of the *T. vaginalis* U6 gene to drive transcription of an internally altered U6 gene indicates that the *T. vaginalis* U6 gene uses an upstream promoter as is found in metazoans and plants, and does not rely on internal promoter sequences as described for some unicellular eukaryotes (e.g. yeast and trypanosomes)^{60–62}. These data also demonstrate that the *T. vaginalis* U6 promoter can be used to drive transcription of a sequence-customizable gRNA. In metazoan and plants, the core promoter of the U6 snRNA gene sits within the first ~70 bp upstream of the TSS⁶⁰. In *T. vaginalis*, the core promoter of the U6 snRNA gene is unknown however we observed by end-point RT-PCR that there was no effect on transcription when the upstream region was reduced from 360 bp to 131 bp (data not shown). All additional gRNA plasmids produced contain the 360 nt sequence 5' of the U6 gene (Fig. 1C) preserving the +1 adenosine followed immediately by a 19 nt seed region that is customized to target the gene of interest.

Increasing transfection efficiency of *Trichomonas vaginalis*. Previous reports on transfection of *T. vaginalis* have used electroporation to deliver plasmids, linearized DNA or small oligonucleotides into the cell⁵³. Although sufficient to introduce DNA, transfection efficiency using this method is low. With the need

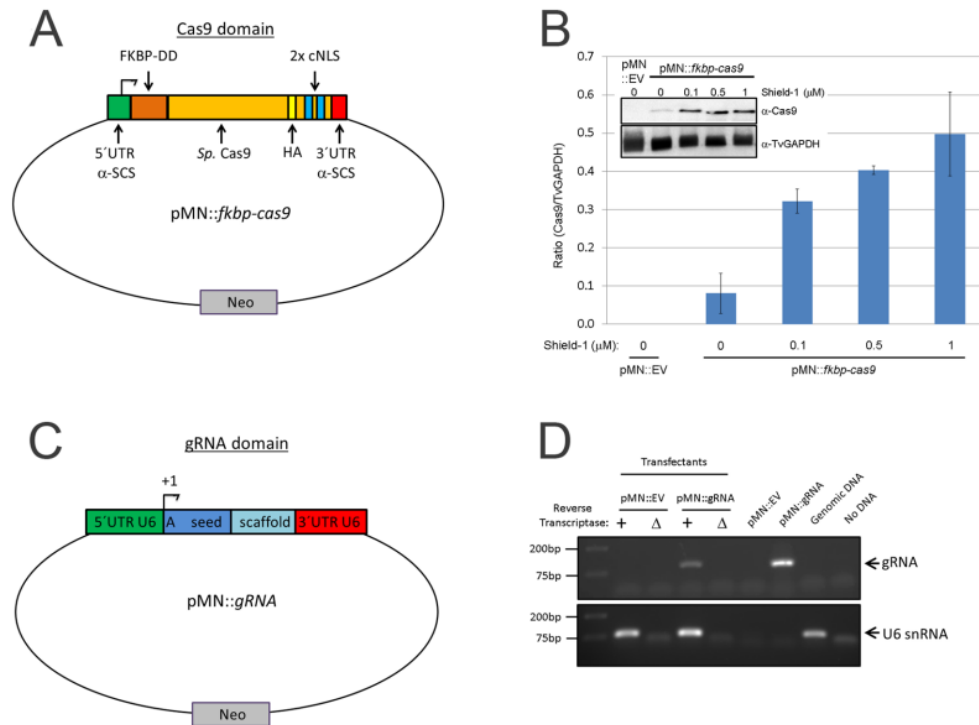


Figure 1. Setup of pMN::fkbp-cas9 and pMN::gRNA constructs. (A) Cartoon representation (not to scale) of pMN::fkbp-cas9 plasmid. The *T. vaginalis* gene α -SCS 5' and 3' UTRs of the pMasterNEO plasmid (pMN)⁵³ drive expression of the fkbp(FKBP destabilization domain)-cas9 fusion gene. The cas9 variant used is the human codon optimized version with 2 SV40 nuclear localization signals at the C-terminus⁵⁶. (B) Representative immunoblot analysis (inset) and quantification of replicate samples of pMN::fkbp-cas9 expression. Samples were induced for 24 hours with 0, 0.1, 0.5 or 1 μ M Shield-1 ligand before protein was collected and resolved by SDS-PAGE. Inset, upper: anti-Cas9 immunoblot (Clontech); Inset, lower: anti-TvGAPDH antibody (Cocalico Biologicals). Control sample used a pMN::EV (pMasterNEO::empty vector) transfectant. Quantitative comparison of samples utilized normalized signal of Cas9 (upper blot) to GAPDH signal (lower blot) taken from within an experiment and analyzed in parallel on separate immunoblots using a Bio-Rad Gel Doc and ImageLab software. Bar graph represents average \pm standard deviation of two independent analyses. (C) Cartoon representation (not to scale) of pMN::gRNA – 360 bp of the *T. vaginalis* U6 5' UTR and 37 bp of the 3' UTR flank the gRNA. A 20 nt seed region with the first nucleotide always an adenine residue followed by 19 nt seed region used for specific targeting and the gRNA scaffold. (D) RT-PCR products amplifying either the gRNA sequence or the U6 snRNA (control). Total RNA was subjected to \pm reverse transcriptase then amplified by PCR using gRNA- or U6 snRNA-specific primers. Control PCRs included the pMN::EV and pMN::gRNA plasmids, genomic DNA and no DNA template. PCR products were imaged using a Bio-Rad Gel Doc and ImageLab software. Full length blots/gels are presented in Supplementary Figure S5.

to introduce multiple DNAs into the same cell to achieve CRISPR/Cas9 editing, we sought to improve the transfection efficiency using the Amaxa nucleofection system^{39,63–65}. We first compared electroporation versus nucleofection using the nanoluciferase reporter system^{47,63}. Nanoluciferase (also termed NanoLuc) is a newly developed luciferase gene from a deep sea shrimp that produces stronger bioluminescence than the firefly luciferase (Promega). After normalization of parasite numbers, we subjected cells to either electroporation using our previously described protocol³³ or nucleofection to introduce the wild-type nanoluciferase gene with a duplicate hemagglutinin (HA) tag at the 3' end (pMN::nluc) (Fig. 2A). To optimize nucleofection, multiple programs and buffers were tested. Two of the programs tested (D-023 and X-001) and buffer (Parasite-2) resulted in detection of nanoluciferase signal compared to controls, however the signal was less than that obtained using standard electroporation (Supplemental Figure 1 and Fig. 2B). We found that one program (U-033) yielded better nanoluciferase signal, although parasite survival was low (<25% of untransfected controls at +24 hours post transfection, comparable to electroporation). Increased nanoluciferase signal was observed for two nucleofection buffers tested, T-cell and Parasite-1. As predicted, cells transfected with the pMN::nluc(stop) plasmid containing a premature stop codon that eliminates nanoluciferase protein production (Fig. 2A and B) produced only background signals. In comparison to the signal intensity achieved using nucleofection we found that nanoluciferase signals measured from parasites electroporated with pMN::nluc barely increased over background signal (Fig. 2B). This is consistent with the low frequency of transfection of parasites by electroporation, 3% at best for surviving

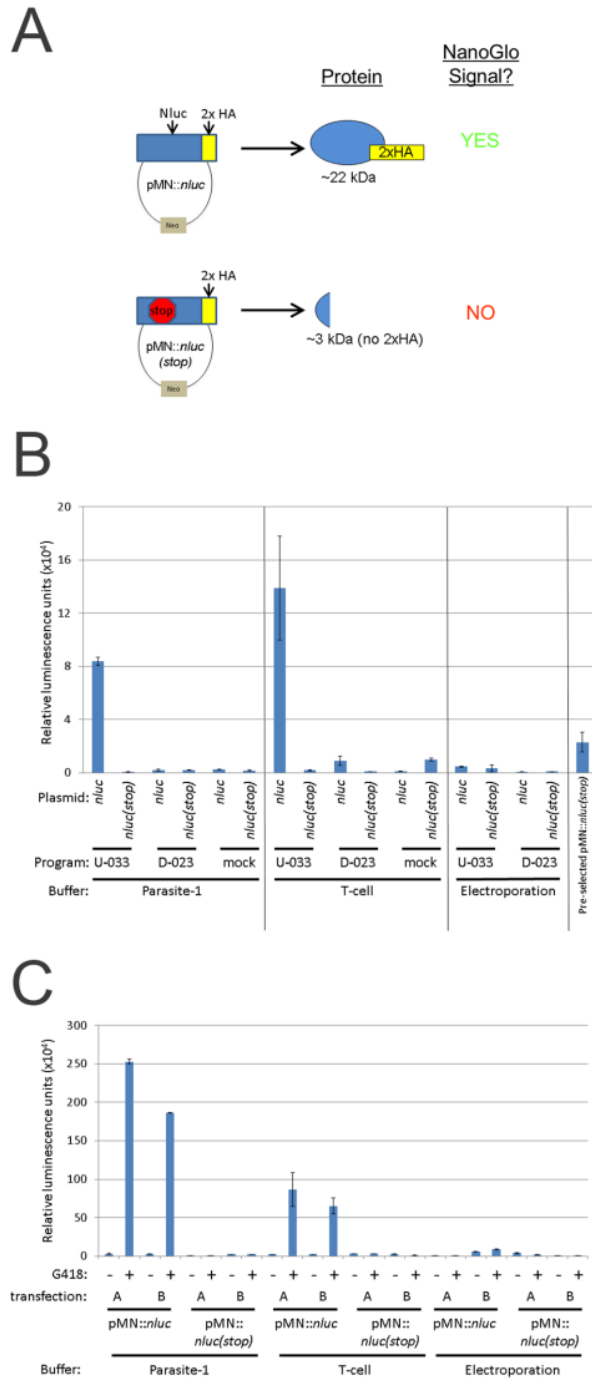


Figure 2. Parameters for transfection of *Trichomonas vaginalis* for detection of nanoluciferase activity. **(A)** Cartoon representation of nanoluciferase plasmids and predicted outcome for protein production. **(B)** A total of 1×10^7 parasites were either nucleofected using the U-033 (“U”) or D-023 (“D”) programs (Amaxa) or mock (no nucleofection) with $10 \mu\text{g}$ of pMN::nluc or pMN::nluc(stop) in buffers Parasite-1 or T-cell (Lonza) or electroporated ($975 \mu\text{F}$, 350V , Bio-Rad) in completed TYM media. Plasmids are pMN::nluc, denoted as “nluc” and pMN::nluc(stop), denoted as “nluc(stop)” where indicated. Parasites were immediately recovered in completed TYM media. After 24 hours, a total of 1×10^6 parasites were collected and nanoluciferase activity was measured by NanoGlo assay (Promega). Graph represents the average relative luminescence value \pm standard deviation of two transfections per condition. **(C)** Samples transfected with the pMN::nluc or pMN::nluc(stop) constructs and the U-033 program from Fig. 2B were subjected to G418-selection and allowed to grow for an additional +24 hours (+48 hours total, post-transfection). Equivalent numbers of parasites (1×10^6) were assayed for nanoluciferase activity and the graph represents the average relative luminescence value \pm standard deviation of two attempts per condition.

cells⁶⁶. Nucleofection with the U-033 program increased nanoluciferase signal 18-fold using Parasite-1 buffer and 30-fold using T-cell buffer, relative to signals detected using electroporation.

To determine if signal was stable and detectable at later time points, we passaged the parasites in the presence or absence of 100 $\mu\text{g/ml}$ G418 to select for the pMN::*nluc* and pMN::*nluc(stop)* plasmids (Fig. 2C). We noted that G418 selection for the pMN::*nluc* plasmid resulted in high levels of detectable nanoluciferase activity compared to transient nucleofection (Figures S2 and S3). The overall nanoluciferase signal for the unselected pMN::*nluc* parasites was reduced at +48 hours post-nucleofection compared to +24 hours. Selection for parasites harboring the pMN::*nluc* plasmids using G418 resulted in a dramatic increase with greater than 20 fold higher nanoluciferase signal compared to those transiently nucleofected (Fig. 2C). Electroporation did not yield the same increase (average ~1.2-fold) over the unselected counterparts (Fig. 2C and Fig. S3). Based on these data, we selected the U-033 program and the T-cell buffer as the optimal conditions to use for nucleofection of this strain of *T. vaginalis*. Together, these data demonstrate that nucleofection greatly improves transfection efficiency of *T. vaginalis*.

CRISPR repair of a dead-luciferase gene in *Trichomonas vaginalis*. To test the activity of Cas9, we used the highly-sensitive nanoluciferase repair assay originally described by Striepen and colleagues⁴⁷. To express the DD- Cas9 and gRNAs together in *T. vaginalis*, we first constructed a plasmid containing both elements as well as a puromycin acetyltransferase (PAC) gene, pCas9-gRNA(*nluc*) (Fig. 3A). As outlined in Fig. 2A, we then preselected parasites containing the plasmid that expresses a dead luciferase (i.e. pMN::*nluc(stop)*) using G418. We subsequently co-nucleofected preselected parasites with the pCas9-gRNA(*nluc*) plasmid expressing a gRNA targeting the premature stop codon (Y18ochre) region of the gene and pre-annealed oligos capable of both repairing the stop codon (“repaired”, ochre18Y) and introducing a mutation that eliminates the PAM (AGG- > AGC). Mutation of the PAM requires the correction of two sites by oligo template-directed repair, increasing the confidence that repair is Cas9-gRNA directed, and not due to random point mutation that changed a stop codon back to a tyrosine codon. Mutation also prevents further targeting of the repair site by Cas9-gRNA(*nluc*). Transient nucleofection was used, without drug selection for expression of the gRNA or Cas9. Using this approach, we were able to demonstrate that CRISPR/Cas9 is capable of repairing the mutation to allow detection of nanoluciferase signal above background levels in *T. vaginalis* (Fig. 3).

The nanoluciferase repair assays were done using different lengths of oligos (50 nt and 125 nt) and we found that although the 50 bp annealed oligos yielded similar or better efficiency of repair, more variability was also observed (Fig. 3B). We also tested the use of PCR products corresponding to the 125 bp annealed oligos and the full length *nluc* gene. These also repaired pMN::*nluc(stop)*, restoring nanoluciferase activity (Fig. 3C) however, the efficiency was not increased.

To further explore the ability to utilize CRISPR/Cas9 in *T. vaginalis*, we co-nucleofected parasites with pCas9-gRNA(*nluc*), pMN::*nluc(stop)* and either the 50 bp or 125 bp annealed repair oligos and selected for parasites containing both the pCas9-gRNA(*nluc*) (puromycin selection) and pMN::*nluc(stop)* (G418 selection) plasmids (Fig. 4A). Assaying for nanoluciferase signal 24 hours post-nucleofection, prior to drug selection, yielded a low overall signal compared to previous nucleofections (Fig. 4B). This is likely the result of requiring the same parasite to acquire all three DNAs to allow Cas9-directed repair. We also found that the 50 bp annealed oligo treatment did not work effectively, compared to previous experiments using parasites preselected to contain pMN::*nluc(stop)* target. Conversely, treatment with the 125 bp annealed oligos yielded a ~six-fold increase in nanoluciferase signal over background (water).

We then subjected the nucleofected parasites to selection with G418 and puromycin for either 7 or 14 days and tested for nanoluciferase activity. The amount of nanoluciferase signal observed was very high for parasites nucleofected with the 125 bp repair oligos (Fig. 4C). This signal did not increase between the 7 and 14 day measurements. To confirm expression of intact nanoluciferase protein at 14 days, total protein was extracted and analyzed by immunoblot analysis for the presence of repaired nanoluciferase-2xHA. We observed expression of the protein in parasites nucleofected with all three DNAs (pCas9-gRNA(*nluc*), pMN::*nluc(stop)*) and the 125 bp annealed repair oligos), but not in parasites where the pCas9-gRNA (*nluc*) was replaced with an empty vector (pMPAC::EV) (Fig. 4C, inset), consistent with the nanoluciferase activity assay. These data show that the repair of the dead luciferase was dependent on the presence of both essential components of the CRISPR/Cas9 system: the Cas9 and gRNA.

To confirm the repair of nanoluciferase by directly examining the DNA sequence of the luciferase gene, we cloned parasites from a selected population demonstrated to express the enzyme by activity and immunoblot assays, using limiting dilution. We then assayed 79 clones for nanoluciferase activity and observed that 91% (72 clones) gave signal above background, while 9% (7 clones) were below a cutoff of 30,000 relative luminescence units. The high percentage of clones expressing nanoluciferase indicates that the majority of parasites in the culture were expressing a repaired nanoluciferase gene. To support this observation, we collected total protein from 8 clones and performed immunoblot analysis (Fig. 4D, upper). Although varied in amount of observable signal, we were able to detect nanoluciferase signal in all 8 clones. We further PCR amplified and then sequenced the *nluc* gene from total gDNA extracts of 8 clones (Fig. 4D, lower). In all 8 clones, the codon 17 contained a mixed population of guanine (GGA, glycine) and cytosine (GCA, alanine) sequence. Additionally, without exception, codon 18 contained a mixed population of thymine (TAT, tyrosine) and adenine (TAA, ochre/stop). The presence of a mixed population of *nluc(stop)* (GGATAA or GCATAA) and *nluc(repaired)* (GGATAT or GCATAT) sequences in the examined clones is expected. Our previous study indicates that ~15–20 episomes are maintained per *T. vaginalis* cell⁵³, hence CRISPR/Cas9-mediated repair may not reach every single plasmid copy within a cell. In fact, repair of a single modified *nluc(stop)* gene would likely be sufficient to be detectable by DNA sequencing and to produce enough luciferase activity for detection using the sensitive NanoGlo assay (Figure S2). Together, the data presented clearly demonstrate that the expression of Cas9 & gRNAs in *T. vaginalis* can mediate gene repair via the CRISPR/Cas9 pathway.

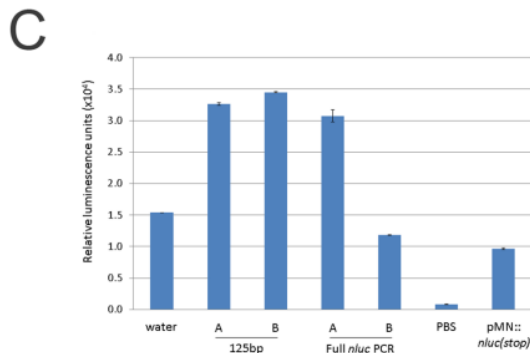
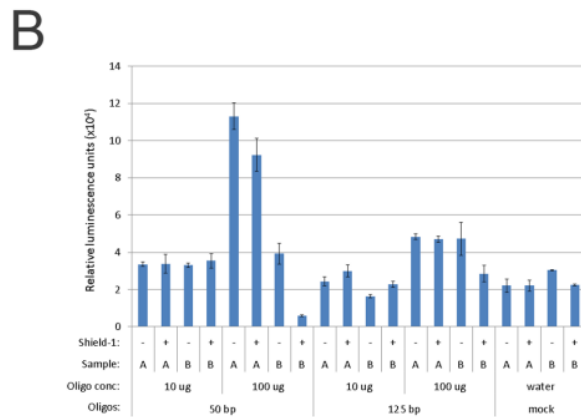
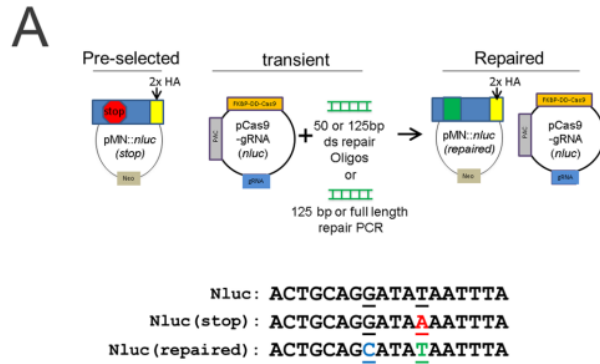


Figure 3. Nanoluciferase repair assay. (A) Upper: cartoon representation of nanoluciferase repair assay. Below: Cas9-gRNA(*nluc*) editing sites of *nluc(stop)* with mutation to create a premature stop codon (red, underlined). Also represented are the wild-type (*nluc*) and repaired (*nluc(repaired)*) versions. (B) A total of 5×10^7 parasites pre-selected for the pMN::*nluc(stop)* plasmid were nucleofected in T-cell buffer using the U-033 program (Amaya) with 10 μ g or 100 μ g of annealed repair oligos and 10 μ g of pCas9-gRNA(*nluc*). Oligos contained the repair sequence and either 50 bp or 125 bp annealed repair oligos. Parasites were immediately recovered in completed TYM media +/- 1 μ M Shield-1 and assayed for nanoluciferase activity after 24 hours. Equivalent numbers of parasites (1×10^6) were assayed for nanoluciferase activity and the graph represents the average relative luminescence value +/- standard deviation for each condition. (C) A total of 5×10^7 parasites pre-selected for pMN::*nluc(stop)* were nucleofected in T-cell buffer using the U-033 program (Amaya) with 10 μ g pCas9-gRNA(*nluc*) and either 100 μ g of PCR-amplified 125 bp repair sequence (equivalent to ds repair oligos) or the full length *nluc* ("Full *nluc* PCR") sequence. Parasites were immediately recovered in completed TYM media + 1 μ M Shield-1 and assayed for nanoluciferase activity after 24 hours. Equivalent numbers of parasites (1×10^6) were assayed for nanoluciferase activity and the graph represents the average relative luminescence value +/- standard deviation for each condition.

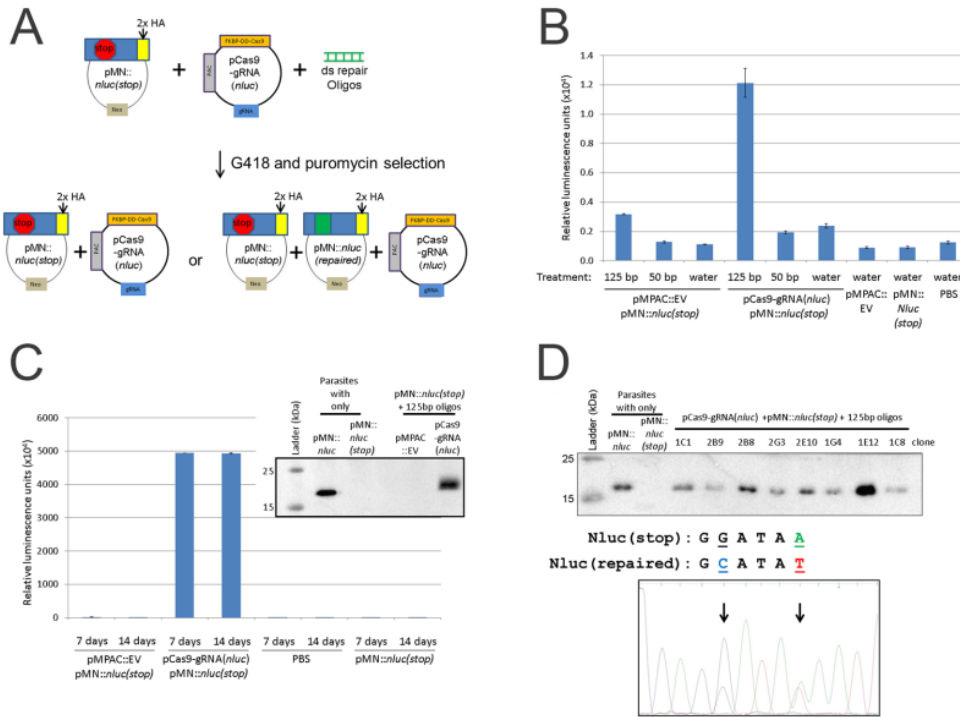


Figure 4. Transient transfection, selection and screening for nanoluciferase repair. (A) Cartoon representation of transient nanoluciferase repair activity followed by selection with puromycin and G418. (B) A total of 5×10^7 parasites were nucleofected with 10 μ g of pCas9-gRNA(*nluc*), 10 μ g pMN::*nluc(stop)* and 100 μ g of either 50 bp or 125 bp annealed repair oligos or water using T-cell buffer (Lonza) and the U-033 program (Amaza). Parasites were immediately recovered in completed TYM media + 1 μ M Shield-1. After 24 hours of recovery, equivalent numbers of parasites (1×10^6) were assayed for nanoluciferase activity and the graph represents the average relative luminescence value \pm standard deviation from duplicate samples for each condition (C). After 24 hours of recovery, one transfection population of the pMPAC::EV- and pCas9-gRNA(*nluc*)-treated parasites from Fig. 4B was treated with 30 μ g/ml puromycin and 50 μ g/ml G418 to select for parasites transfected with both plasmids. After 7 and 14 days (post-nucleofection), parasites were re-tested for nanoluciferase activity by assay of equivalent numbers of parasites (1×10^6). The graph represents the average relative luminescence value \pm standard deviation for each condition. Inset: Anti-HA epitope immunoblot analysis of control samples (pre-selected parasites) compared to protein isolated from puromycin/G418 selected parasites grown for two weeks. (D) Upper: anti-HA epitope immunoblot analysis of controls (pre-selected plasmids) and representative clones from 14 day puromycin/G418 selected pCas9-gRNA(*nluc*) + pMN::*nluc(stop)* + 125 bp oligo parasites in Fig. 4C. Lower: representative DNA sequencing trace (Genewiz sequencing and FinchTV sequence viewer) of PCR products amplifying the nanoluciferase gene from *T. vaginalis* genomic DNA preparations. Highlighted (and arrows) are residues G50C and A54T which are the site of the two predicted modifications for repair of the stop codon (A54T) and oligo-modification confirmatory mutation (G50C). Immunoblot analyses in Fig. 4C and D were imaged using a Bio-Rad Gel Doc and ImageLab software. Full length blots/gels are presented in Supplementary Figure S5.

CRISPR knockout of the Ferredoxin-1 and Mif genes from the *T. vaginalis* genome. To test whether the CRISPR/Cas9 system we have established is capable of knocking out a gene in the complex *T. vaginalis* genome, we first attempted to knockout the *ferredoxin-1* (Fd-1) gene previously shown to be non-essential to the parasite^{29,67}. A neomycin resistance (NeoR) gene flanked by \sim 1000 bp of the 5' and 3' UTRs of Fd-1 was constructed (Fig. 5A). Parasites were co-nucleofected with either the pMPAC::EV or the pCas9-gRNA(Fd) plasmid that expresses a gRNA targeting the 5' end of the gene and an \sim 2800 bp PCR product containing the NeoR genes flanked by Fd-1 gene 5' and 3' UTRs (Fig. 5A). After selection for parasites resistant to G418, parasites were screened for the presence of the NeoR gene in the Fd-1 locus, using PCR and primers that sit just outside the Fd-1 UTRs included in the \sim 2800 bp PCR product. Positive amplicons of expected size were observed in the pCas9-gRNA(Fd) nucleofected parasites, while the pMPAC::EV parasites did not grow as expected. We then obtained cloned parasites from a NeoR positive population using limited-dilution cloning. Two clones (2-2 G4 " Δ Fd-1 clone 1" and 2-1 D9 " Δ Fd-1 clone 2") were randomly selected and tested for the presence of the NeoR gene as well as the wild-type Fd-1 gene (Fig. 5B). Confirmation of the sequence of all PCR products clearly demonstrates that both clones contain the NeoR gene in the Fd-1 locus and to also lack the endogenous Fd-1 gene (Fig. 5B). Immunoblot analysis using an antibody that detects Fd-1⁶⁷ also confirmed the loss of Fd-1 protein in both clones (Fig. 5C).

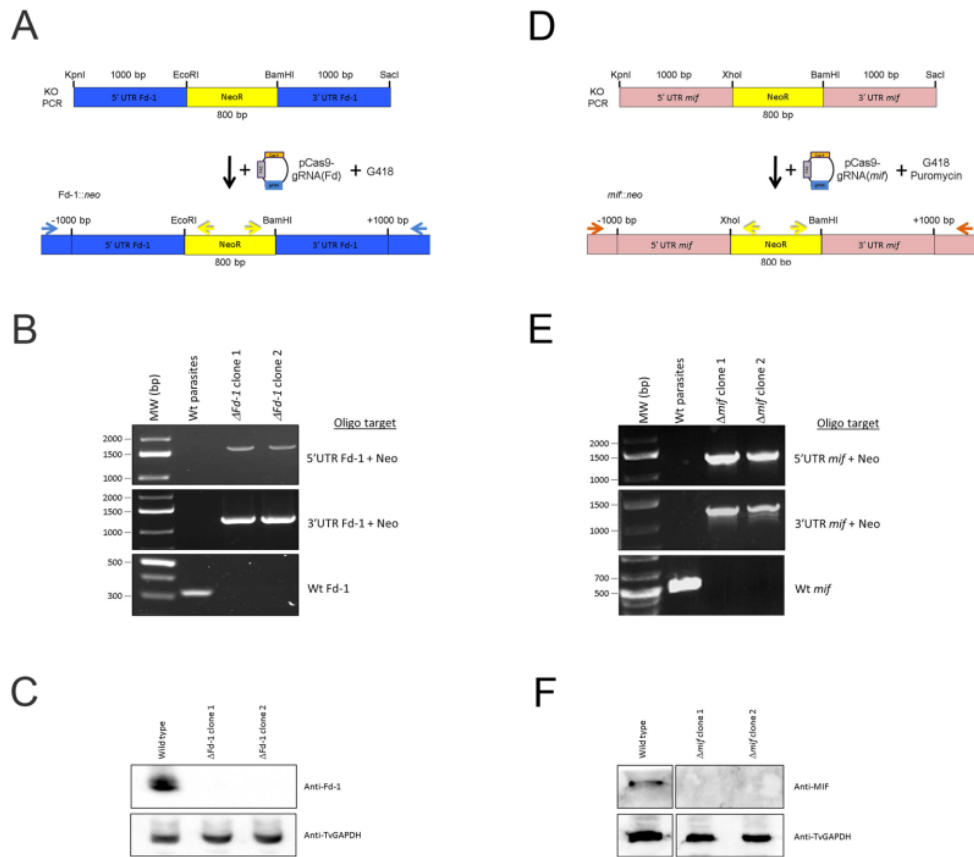


Figure 5. CRISPR-directed KO of ferredoxin-1 and *mif*. **(A)** Cartoon representation of the KO scheme using nucleofection of parasites with a linearized neo resistance gene flanked by the ferredoxin-1 UTRs and a plasmid containing Cas9 and Fd gRNA (pCas9-gRNA(*Fd*)) followed by selection for G418-resistance (image not to scale). The resulting parasites were then screened for the presence of the KO and wt alleles using sequence-specific primers (horizontal arrows). **(B)** PCR analysis of G418-resistant clones for the presence of the neo resistance gene in the ferredoxin-1 locus. PCR screens utilized primers specific to the neo resistance gene (yellow arrows in 5A) combined with primers specific to the ferredoxin-1 locus (blue arrows in 5A) in regions outside the region present in the original KO PCR introduced by nucleofection. The 5' end PCR screen (upper panel) predicts a product of 1665 bp and the 3' PCR screen (middle panel) predicts a product of 1236 bp if the neo gene is present in the ferredoxin-1 locus. Lowest panel: PCR analysis of the ferredoxin-1 gene in clones. Amplification utilized primers specific to the wild-type ferredoxin-1 (yielding a 324 bp product, if present). The PCR products for the different panels were run in parallel from reactions on 100 ng of the indicated genomic DNA extracts and resolved on separate agarose gels then imaged using a Bio-Rad Gel Doc and ImageLab software. **(C)** Immunoblot protein analysis of the clones yielding positive PCR products for KO in Fig. 5B. Total protein extracts were resolved by SDS-PAGE and immunoblotted using anti-Ferredoxin-1 and TvGAPDH antibodies. All immunoblots contained equal amounts of the same experimental samples and were analyzed in parallel using a Bio-Rad Gel Doc and ImageLab software. **(D)** Cartoon representation of the KO scheme using nucleofection of parasites with a linearized neo resistance (NeoR) gene flanked by the *mif* UTRs and a plasmid containing Cas9 and *mif* gRNAs (pCas9-gRNA(*mif*)), followed by selection for G418- and puromycin-resistance (image not to scale). The resulting parasites were then screened for the presence of the KO and wt alleles using sequence-specific primers (horizontal arrows). **(E)** PCR analysis of G418 and puromycin-resistant clones for the presence of the neo resistance gene in the *mif* locus. PCR screens utilized primers specific to the neo resistance gene (yellow arrows in 5D) combined with primers specific to the *mif* locus (orange arrows in 5D) in regions outside the region present in the original KO PCR introduced by nucleofection. The 5' end PCR screen (upper panel) predicts a product of 1290 bp and the 3' PCR screen (middle panel) predicts a product of 1220 bp if the neo gene is present in the *mif* locus. Lowest panel: PCR analysis of the *mif* gene in clones. Amplification utilized primers specific to the wild-type *mif* gene (yielding a 500 bp product, if present). The PCR products for the different panels were run in parallel from reactions on 100 ng of the indicated genomic DNA extracts and resolved on separate agarose gels then imaged using a Bio-Rad Gel Doc and ImageLab software. **(F)** Immunoblot protein analysis of the clones yielding positive PCR products for KO in Fig. 5E. Total protein extracts were resolved by SDS-PAGE and immunoblotted using anti-MIF and TvGAPDH antibodies. All immunoblots contained equal amounts of the same experimental samples and were analyzed in parallel using a Bio-Rad Gel Doc and ImageLab software. Full length blots/gels are presented in Supplementary Figure S5.

To further test the CRISPR/Cas9 system, we attempted to knockout the single copy *mif* gene, which codes for a homologue of the human macrophage migration inhibitory factor (MIF) and was recently reported to affect host cell physiology⁶⁸. A neomycin resistance (NeoR) gene flanked by ~1000 bp of the 5' and 3' UTRs of *mif* was constructed (Fig. 5D). To illustrate the ability to use CRISPR/Cas9 in multiple *T. vaginalis* strains, the B7RC2 strain²² was used. Parasites were co-nucleofected with the pCas9-gRNA(*mif*) plasmid expressing a gRNA targeting the 5' end of the gene and an ~2800 bp PCR product containing the NeoR gene flanked by *mif* gene 5' and 3' UTRs (Fig. 5D). After selection for parasites resistant to G418 and puromycin, parasites were screened for the presence of the NeoR gene in the *mif* locus, using PCR and primers that sit just outside the *mif* UTRs included in the ~2800 bp PCR product. Positive amplicons of expected size were observed in the pCas9-gRNA(*mif*) nucleofected parasites (Fig. 5E). Control reactions wherein parasites were nucleofected with only the linear KO PCR product survived G418 selection, however no positive PCR signal was observed for the NeoR gene in the *mif* locus (Supplementary Figure S4). We further examined these control parasites lacking the pCas9-gRNA(*mif*) plasmid by screening 800 cells, split into 40 subpopulations of 20 parasites each to directly test whether the NeoR gene was in the *mif* locus. No PCR product was detected in any of the 40 subpopulations (Supplementary Figure S4). This is in contrast with obtaining positive PCR signal for NeoR integration at the *mif* locus in 39/40 subpopulations of the parasites nucleofected with both the pCas9-gRNA(*mif*) plasmid and the linear KO PCR product. To confirm that the *mif* gene was knocked out in these NeoR PCR positive populations, parasites were cloned using limited-dilution cloning. Two clones ("Δ*mif* clone 1" and "Δ*mif* clone 2") were randomly selected and tested for the presence of the NeoR gene in the *mif* locus and the absence of the wild-type *mif* gene (Fig. 5E). Confirmation of the sequence of all PCR products clearly demonstrated that both clones contain the NeoR gene in the *mif* locus and also lack the endogenous *mif* gene (Fig. 5E). Immunoblot analysis using an antibody that detects MIF likewise confirmed the loss of the MIF protein in both clones (Fig. 5F). Together, our findings demonstrate that CRISPR/Cas9 can be used to disrupt gene sequences in the *T. vaginalis* genome by a homology-directed repair pathway.

Discussion

Here we describe the development of a system to achieve CRISPR/Cas9 gene modification and gene knockout in *Trichomonas vaginalis*. Three technical advances made this possible. One was to decrease the toxicity of Cas9 when expressed in *T. vaginalis* by using FKBP-DD/Shield-1 regulated expression of the endonuclease. The second was to increase transfection efficiency using nucleofection. These together, with the use of a sensitive nanoluciferase reporter assay to detect homology directed repair of a premature stop codon back to wild-type firstly described by Streipen and colleagues^{47,69}, provided a sensitive assay to facilitate identifying optimal nucleofection parameters. Finally, we were able to utilize the strong RNA polymerase III *T. vaginalis* U6 promoter to drive transcription of a sequence-customizable gRNA. This, the first report of CRISPR/Cas9 gene modification in *T. vaginalis*, will greatly enhance the ability to test gene function in this pathogen.

It has been previously reported that expression of Cas9 in various organisms leads to cell growth issues⁴³. We found that initial attempts at plasmid-based Cas9 expression by transfection and selection of *T. vaginalis* repeatedly failed. Different reports have addressed decreased cell growth by transient transfection of *cas9*-gRNA from plasmids or transfecting with Cas9 mRNA or holoenzymes⁷⁰⁻⁷². We chose to regulate Cas9 expression at the protein through fusion to the FKBP-destabilization domain (FKBP-DD), which by default sends proteins for proteolytic degradation. In the presence of a stabilizing ligand Shield-1, the protein accumulates^{54,55}. We found that this method allowed the regulation of cellular Cas9 levels in *T. vaginalis*, which in turn yielded viable parasites expressing sufficient, but not toxic, levels of Cas9.

Testing the biological role of genes in *T. vaginalis* has previously been severely compromised by limited technologies to alter the highly, repetitive genome of this parasite⁵². Only two previous reports have successfully knocked out *T. vaginalis* genes^{28,29} and knockdown of gene expression is limited to four reports³⁰⁻³³. Lacking the ability to knockout gene expression, researchers have primarily relied on episomal over-expression of gene variants to study protein function.

One reason that homologous gene replacement has been hampered in *T. vaginalis* is the poor transfection efficiency achieved with standard electroporation. Here, using nucleofection^{64,73}, we have greatly enhanced the transfection efficiency by 20-fold or greater as compared to that achieved using electroporation method. This enhancement of transfection efficiency has enhanced both the probability of successful modification of genes and the ability to detect the modifications by sensitive techniques such as nanoluciferase activity assays or PCR. Thus, developing successful nucleofection methods allowing sensitive screening and selection for gene modifications was key to our ability to achieve and monitor CRISPR/Cas9 modification of *T. vaginalis* genes.

Our analyses of the *T. vaginalis* genome for homologs of NHEJ pathway components indicated that this pathway is absent or highly divergent from other organisms. Based on this observation, we focused on homology-directed repair pathways to establish the use of CRISPR/Cas9 in this parasite. We were able to detect CRISPR activity using the sensitive technique of early termination mutation repair first used to demonstrate CRISPR in *Cryptosporidium parvum*⁴⁷. Using a 125 bp repair template of annealed oligonucleotides with flanks on both sides of the CRISPR cut site, we were able to repair an early termination codon restoring nanoluciferase activity as demonstrated by enzyme activity assays, immunoblot analysis and DNA sequencing. The repair template makes two specific point mutations both changing the stop codon to a tyrosine and a proximal glycine to alanine. The nanoluciferase repair assay demonstrates that small oligonucleotides are sufficient to modify multi-target episomally maintained genes and thus the length of a homology template may not have to be large. Repair is due to homology-directed repair (HDR) using the oligonucleotide template, as opposed to NHEJ activity. Notably, in the absence of the HDR template, we did not observe signal of repaired nanoluciferase above background signal, consistent with the lack of NHEJ-mediated repair.

Nucleofection of pre-selected pMN::*nluc(stop)* parasites with pCas9-gRNA(*nluc*) and repair oligos resulted in an increase of nanoluciferase activity. This varied based on concentration of oligos with 100 µg working more effectively than 10 µg. Transient co-nucleofection of all DNA components (pMN::*nluc(stop)*, pCas9-gRNA(*nluc*) and repair oligos) resulted in lower nanoluciferase signals, however, this could be overcome using drug selection to enrich for parasite populations containing DNAs required for CRISPR/Cas9-mediated repair. Using drug selection and cell cloning by limited dilution, we found that 91% of the clones had nanoluciferase activity above background. DNA sequencing of the clones confirmed the modification of the *nluc(stop)* to *nluc(repaired)*, demonstrating CRISPR-Cas9 mediated repair of the *nluc(stop)* gene.

We have also demonstrated the ability to use CRISPR-Cas9 mediated homology-repair to eliminate two genes (*ferredoxin-1* and *mif*) from the genome of *T. vaginalis*. CRISPR-mediated gene knock-out was achieved in two different *T. vaginalis* strains. The methods we have developed to increase transfection efficiency for both plasmids and KO cassettes and to direct CRISPR/Cas9 gene modification will greatly increase the success rate of gene knockouts in this parasite. The expanded toolkit for molecular modification of the *T. vaginalis* genome will significantly enhance the ability to assess gene function in this medically-important pathogen.

Methods

Parasite culture. Parasites (*T. vaginalis* strain B7RC2²² and MSA 1103⁷⁴) were maintained by daily passage in modified TYM media⁷⁵ supplemented with 10% heat-inactivated horse serum (Sigma), 10 U/ml penicillin/10 µg/ml streptomycin (Invitrogen), 180 µM ferrous ammonium sulfate and 28 µM sulfosalicylic acid (completed TYM media). To select for the pMasterPAC (pMPAC)^{53,76} or pMasterNEO (pMN)²² plasmids, puromycin (AG scientific) or G418 (Invitrogen) was added to cultures to a final concentration of 30 µg/ml and 100 µg/ml, respectively.

Plasmid constructs. Plasmid pMN::*cas9* was created by PCR amplification of the human codon optimized *cas9* gene of plasmid pMJ920⁵⁶ using primers For-hcas9-SacII and Rev-hcas9-Bam. All oligos used in this study are listed in Supplemental Table 1. The resulting hcas9 product was digested with SacII/BamHI and ligated to pMN::*fkbp*. The resulting construct was then PCR amplified using primers For-dS-HuCas9 and Rev-MN3UTR to silently mutate an internal SacI sequence. This product was then used in megaprimer PCR with primer For-MN-SacXho and subsequently digested with SacI/BamHI and ligated into pMN::*fkbp* to produce pMN::*fkbp-cas9*. To create the pMPAC::*fkbp-cas9* construct, pMN::*fkbp-cas9* was digested with SacI/BamHI and the product cloned into the pMPAC-empty vector plasmid (pMPAC::EV). The gRNA cassette was constructed by PCR amplification of a synthetic gene construct (Table S1) containing the U6 seed region and gRNA scaffold flanked upstream by the 360 bp 5' of the U6 start nucleotide and downstream with 37 bp of the 3' UTR of the U6 gene using primer U6_SacI_F1 and downstream 3' UTR with primer U6_SacI_R1. The resulting product was then digested with SacI and ligated to the unique SacI site in pMasterNEO⁵³. The *nluc* gRNA was constructed by megaprimer amplification of the gRNA scaffold using primers For-Nluc-gRNA and U6_SacI_R1 and then used in a megaprimer PCR with U6_SacI_F1. The resulting PCR product was digested with SacI and ligated to pMPAC::*fkbp-cas9*. The final construct was termed to pMPAC::*fkbp-cas9-gRNA(nluc)*, abbreviated as pCas9-gRNA(*nluc*).

Construction of nanoluciferase plasmids utilized codon-optimized plasmid templates of *nluc* (wt) and *nluc* (Y18ochre, "dead"/stop) from the Nluc-Neo and Dead Nluc-Neo plasmids (a generous gift from the Boris Striepen laboratory, University of Georgia)⁴⁷, respectively. For each *nluc* variant, a megaprimer PCR was performed utilizing primers For-MN-SacXho and Rev-Nluc-Nde to amplify the 5' UTR of a-SCS on pMasterNEO with a portion of the 5' end of the *nluc* gene. The resulting products were gel-purified and used with primer Rev-Nluc-Kpn to amplify the remainder of *nluc* and *nluc(stop)*. The PCR products were then digested with SacI/KpnI and ligated to pMasterNEO such that the *nluc* (or repaired) sequence would be fused to a 2xHA epitope tag when translated. These plasmids were termed pMN::*nluc* and pMN::*nluc(stop)*.

For construction of the pCas9-gRNA construct targeting the *ferredoxin-1* gene (TVAG_003900), the 20 nt seed region of pMPAC::*fkbp-cas9-gRNA(nluc)* was replaced after the adenosine residue start with 19 nucleotides of the *ferredoxin-1* gene (residues 5–23, 5' - TCT CTC AAG TTT GCC GCT T) which lie 5' upstream of a TGG PAM sequence. This was constructed by PCR amplification with primers For-gRNA-Fer-1 and U6_SacI_R1. The resulting PCR product was purified and used in a second PCR with primer U6_SacI_F1, followed by digestion with SacI and cloning into pMPAC::*fkbp-cas9-gRNA(nluc)*. The resulting plasmid was termed pCas9-gRNA(*Fd*). For construction of the pCas9-gRNA construct targeting the *mif* gene (TVAG_219770), a dual gRNA was constructed. For each of the gRNAs the 20 nt seed region of pMPAC::*fkbp-cas9-gRNA(nluc)* was replaced after the adenosine residue start with 19 nucleotides of the *mif* gene. The *mif* sequences "g300" (5' - CAA AGA GTG CTG AGG ACT G) and "g301" (5' -CCA AAG AGTGCT GAG GAC T) were used to construct 19 nucleotides after the A in the seed region. Briefly, "g300" gRNA was constructed using PCR primers For-gRNA-g300 + U6-KpnI-R. The resulting product was purified and used in a second PCR with primer U6_SacI_F1. For "g301" gRNA was constructed using PCR primers For-gRNA-g301 + U6_SacI_R1. The resulting product was purified and used in a second PCR with primer U6-KpnI-F. Both PCR products were digested with KpnI, ligated together and gel purified. The resulting ligated product was then digested with SacI and ligated into pMPAC::*fkbp-cas9-gRNA(nluc)* producing the plasmid pMPAC::*fkbp-cas9-gRNA(mif)*.

Construction of the ferredoxin KO cassette utilized 1000 bp upstream of the *ferredoxin-1* start codon and 1000 bp downstream of the stop codon. Briefly, the *neo* resistance gene was PCR amplified using primer For-Neo-Eco and Rev-Neo-Bam. The resulting product was cloned into pSC-A (Stratagene) to produce the plasmid pSC-A::*neo*. PCR amplification of the 5' UTR of ferredoxin utilized For-Fer-Kpn and Rev-Fer-Eco. The product was then digested with KpnI and EcoRI and cloned into the pSC-A::*neo* plasmid resulting in plasmid pSC-A::*5'UTR-Fd-neo*. Amplification of the 3' UTR of ferredoxin utilized For-Fer-Bam and Rev-Fer-Sac. The

resulting product was digested with BamHI and SacI and cloned into the pSC-A::5'UTR-Fd-neo plasmid to produce plasmid pSC-A::5'UTR-Fd-neo-3'UTR-Fd (termed pKO-Fd).

Construction of the *mif* KO cassette utilized the same method used to generate the ferredoxin KO cassette except using *mif* gene-specific primers. Briefly, the 1000 bp upstream of the *mif* start codon and downstream of the stop codon were ligated to the NeoR gene. PCR amplification of the 1000 bp 5' UTR upstream of the *mif* start codon utilized primers For-MIF-Kpn and Rev-MIF-Xho. The resulting product was digested with KpnI and XhoI and ligated to the pSC-A::neo plasmid resulting in plasmid pSC-A::5'UTR-*mif*-neo. PCR amplification of the 1000 bp 3' UTR downstream of the *mif* stop codon utilized primers For-MIF-Bam and Rev-MIF-Sac. The resulting products were digested with BamHI and SacI and ligated to pSC-A::5'UTR-*mif*-neo to produce plasmid pSC-A::5'UTR-*mif*-neo-3'UTR-*mif* (termed pKO-*mif*).

Repair oligos/PCR. Repair oligos were constructed to target mutations in the *nluc*(*stop*) gene (Operon). Annealing of the 125 nt repair oligos utilized Repair-oligo-F and Repair-oligo-R. Annealing of the 50 nt repair oligos utilized Repair-oligo-F50 and Repair-oligo-R50. An equal concentration of each repair oligo (200 μ g) was annealed in 1x NEB T4 ligase buffer to create a stock of anneal oligos. For PCR amplification of the 125 bp repair sequence, primers For-125bp and Rev-125bp were used on the annealed 125 bp oligos above. For full length PCR of *nluc*, the digested (SacI/KpnI) and gel purified template of pMN::nluc was used as a PCR template using primers For-pMN-5UTR and Rev-Nluc-Kpn. The resulting product was treated with DpnI and then gel purified and amplified using the same primers. The final PCR product was precipitated, resuspended and quantified.

PCR amplification of the *ferredoxin-1::neo* knockout utilized the primers For-Fer-Kpn and Rev-Fer-Sac on a gel-purified product from a KpnI and SacI digestion of pKO-Fd. PCR amplification of the *mif::neo* knockout utilized the same method described above with *mif*-specific primers For-MIF-Kpn and Rev-MIF-Sac. The resulting PCR products were treated with DpnI and confirmed to be free of template plasmid. The final KO PCR product was precipitated, resuspended and quantified.

Protein and Immunoblot analysis. For Shield-1 (Clontech) titration, parasites were seeded at 1×10^5 cells/ml and treated with the indicated concentrations for 24 hours. For all immunoblot analyses, total protein was extracted and analyzed by SDS-PAGE using equal amount of soluble protein (10 μ g). Protein was then transferred to a membrane which was subsequently incubated with an anti-Cas9 antibody (Clontech). For TvGAPDH detection, the membrane was incubated with an anti-TvGAPDH antibody (Cocalico Biologicals). Images were captured and analyzed by Bio Rad Gel Doc and ImageLab software (v. 5.1, Bio Rad). Resulting values were normalized to TvGAPDH signal and presented as the average \pm the standard deviation from two independent analyses. For detection of nanoluciferase-2xHA protein, total protein was extracted from parasites, resolved by SDS-PAGE, transferred to a PVDF membrane and incubated with an anti-HA antibody (Covance). For immunoblot analysis of the Ferredoxin-1 and MIF KO samples, total soluble protein from parasite samples was resolved by SDS-PAGE, transferred to a membrane and incubated with an anti-Ferredoxin-1⁶⁷, anti-MIF⁶⁸ and anti-TvGAPDH (Cocalico Biologicals) antibodies. Uncropped images for the corresponding immunoblots are included in Figure S5.

Nanoluciferase activity assay. A total of 1×10^6 parasites were harvested per reaction (in duplicate), washed in ice-cold 1x PBS with 5% sucrose (w/v) and resuspended at a concentration of 1×10^6 cells/100 μ l in the same PBS/sucrose solution. Each 100 μ l aliquot was mixed with 100 μ l of completed NanoGlo luciferase assay reagent (Promega) and transferred to round bottomed white walled 96-well plates (Costar). Luciferase activity was analyzed by measurement with a Victor 3 model 1420 plate reader at 460 nm. Relative luminescence signal was measured in duplicate or triplicate for each assay and the average signal calculated \pm standard deviation.

Transfection of *T. vaginalis* using nucleofection and electroporation. Parasites were collected by centrifugation and resuspended in 100 μ l T-cell, Parasite-1 or Parasite-2 buffers (Lonza) and the indicated amounts of DNA and parasites (1×10^7 or 5×10^7). Typically, 10 μ g plasmid(s) and/or 100 μ g of anneal oligos or PCR product was added. After five minutes of incubation at room temperature, parasites were nucleofected using an Amaxa nucleofector using the programs U-033, D-023 or X-100. For parasite electroporation, 5×10^7 parasites were resuspended in 100 μ l of completed TYM media and placed into electrocuvettes with the indicated DNA. Parasites were then electroporated using a single pulse of 350 V with 975 μ F capacitance using a Bio Rad Gene Pulser II⁵³. For both nucleofection and electroporation parasites were immediately resuspended into 50 ml of fresh completed TYM media. During recovery, parasites were treated with 1 μ M Shield-1 where indicated.

Knockout of the *ferredoxin-1* gene (TVAG_003900) in the MSA 1103 *T. vaginalis* strain⁷⁴ utilized the nucleofection conditions (U-033 and T-cell buffer) with the substitution of pCas9-gRNA(*Fd*) or pMPAC::EV and 50 μ g of KO PCR product in duplicate. Parasites were recovered in completed TYM media for four hours and then selected for resistance to 50 μ g/ml of G418. After an additional 16 hours, the parasites were harvested and resuspended in fresh completed TYM media and 100 μ g/ml G418. After outgrowth from selection to 1×10^6 parasites/ml, genomic DNA was extracted from $\sim 1.5 \times 10^7$ parasites samples and PCR screening was done for the presence of the KO allele at the *ferredoxin-1* locus (see below). The cultures with signal positive for *ferredoxin-1* disruption were diluted and re-screened using limiting dilution until clones were obtained. The clones were screened for the presence of the *neo* gene at the ferredoxin locus as well as for the presence of the wild type *ferredoxin-1* gene. All PCRs were performed on 100 ng of purified genomic DNA and utilized NEB Phusion polymerase, per the manufacturers' instructions. Screening for the wild-type gene used primers For-003900-1 and Rev-003900-1 (PCR cycle: 95°C- 30 sec, 60°C- 30 sec, 72°C- 90 sec). Screening for the 5' end of the *ferredoxin-1::neo* KO locus used primers For-003900-5UTR-1 and Rev-Neo-Int3 (PCR cycle: 95°C- 30 sec, 60°C- 30 sec, 72°C- 90 sec). Screening

for the 3' end of the *ferredoxin-1::neo* KO locus used primers For-Neo-Int2 and Rev-003900-3UTR-2 (PCR cycle: 95°C- 30 sec, 64°C- 30 sec, 72°C- 90 sec). All PCR products were confirmed by DNA sequencing.

Knockout of the *mif* gene (TVAG_219770) in *T. vaginalis* strain B7RC2²² utilized nucleofection conditions described for the knockout of ferredoxin-1 above, except the D-023 program and V-kit buffer were utilized, and pCas9-gRNA(*mif*) or water (for the negative control) and 100 µg of KO PCR product was used. B7RC2 parasites were recovered in completed TYM media for 24 hours and selected for resistance to 100 µg/ml of G418, and 30 µg/ml of puromycin for the parasites that received pCas9-gRNA(*mif*). Negative control parasites that did not receive pCas9-gRNA(*mif*) were only selected with 100 µg/ml of G418. After an additional 24 hours, the parasites that received pCas9-gRNA(*mif*) were re-dosed with the 100 µg/ml G418, and 30 µg/ml of puromycin and control parasites were re-dosed with just 100 µg/ml G418. Drug selected parasites were then sub-populated into 20 cells per well in a 96-well plate. When the parasites reached $\sim 1 \times 10^7$ parasites/ml, genomic DNA was prepared for PCR screening. Initial screening was done utilizing the 5' end of the *mif::neo* KO with primers For-219770-5UTR-1 and Rev-Neo-Int4 (PCR cycle: 95°C- 30 sec, 55°C- 30 sec, 72°C- 90 sec). A subpopulation with the correct Neo replacement based on 5' UTR PCR analyses was cloned and then screened for the presence of the NeoR gene in the *mif* locus using both the 5' primer described above and the 3' primer For-Neo-Int3 and Rev-219770-3UTR-1 (PCR cycle: 95°C- 30 sec, 55°C- 30 sec, 72°C- 90 sec). Screening for the wild-type *mif* gene used primers For-219770-1 and Rev-219770-1 (PCR cycle: 95°C- 30 sec, 55°C- 30 sec, 72°C- 30 sec). All PCR products were confirmed by DNA sequencing.

RT-PCR analysis of gRNA expression. Total RNA was isolated from $\sim 1.5 \times 10^7$ parasites using the Direct-zol RNA Miniprep kit (Zymo) and then fractionated into small RNAs using the RNA Clean and Concentrator kit (Zymo). Small RNAs were further treated with the *TURBO DNA-free* kit (Ambion). Poly-A tails were then added using the Poly(A) polymerase tailing Kit (Ambion). Small RNAs were quantified and cDNA created by utilizing an equivalent amount of RNA in the Superscript III first strand synthesis system for RT-PCR (Invitrogen) using the provided oligo-dT₂₀ primer. All PCRs were performed on one microliter of the resulting cDNA and utilized NEB Phusion polymerase, per the manufacturers' instructions. For the gRNA, primers For-gRNA and Rev-gRNA were used to detect the gRNA and primers For-U6 and Rev-U6 were used to detect the U6 snRNA (for both, the PCR cycle: 98°C- 10 sec, 55°C- 20 sec, 72°C- 8 sec). All samples were resolved on agarose-TBE gels, stained with ethidium bromide and imaged by Bio-Rad Gel Doc, as above.

Data Availability. All data generated or analysed during this study are included in this published article (and its Supplementary Information files).

References

1. Rowley RTaN, F. Global incidence and prevalence of selected curable sexually transmitted infections-2008. 20 (World Health Organization, 2012).
2. Hirt, R. P. & Sherrard, J. Trichomonas vaginalis origins, molecular pathobiology and clinical considerations. *Curr Opin Infect Dis* **28**, 72–79, <https://doi.org/10.1097/QCO.0000000000000128> (2015).
3. Swygard, H., Sena, A. C., Hobbs, M. M. & Cohen, M. S. Trichomoniasis: clinical manifestations, diagnosis and management. *Sex Transm Infect* **80**, 91–95 (2004).
4. Kirkcaldy, R. D. *et al.* Trichomonas vaginalis antimicrobial drug resistance in 6 US cities, STD Surveillance Network, 2009–2010. *Emerg Infect Dis* **18**, 939–943, <https://doi.org/10.3201/eid1806.111590> (2012).
5. Schwabke, J. R. & Barrientes, F. J. Prevalence of Trichomonas vaginalis isolates with resistance to metronidazole and tinidazole. *Antimicrob Agents Chemother* **50**, 4209–4210, <https://doi.org/10.1128/AAC.00814-06> (2006).
6. Snipes, L. J. *et al.* Molecular epidemiology of metronidazole resistance in a population of Trichomonas vaginalis clinical isolates. *J Clin Microbiol* **38**, 3004–3009 (2000).
7. Upcroft, J. A. *et al.* Metronidazole resistance in Trichomonas vaginalis from highland women in Papua New Guinea. *Sex Health* **6**, 334–338, <https://doi.org/10.1071/SH09011> (2009).
8. Conrad, M. D., Bradic, M., Warring, S. D., Gorman, A. W. & Carlton, J. M. Getting trichy: tools and approaches to interrogating Trichomonas vaginalis in a post-genome world. *Trends Parasitol* **29**, 17–25, <https://doi.org/10.1016/j.pt.2012.10.004> (2013).
9. Hirt, R. P. *et al.* Trichomonas vaginalis pathobiology new insights from the genome sequence. *Adv Parasitol* **77**, 87–140, <https://doi.org/10.1016/B978-0-12-391429-3.00006-X> (2011).
10. Leitsch, D., Drinic, M., Kolarich, D. & Duchene, M. Down-regulation of flavin reductase and alcohol dehydrogenase-1 (ADH1) in metronidazole-resistant isolates of Trichomonas vaginalis. *Mol Biochem Parasitol* **183**, 177–183, <https://doi.org/10.1016/j.molbiopara.2012.03.003> (2012).
11. Leitsch, D., Janssen, B. D., Kolarich, D., Johnson, P. J. & Duchene, M. Trichomonas vaginalis flavin reductase 1 and its role in metronidazole resistance. *Mol Microbiol* **91**, 198–208, <https://doi.org/10.1111/mmi.12455> (2014).
12. Alvarez-Sanchez, M. E. *et al.* A novel cysteine proteinase (CP65) of Trichomonas vaginalis involved in cytotoxicity. *Microb Pathog* **28**, 193–202, <https://doi.org/10.1006/mpat.1999.0336> (2000).
13. Gould, S. B. *et al.* Deep sequencing of Trichomonas vaginalis during the early infection of vaginal epithelial cells and amoeboid transition. *Int J Parasitol* **43**, 707–719, <https://doi.org/10.1016/j.ijpara.2013.04.002> (2013).
14. Noel, C. J. *et al.* Trichomonas vaginalis vast BspA-like gene family: evidence for functional diversity from structural organisation and transcriptomics. *BMC Genomics* **11**, 99, <https://doi.org/10.1186/1471-2164-11-99> (2010).
15. Conrad, M. D. *et al.* Extensive genetic diversity, unique population structure and evidence of genetic exchange in the sexually transmitted parasite Trichomonas vaginalis. *PLoS Negl Trop Dis* **6**, e1573, <https://doi.org/10.1371/journal.pntd.0001573> (2012).
16. Morada, M. *et al.* Arginine metabolism in Trichomonas vaginalis infected with Mycoplasma hominis. *Microbiology* **156**, 3734–3743, <https://doi.org/10.1099/mic.0.042192-0> (2010).
17. Huang, K. Y. *et al.* Comparative transcriptomic and proteomic analyses of Trichomonas vaginalis following adherence to fibronectin. *Infect Immun* **80**, 3900–3911, <https://doi.org/10.1128/IAI.00611-12> (2012).
18. Pachano, T. *et al.* Epigenetics regulates transcription and pathogenesis in the parasite Trichomonas vaginalis. *Cell Microbiol* **19**, <https://doi.org/10.1111/cmi.12716> (2017).
19. Bradic, M. *et al.* Genetic indicators of drug resistance in the highly repetitive genome of Trichomonas vaginalis. *Genome Biol Evol*, <https://doi.org/10.1093/gbe/evx110> (2017).
20. Johnson, P. J., Schuck, B. L. & Delgadillo, M. G. Analysis of a single-domain P-glycoprotein-like gene in the early-diverging protist Trichomonas vaginalis. *Mol Biochem Parasitol* **66**, 127–137 (1994).

21. Quon, D. V., d'Oliveira, C. E. & Johnson, P. J. Reduced transcription of the ferredoxin gene in metronidazole-resistant *Trichomonas vaginalis*. *Proc Natl Acad Sci USA* **89**, 4402–4406 (1992).
22. de Miguel, N. *et al.* Proteome analysis of the surface of *Trichomonas vaginalis* reveals novel proteins and strain-dependent differential expression. *Mol Cell Proteomics* **9**, 1554–1566, <https://doi.org/10.1074/mcp.M000022-MCP201> (2010).
23. Bastida-Corcucera, F. D., Okumura, C. Y., Colocoussi, A. & Johnson, P. J. *Trichomonas vaginalis* lipophosphoglycan mutants have reduced adherence and cytotoxicity to human ectocervical cells. *Eukaryot Cell* **4**, 1951–1958, <https://doi.org/10.1128/EC.4.11.1951-1958.2005> (2005).
24. Land, K. M., Clemens, D. L. & Johnson, P. J. Loss of multiple hydrogenosomal proteins associated with organelle metabolism and high-level drug resistance in trichomonads. *Exp Parasitol* **97**, 102–110, <https://doi.org/10.1006/expr.2001.4587> (2001).
25. Wright, J. M., Webb, R. L., O'Donoghue, P., Upcroft, P. & Upcroft, J. A. Hydrogenosomes of laboratory-induced metronidazole-resistant *Trichomonas vaginalis* lines are down-sized while those from clinically metronidazole-resistant isolates are not. *J Eukaryot Microbiol* **57**, 171–176, <https://doi.org/10.1111/j.1550-7408.2009.00455.x> (2010).
26. Kulda, J., Tachezy, J. & Cerkasovova, A. *In vitro* induced anaerobic resistance to metronidazole in *Trichomonas vaginalis*. *J Eukaryot Microbiol* **40**, 262–269 (1993).
27. Tachezy, J., Kulda, J. & Tomkova, E. Aerobic resistance of *Trichomonas vaginalis* to metronidazole induced *in vitro*. *Parasitology* **106**(Pt 1), 31–37 (1993).
28. Bras, X. P. *et al.* Knockout of the abundant *Trichomonas vaginalis* hydrogenosomal membrane protein TvHMP23 increases hydrogenosome size but induces no compensatory up-regulation of paralogous copies. *FEBS Lett* **587**, 1333–1339, <https://doi.org/10.1016/j.febslet.2013.03.001> (2013).
29. Land, K. M. *et al.* Targeted gene replacement of a ferredoxin gene in *Trichomonas vaginalis* does not lead to metronidazole resistance. *Mol Microbiol* **51**, 115–122 (2004).
30. Hsu, H. M., Ong, S. J., Lee, M. C. & Tai, J. H. Transcriptional regulation of an iron-inducible gene by differential and alternate promoter entries of multiple Myb proteins in the protozoan parasite *Trichomonas vaginalis*. *Eukaryot Cell* **8**, 362–372, <https://doi.org/10.1128/EC.00317-08> (2009).
31. Ong, S. J., Hsu, H. M., Liu, H. W., Chu, C. H. & Tai, J. H. Activation of multifarious transcription of an adhesion protein ap65-1 gene by a novel Myb2 protein in the protozoan parasite *Trichomonas vaginalis*. *J Biol Chem* **282**, 6716–6725, <https://doi.org/10.1074/jbc.M610484200> (2007).
32. Munoz, C. *et al.* A protein phosphatase 1 gamma (PP1gamma) of the human protozoan parasite *Trichomonas vaginalis* is involved in proliferation and cell attachment to the host cell. *Int J Parasitol* **42**, 715–727, <https://doi.org/10.1016/j.ijpara.2012.03.012> (2012).
33. Ravae, R., Ebadi, P., Hatam, G., Vafafar, A. & Ghahramani Seno, M. M. Synthetic siRNAs effectively target cysteine protease 12 and alpha-actinin transcripts in *Trichomonas vaginalis*. *Exp Parasitol* **157**, 30–34, <https://doi.org/10.1016/j.exppara.2015.06.012> (2015).
34. Cong, L. *et al.* Multiplex genome engineering using CRISPR/Cas systems. *Science* **339**, 819–823, <https://doi.org/10.1126/science.1231143> (2013).
35. Cui, Y. & Yu, L. Application of the CRISPR/Cas9 gene editing technique to research on functional genomes of parasites. *Parasitol Int* **65**, 641–644, <https://doi.org/10.1016/j.parint.2016.08.011> (2016).
36. Doudna, J. A. & Charpentier, E. Genome editing. The new frontier of genome engineering with CRISPR-Cas9. *Science* **346**, 1258096, <https://doi.org/10.1126/science.1258096> (2014).
37. Mali, P. *et al.* RNA-guided human genome engineering via Cas9. *Science* **339**, 823–826, <https://doi.org/10.1126/science.1232033> (2013).
38. Mali, P., Esvelt, K. M. & Church, G. M. Cas9 as a versatile tool for engineering biology. *Nat Methods* **10**, 957–963, <https://doi.org/10.1038/nmeth.2649> (2013).
39. Beneke, T. *et al.* A CRISPR Cas9 high-throughput genome editing toolkit for kinetoplasts. *R Soc Open Sci* **4**, 170095, <https://doi.org/10.1098/rsos.170095> (2017).
40. Ghorbal, M. *et al.* Genome editing in the human malaria parasite *Plasmodium falciparum* using the CRISPR-Cas9 system. *Nat Biotechnol* **32**, 819–821, <https://doi.org/10.1038/nbt.2925> (2014).
41. Lander, N., Chiurillo, M. A., Storey, M., Vercesi, A. E. & Docampo, R. CRISPR/Cas9-mediated endogenous C-terminal Tagging of *Trypanosoma cruzi* Genes Reveals the Acidocalcisome Localization of the Inositol 1,4,5-Trisphosphate Receptor. *J Biol Chem* **291**, 25505–25515, <https://doi.org/10.1074/jbc.M116.749655> (2016).
42. Lander, N., Li, Z. H., Niyogi, S. & Docampo, R. CRISPR/Cas9-Induced Disruption of Paraflagellar Rod Protein 1 and 2 Genes in *Trypanosoma cruzi* Reveals Their Role in Flagellar Attachment. *MBio* **6**, e01012, <https://doi.org/10.1128/mBio.01012-15> (2015).
43. Peng, D., Kurup, S. P., Yao, P. Y., Minning, T. A. & Tarleton, R. L. CRISPR-Cas9-mediated single-gene and gene family disruption in *Trypanosoma cruzi*. *MBio* **6**, e02097–02014, <https://doi.org/10.1128/mBio.02097-14> (2014).
44. Shen, B., Brown, K. M., Lee, T. D. & Sibley, L. D. Efficient gene disruption in diverse strains of *Toxoplasma gondii* using CRISPR/CAS9. *MBio* **5**, e01114–01114, <https://doi.org/10.1128/mBio.01114-14> (2014).
45. Sidik, S. M., Hackett, C. G., Tran, F., Westwood, N. J. & Lourido, S. Efficient genome engineering of *Toxoplasma gondii* using CRISPR/Cas9. *PLoS One* **9**, e100450, <https://doi.org/10.1371/journal.pone.0100450> (2014).
46. Sollelis, L. *et al.* First efficient CRISPR-Cas9-mediated genome editing in *Leishmania* parasites. *Cell Microbiol* **17**, 1405–1412, <https://doi.org/10.1111/cmi.12456> (2015).
47. Vinayak, S. *et al.* Genetic modification of the diarrhoeal pathogen *Cryptosporidium parvum*. *Nature* **523**, 477–480, <https://doi.org/10.1038/nature14651> (2015).
48. Wagner, J. C., Platt, R. J., Goldfless, S. J., Zhang, F. & Niles, J. C. Efficient CRISPR-Cas9-mediated genome editing in *Plasmodium falciparum*. *Nat Methods* **11**, 915–918, <https://doi.org/10.1038/nmeth.3063> (2014).
49. Zhang, C. *et al.* Efficient editing of malaria parasite genome using the CRISPR/Cas9 system. *MBio* **5**, e01414–01414, <https://doi.org/10.1128/mBio.01414-14> (2014).
50. Zhang, W. W. & Matlashewski, G. CRISPR-Cas9-Mediated Genome Editing in *Leishmania donovani*. *MBio* **6**, e00861, <https://doi.org/10.1128/mBio.00861-15> (2015).
51. Zamanian, M. & Andersen, E. C. Prospects and challenges of CRISPR/Cas genome editing for the study and control of neglected vector-borne nematode diseases. *FEBS J* **283**, 3204–3221, <https://doi.org/10.1111/febs.13781> (2016).
52. Carlton, J. M. *et al.* Draft genome sequence of the sexually transmitted pathogen *Trichomonas vaginalis*. *Science* **315**, 207–212, <https://doi.org/10.1126/science.1132894> (2007).
53. Delgado, M. G., Liston, D. R., Niazi, K. & Johnson, P. J. Transient and selectable transformation of the parasitic protist *Trichomonas vaginalis*. *Proc Natl Acad Sci USA* **94**, 4716–4720 (1997).
54. Banaszynski, L. A., Chen, L. C., Maynard-Smith, L. A., Ooi, A. G. & Wandless, T. J. A rapid, reversible, and tunable method to regulate protein function in living cells using synthetic small molecules. *Cell* **126**, 995–1004, <https://doi.org/10.1016/j.cell.2006.07.025> (2006).
55. Banaszynski, L. A. & Wandless, T. J. Conditional control of protein function. *Chem Biol* **13**, 11–21, <https://doi.org/10.1016/j.chembiol.2005.10.010> (2006).
56. Jinek, M. *et al.* RNA-programmed genome editing in human cells. *Elife* **2**, e00471, <https://doi.org/10.7554/eLife.00471> (2013).
57. Simoes-Barbosa, A., Meloni, D., Wohlschlegel, J. A., Konarska, M. M. & Johnson, P. J. Spliceosomal snRNAs in the unicellular eukaryote *Trichomonas vaginalis* are structurally conserved but lack a 5'-cap structure. *RNA* **14**, 1617–1631, <https://doi.org/10.1261/rna.1045408> (2008).

58. Iijima, O., Fukano, H., Takahashi, H., Shirai, M. & Suzuki, Y. A purine at +2 rather than +1 adjacent to the human U6 promoter is required to prepare effective short hairpin RNAs. *Biochem Biophys Res Commun* **350**, 809–817, <https://doi.org/10.1016/j.bbrc.2006.08.187> (2006).
59. Peng, D. & Tarleton, R. EuPaGDT: a web tool tailored to design CRISPR guide RNAs for eukaryotic pathogens. *Microb Genom* **1**, e000033, <https://doi.org/10.1099/mgen.0.000033> (2015).
60. Hernandez, N. Small nuclear RNA genes: a model system to study fundamental mechanisms of transcription. *J Biol Chem* **276**, 26733–26736, <https://doi.org/10.1074/jbc.R100032200> (2001).
61. Mroczek, S. & Dziembowski, A. U6 RNA biogenesis and disease association. *Wiley Interdiscip Rev RNA* **4**, 581–592, <https://doi.org/10.1002/wrna.1181> (2013).
62. Tschudi, C. & Ullut, E. Unconventional rules of small nuclear RNA transcription and cap modification in trypanosomatids. *Gene Expr* **10**, 3–16 (2002).
63. Boute, N. *et al.* NanoLuc Luciferase - A Multifunctional Tool for High Throughput Antibody Screening. *Front Pharmacol* **7**, 27, <https://doi.org/10.3389/fphar.2016.00027> (2016).
64. Burkard, G., Fragoso, C. M. & Roditi, I. Highly efficient stable transformation of bloodstream forms of *Trypanosoma brucei*. *Mol Biochem Parasitol* **153**, 220–223, <https://doi.org/10.1016/j.molbiopara.2007.02.008> (2007).
65. Glover, L. & Horn, D. Site-specific DNA double-strand breaks greatly increase stable transformation efficiency in *Trypanosoma brucei*. *Mol Biochem Parasitol* **166**, 194–197 (2009).
66. Wang, S. E., Brooks, A. E. S., Cann, B. & Simoes-Barbosa, A. The fluorescent protein iLOV outperforms eGFP as a reporter gene in the microaerophilic protozoan *Trichomonas vaginalis*. *Mol Biochem Parasitol* **216**, 1–4, <https://doi.org/10.1016/j.molbiopara.2017.06.003> (2017).
67. Johnson, P. J., d'Oliveira, C. E., Gorrell, T. E. & Muller, M. Molecular analysis of the hydrogenosomal ferredoxin of the anaerobic protist *Trichomonas vaginalis*. *Proc Natl Acad Sci USA* **87**, 6097–6101 (1990).
68. Twu, O. *et al.* *Trichomonas vaginalis* homolog of macrophage migration inhibitory factor induces prostate cell growth, invasiveness, and inflammatory responses. *Proc Natl Acad Sci USA* **111**, 8179–8184, <https://doi.org/10.1073/pnas.1321884111> (2014).
69. Beverley, S. M. Parasitology: CRISPR for *Cryptosporidium*. *Nature* **523**, 413–414, <https://doi.org/10.1038/nature14636> (2015).
70. Kim, S., Kim, D., Cho, S. W., Kim, J. & Kim, J. S. Highly efficient RNA-guided genome editing in human cells via delivery of purified Cas9 ribonucleoproteins. *Genome Res* **24**, 1012–1019, <https://doi.org/10.1101/gr.171322.113> (2014).
71. Liang, X. *et al.* Rapid and highly efficient mammalian cell engineering via Cas9 protein transfection. *J Biotechnol* **208**, 44–53, <https://doi.org/10.1016/j.jbiotec.2015.04.024> (2015).
72. Yin, H., Kauffman, K. J. & Anderson, D. G. Delivery technologies for genome editing. *Nat Rev Drug Discov* **16**, 387–399, <https://doi.org/10.1038/nrd.2016.280> (2017).
73. Glover, L., McCulloch, R. & Horn, D. Sequence homology and microhomology dominate chromosomal double-strand break repair in African trypanosomes. *Nucleic Acids Res* **36**, 2608–2618, <https://doi.org/10.1093/nar/gkn104> (2008).
74. Lustig, G., Ryan, C. M., Secor, W. E. & Johnson, P. J. *Trichomonas vaginalis* contact-dependent cytolysis of epithelial cells. *Infect Immun* **81**, 1411–1419, <https://doi.org/10.1128/IAI.01244-12> (2013).
75. Clark, C. G. & Diamond, L. S. Methods for cultivation of luminal parasitic protists of clinical importance. *Clin Microbiol Rev* **15**, 329–341 (2002).
76. Riestra, A. M. *et al.* A *Trichomonas vaginalis* Rhomboid Protease and Its Substrate Modulate Parasite Attachment and Cytolysis of Host Cells. *PLoS Pathog* **11**, e1005294, <https://doi.org/10.1371/journal.ppat.1005294> (2015).

Acknowledgements

We thank members of our laboratories for useful discussions, Charlie Ho for technical assistance and Dr. Frances Mercer and Fitz Gerald Diala for helpful comments on the manuscript. We also thank Drs. Boris Striepen and Sumiti Vinayak (University of Georgia) for providing the nanoluciferase constructs and Dr. W. Evan Secor (Center for Disease Control & Prevention) for providing *T. vaginalis* strain MSA 1103. This work was funded by NIH grants AI119721 & AI103182 (to PJJ). Y-PC and BMM received support from Ruth L. Kirschstein National Research Service Awards, AI007323 and GM00718, respectively.

Author Contributions

B.D.J., Y.-P.C., A.S.-B. and P.J.J. conceived of and designed experiments. B.D.J., Y.-P.C., B.M.M., S.E.W. performed experiments and B.D.J., Y.-P.C., A.S.-B. and P.J.J. analyzed data. B.D.J. and P.J.J. wrote the manuscript. P.J.J. secured funding. All authors reviewed the manuscript.

Additional Information

Supplementary information accompanies this paper at <https://doi.org/10.1038/s41598-017-18442-3>.

Competing Interests: The authors declare that they have no competing interests.

Publisher's note: Springer Nature remains neutral with regard to jurisdictional claims in published maps and institutional affiliations.



Open Access This article is licensed under a Creative Commons Attribution 4.0 International License, which permits use, sharing, adaptation, distribution and reproduction in any medium or format, as long as you give appropriate credit to the original author(s) and the source, provide a link to the Creative Commons license, and indicate if changes were made. The images or other third party material in this article are included in the article's Creative Commons license, unless indicated otherwise in a credit line to the material. If material is not included in the article's Creative Commons license and your intended use is not permitted by statutory regulation or exceeds the permitted use, you will need to obtain permission directly from the copyright holder. To view a copy of this license, visit <http://creativecommons.org/licenses/by/4.0/>.

Chapter 5:

Examination of cytokine induction from human innate immune cells by *Trichomonas vaginalis* co-infected with *Mycoplasma hominis* and by the presence of *Tv* protein TvMIF

Abstract

Most infections caused by *Trichomonas vaginalis* (*Tv*) are asymptomatic but chronic and symptomatic infections do exist. To understand how the parasite transitions from acute to long-term infection, we characterized innate immune responses against *T. vaginalis* by setting up an *in vitro* co-culture system to detect cytokine responses elicited by *T. vaginalis* from human monocyte-derived dendritic cells and macrophages. By including *T. vaginalis* symbiont *Mycoplasma hominis* in the study, we found that majority of the cytokine responses are induced by *Tv* in the presence of *M. hominis* but not when *M. hominis* is absent. In addition, a laboratory adapted *Tv* strain triggers significantly stronger inflammatory responses than a clinical *Tv* strain, indicating strain variations could contribute to various infection outcomes. We also examined innate immune responses to *Tv* homologue (TvMIF) of human cytokine macrophage migration inhibitory factor (HuMIF). TvMIF does not induce significant amount of inflammatory cytokine responses from innate immune cells. This could be because the parasite has co-evolved with the host so the parasite homologue of the human cytokine preserves its anti-apoptotic effect on the parasite but does not trigger host immune response during infection. These results lay the groundwork for future studies on host immune responses to *T. vaginalis* infection.

Introduction

Immune responses induced by *T. vaginalis* in infected individuals are largely unknown but remain interesting given that majority of the infections are asymptomatic while chronic symptomatic cases also exist [1]. As a first step towards fighting the chronic *Tv* infection, it is critical to understand how human innate immune system such as monocytes, macrophages, and dendritic cells respond to the parasite. Human monocytes, derived from bone marrow, are known

to circulate and survey bloodstream [2]. When monocytes pass through capillary walls and enter tissues, they differentiate into macrophages which are 5-10 times larger in size and more phagocytic than monocytes [2]. The main defensive roles of macrophages involve phagocytosis, presenting foreign antigens, and initiating inflammatory responses by releasing small signaling molecules called cytokines [2]. Dendritic cells (DCs) develop from bone marrow-derived hematopoietic stem cells but the precise origin of dendritic cells is not well understood [3]. *In vitro*, DCs can be differentiated from bone marrow derived-monocytes by receiving granulocyte-macrophage colony stimulating factor (GM-CSF) and cytokine IL-4 [4]. DCs in tissues are activated by receiving signals such as cytokines from macrophages during an infection [5]. It is also known that during herpes simplex viral infection in mice, bone-marrow-derived precursors differentiate into vaginal epithelial DCs and become activated [6]. Understanding the type of responses DCs and macrophages mount against *Tv* will provide insights into how our innate immune system communicates with adaptive immune responses to result in diverse infection outcomes.

Cytokine responses induced by *T. vaginalis* and its symbionts or products have been examined sporadically. Lipoglycan on *T. vaginalis* surface [7], *T. vaginalis* infected with its endosymbiotic viruses (TVVs) [8], exosomes secreted by the parasite [9], live *T. vaginalis*, and its secretory proteins and lysates [10][11][12][13] induce cytokine production from epithelial host cells or host immune cells. *Mycoplasma hominis* is a natural *T. vaginalis* symbiont and the co-infection exists at a range from 5% to 90% of clinical cases depending on the regions of the isolation [14]. However, only recently, our laboratory systemically tested cytokine responses comparing both clinical and laboratory adapted *T. vaginalis* strains and both *M. hominis*-free and *M. hominis*-positive isogenic strains on primary human monocytes [15] and found that most of

the cytokine responses are triggered by *T. vaginalis* symbiont *M. hominis* instead of the parasite itself except for IL-8 [15], contradictory to the highly immunogenic properties of *T. vaginalis* found in previous reports [11][12][13]. As a result, it is worthwhile to revisit the cytokine responses induced by *T. vaginalis* in the presence and absence of *M. hominis* from other immune cells such as macrophages and dendritic cells.

Trichomonas vaginalis macrophage migration inhibitory factor (TvMIF) is homologue of human pleiotropic cytokine HuMIF [10]. Plenty of pro-inflammatory cytokine properties of mammalian MIFs were characterized in mouse models during infections [16][17][18]. For example, in MIF-depleted mice, pro-inflammatory cytokines from macrophages were reduced in response to *Mycobacterium tuberculosis* infection, or exposure to lipopolysaccharide (LPS) and gram-negative bacteria compared to the wild-type (WT) mice [16][17]. Like HuMIF, parasite MIF homologues modulate human immune responses. *Entamoeba histolytica* MIF [19], *Toxoplasma gondii* MIF [20], and *Plasmodium yoelii* MIF [21] and TvMIF [10] can induce pro-inflammatory cytokine production from host. On the other hand, helminth parasite *Brugia malayi* MIF promotes Th2 response that alleviates inflammatory response [22]. To gain a thorough understanding of immunomodulatory roles of TvMIF, we examined cytokine responses from human macrophages and dendritic cells that were previously unstudied.

We used human bone marrow-derived primary cells as our model because human is the natural host of *T. vaginalis*. Furthermore, current *T. vaginalis* mouse model requires immunosuppressive treatment that is not suitable for studying immune responses from the host [23]. Macrophages and dendritic cells are differentiated from primary human monocytes with a method that is standardly employed in the immunology field [4][24]. In this chapter, we will

present cytokine responses from human macrophages and dendritic cells to *T. vaginalis* and a secreted cytokine homologue TvMIF.

Results

Differentiation of macrophages and dendritic cells

By treating isolated primary human monocytes with granulocyte-macrophage colony stimulating factor (GM-CSF) only or GM-CSF + IL-4 for 4 days, we obtained monocyte-derived macrophages (MDM) or monocyte-derived dendritic cells (MDDC), respectively. We verified the differentiation by examining the surface markers such as CD11c and CD14 [25][26][27] and the cell sizes. MDM has higher CD11c and CD14 expression than monocytes on day 0 and it has a significant size increase shown by a shift of forward side scatter (FSC) to the right on a flow cytometry histogram (Fig. 5-1A). For MDDC, CD14 expression is reduced and the size increased (higher FSC) after the differentiation (Fig. 5-1B). After confirming that the differentiation was successful, we then co-cultured *T. vaginalis* with MDM or MDDC overnight and collected the supernatant for cytokine detection.

Examination of cytokine production by live *T. vaginalis* in the presence or absence of *M. hominis*

We tested a laboratory adapted *Tv* strain G3 and a clinical isolate MSA1103, and *M. hominis*-negative and *M. hominis*-positive for both of these strains. Consistent with our previous examination using primary monocytes in our laboratory [15], most of the cytokine production from both MDM and MDDC are present in *M. hominis*-positive strain but not very much in *M. hominis*-negative strain (Fig. 5-2 & 5-3). In addition, we found that in *M. hominis*-positive strains, laboratory adapted G3 induced much more cytokine productions than clinical isolate

MSA1103 for almost all the inflammatory cytokines tested including IL-1 β , IL-6, IL-8 and TNF- α from both MDCC and MDM (Fig. 5-2 & 5-3). IL-12 was only stimulated in MDCC but not MDM (Fig. 5-2E & 5-3E). The differences between G3- and MSA1103-stimulated cytokines were more dramatic in MDCC than MDM. To test if G3 contains more *M. hominis* than MSA1103, we performed qRT-PCR to measure *M. hominis* levels by using *M. hominis*-specific primers and normalized it to *Tv* housekeeping gene, β -tubulin. The amounts of *M. hominis* were similar in G3 and MSA1103 (Fig. 5-3G) so this suggests that G3 is more immunogenic than MSA1103 but only when *M. hominis* is also present.

Interestingly, anti-inflammatory cytokine IL-10 is also induced in *M. hominis*-positive strains and is significantly more in G3 than MSA1103 when produced by MDM (Fig. 5-3D). The result could suggest that *T. vaginalis* and *M. hominis* co-infection presents a mixture of antigens that stimulate both inflammatory and anti-inflammatory responses from the host immune cells.

Examination of cytokine production in the presence of TvMIF

After we confirmed the differentiation of MDM and MDCC as described in Fig. 5-1, we added 100 ng/ml, 1 μ g/ml, 10 μ g/ml of recombinant TvMIF (rTvMIF) or recombinant HuMIF (rHuMIF) or PBS to MDM or MDCC and the culture was incubated for 16h at 37°C. We found that none of the rTvMIF or rHuMIF concentration tested induced significant pro-inflammatory cytokine production (IL-1 β , IL-6, IL-8 and TNF- α) from MDCC (Fig. 5-4 & 5-5). 10 μ g/ml of rHuMIF caused IL-6, IL-8 and TNF- α production from MDM but none of the rTvMIF induced the pro-inflammatory cytokines from MDM (Fig. 5-5).

Discussion

We examined a panel of cytokine responses induced by live *T. vaginalis* and rTvMIF in MDM and MDDC. By including *M. hominis*-positive, *M. hominis*-negative, laboratory adapted and clinical *Tv* strains, we observed that *Tv* symbiont *M. hominis* plays a significant role in the cytokine stimulation, consistent with our previous study that *T. vaginalis*-induced cytokines from human monocytes are greatly dependent on the presence of *M. hominis* [15]. In addition, all the cytokines tested in the *M. hominis*-positive samples were more abundant in the laboratory adapted strain than the clinical strain, suggesting that the immunogenic property of *M. hominis* is also dependent on *Tv* strains. The striking differences in the cytokine productions between strains and whether *M. hominis* is present could, at least partially, explain the diverse outcomes of *T. vaginalis* infection in humans.

We showed that *T. vaginalis* stimulates immunosuppressive cytokine IL-10 from MDDC and MDM, consistent with Song et al. observation that *T. vaginalis*-derived secretory products up-regulates anti-inflammatory IL-10 from MDDC [11]. On the other hand, the pro-inflammatory cytokines (TNF- α , IL-1 β and IL-6) induced by *M. hominis*-positive *T. vaginalis* samples in MDM are consistent with previous observations with live *Tv*, *Tv* lysates and human plasma-opsinized live *Tv* [12]. Notably, we only saw abundant cytokines from MDDC and MDM using *M. hominis*-positive parasites whose presence was not examined in previous studies on cytokine stimulated by *T. vaginalis* or its products. These results emphasize the importance of taking *M. hominis* into account as majority of the pro-inflammatory responses produced by MDDC and MDM were only present in *M. hominis*-positive samples. In this study, we also observed strain-to-strain variations. As a result, it is critical to compare between different *Tv* strains in the presence or absence of *M. hominis* before drawing any conclusion whether a *T.*

vaginalis protein, secretory products, and *Tv* molecules have true immunogenic effects on the host.

Induction of either pro-inflammatory or immunosuppressive cytokines by *Tv* from immune cells have been reported in independent studies [1]. However, this is the first time that we found the presence both anti-inflammatory and immunosuppressive responses induced by *Tv* by the same cell types. The same observation was made in sepsis during pathogen infection and it was reasoned that the increase in pro-inflammatory cytokines is to fight off the infection and the immunosuppressive cytokines are made to prevent organ failure from excessive inflammation [28]. Moreover, it was also found that *Mycoplasma*-infected human tumor exosomes stimulated both pro-inflammatory IFN- γ and immunosuppressive IL-10 from B cells but these cytokines were absent in *Mycoplasma*-negative exosomes [29]. This further highlights that the immunogenic properties of *Tv* described previously may attribute to the presence of *M. hominis*.

Contrary to seen in human monocytes [15] and MDM, IL-12 that induces Th1 responses was elicited in MDDC by live *Tv* (Fig 5-2E & 5-3E). The different immune cell types used may contribute to the observed differences. Future analyses are required to determine whether our laboratory adapted strain that induces significantly more pro-inflammatory cytokines from both MDM and MDDC are more susceptible to attack by immune cells.

In this study, rHuMIF induced IL-6, IL-8 and TNF- α responses produced by MDM as HuMIF plays a pro-inflammatory role in human cells although only at high concentration (10 $\mu\text{g/ml}$). However, almost no cytokine tested was induced by rTvMIF or lower concentrations of rHuMIF. We suspect that this is because of the production method of the recombinant proteins we used. Both rTvMIF and rHuMIF have C-terminal His tags that can inhibit the oligomerization

of MIF proteins [30]. The trimeric MIF proteins are primarily responsible for binding to MIF receptor and induce the cytokine responses [31]. As a result, our rMIF with C-terminal His tags may not be able to induce the cytokine production. Another explanation for the difference is that most of the pro-inflammatory roles of mammalian MIFs were studied in MIF knockout mice during pathogenic infections [16][17][18][32]. Purified MIF proteins may not stimulate cytokine responses on isolated immune cells in the absence of an infection. We previously observed that rTvMIF was able to induce IL-8 signal from monocytes [10]. In several studies, macrophages and DC were found to produce less cytokines than their precursor monocytes when treated with the same agonists. Seow et al and Daigneault et al reported that macrophages produce less pro-inflammatory cytokines than monocytes in response to LPS and TLR1/2 agonist Pam3CSK4, respectively [33][34]. MDDC produce less pro-inflammatory cytokine than monocytes in response to LPS, *Staphylococcus epidermis* and TLR2 ligand [35]. The less abundant cytokine production from MDDC and MDM may explain the absence of rTvMIF-induced cytokine release.

TvMIF has been shown to bind HuMIF receptor CD74 [10] and both MIFs can inhibit the parasite death under nutrient starvation [36]. However, TvMIF may not be as immunogenic to the host as we hypothesized. This could be the parasite reaching a balance of mimicking host survival factor while avoiding the immune consequence of having a pro-inflammatory cytokine in the parasite. TvMIF may demonstrate an intricate example of co-evolution of host and parasite.

Material and Methods

***Trichomonas vaginalis* culture**

T. vaginalis strains G3 and MSA1103 were cultured in complete Diamond's media as previously described [37]. The cells were passaged for 2 weeks or less. *M. hominis*-negative *T. vaginalis* culture was treated with 50 µg/ml of chloramphenicol and 5 µg/ml of tetracycline daily for at least 3 days and *M. hominis*-positive *Tv* was cultured without the antibiotic treatment [15].

Acquisition of human monocyte-derived macrophages and monocyte-derived dendritic cells

Primary human monocytes were isolated by adherence to plastic by UCLA Virology Core. Monocyte-derived macrophages (MDM) and monocyte-derived dendritic cells (MDDC) were differentiated *in vitro* as previously described [4][15]. Briefly, 20 ng/ml of GM-CSF (Biolegend) was added to induce MDM differentiation. 20 ng/ml of GM-CSF and 20 ng/ml of IL-4 were added to induce MDDC differentiation. Both MDM and MDDC were differentiated for 4 days in RPMI 1640 media supplemented with 10% fetal bovine serum (Thermo Fisher Scientific), 100 U/ml penicillin + 100 µg/ml streptomycin (Thermo Fisher Scientific), GlutaMAX (Thermo Fisher Scientific) and MEM non-essential amino acids (Thermo Fisher Scientific) before co-culture with *Tv*. Successful differentiation was determined by increase in sizes for both cell types, increase in CD11c and CD14 for MDM, and decrease in CD14 for MDDC. The differentiated cells were stained with 20 µg/ml CD11c-FITC (BioLegend) and 50 µg/ml of CD14-PE (BioLegend) for 30 min at 4 °C in the dark. The stained cells were read on BD LSR Fortessa and the data were analyzed by FlowJo 7.6.

Co-culture of MDM or MDDC with *Tv* and cytokine production analysis

M. hominis-free and *M. hominis*-positive *Tv* were counted and resuspended in complete RPMI media to be incubated with MDM or MDDC at an multiplicity of infection (MOI) of 1 for 16 hours. 100 ng/ml lipopolysaccharide (LPS) (Sigma) alone or 100 ng/ml LPS + 1000 U/ml interferon gamma (IFN- γ) (BioLegend) was used as positive controls to stimulate cytokine production. After the incubation, the cells were centrifuged and the supernatants were collected for cytokine detection. Cytometric Bead Array (Becton-Dickenson) was used to measure IL-1 β , IL-6, IL-8, IL-10, IL-12 and TNF- α cytokines. The results were read on BD LSR Fortessa and the data were analyzed by FlowJo 7.6.

rTvMIF induction of cytokine

Recombinant TvMIF protein was made according to the method described in [10]. In brief, TvMIF or HuMIF in pET200 expression vector grown in *Escherichia coli* BL21 StarTM(DE3) cells (Thermo Fisher Scientific) was purified using His FastFlow Columns (GE healthcare) against the C-terminal His tags on both proteins. Endotoxin was removed from both proteins using Detoxi-Gel Endotoxin Removing Columns (Thermo Fisher Scientific). The protein concentrations were determined by Pierce BCA Protein Assay Kit (Thermo Fisher Scientific).

100 ng/ml, 1 μ g/ml or 10 μ g/ml of rTvMIF was added to MDM or MDDC to induce cytokine production. PBS and LPS (Sigma) were used as the negative and positive controls, respectively. The supernatants of MDM and MDDC were collected by spinning the cells and the cytokine detection was measured and analyzed by the same method described in *Tv*-induced cytokine analysis.

Quantification of *M. hominis* in *T. vaginalis* by qRT-PCR

T. vaginalis along with *M. hominis* total RNA was extracted with TRIzol (Life Technologies) and treated with TURBO DNase (Invitrogen). cDNA and qRT-PCR were performed using SuperScript III (Thermo Fisher Scientific) and Platinum SYBR Green qPCR SuperMix-UDG kits (Thermo Fisher Scientific). The *M. hominis*-specific primers were described in [38] and their Cq values were normalized to *T. vaginalis* β -tubulin gene Cq values [39].

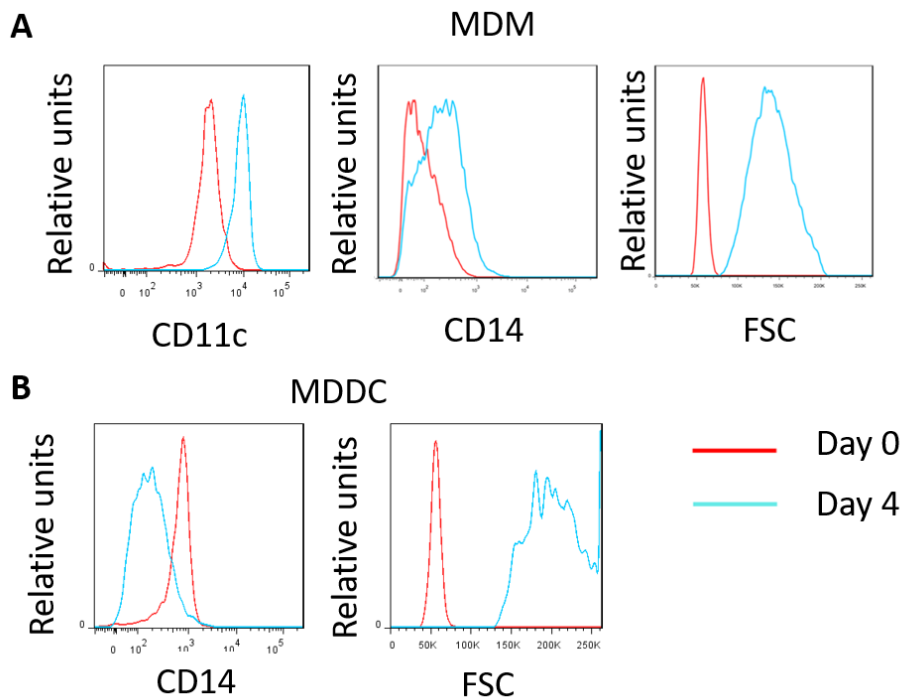


Figure 5-1: MDM and MDDC differentiation were verified by the surface markers and their size changes. (A) After 4 days of differentiation, MDM gained CD11c and CD14 signals and had a size increase (FSC). (B) MDDC (day 4) had a lower CD14 and smaller size (FSC) compared to day 0.

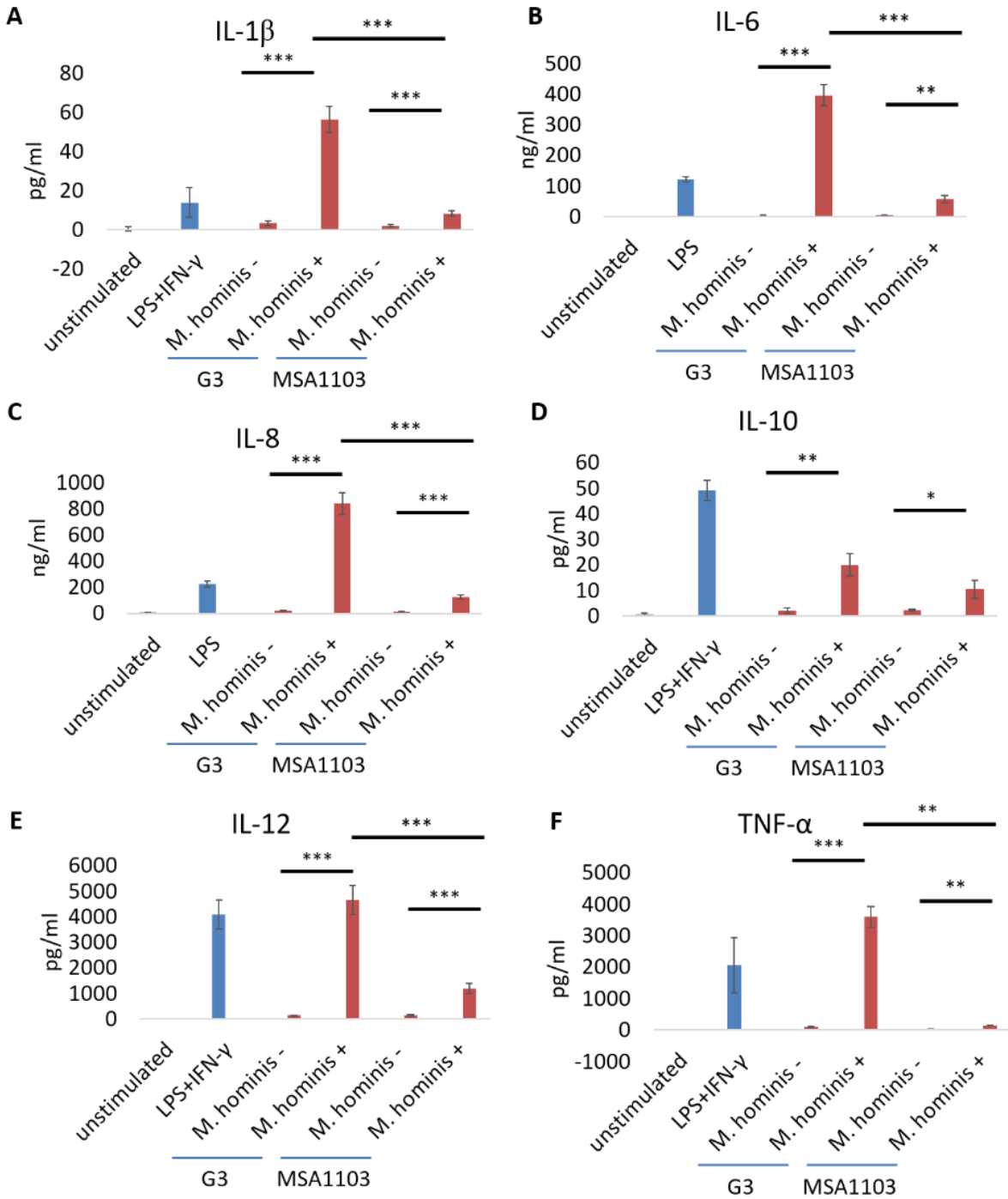


Figure 5-2: Cytokines IL-1 β , IL-6, IL-8, IL-10, IL-12 and TNF- α from MDCC are induced by *M. hominis*-positive live *T. vaginalis* and significantly more in the laboratory adapted strain G3 than the clinical strain MSA1103. (A-F) Unstimulated is PBS-treated. LPS or LPS + IFN- γ are the positive controls. Live G3 or MSA1103 parasites were co-cultured with MDCC at multiplicity of infection = 1 for 16 hours. * = $p \leq 0.05$, ** = $p \leq 0.01$, * = $p \leq 0.001$**

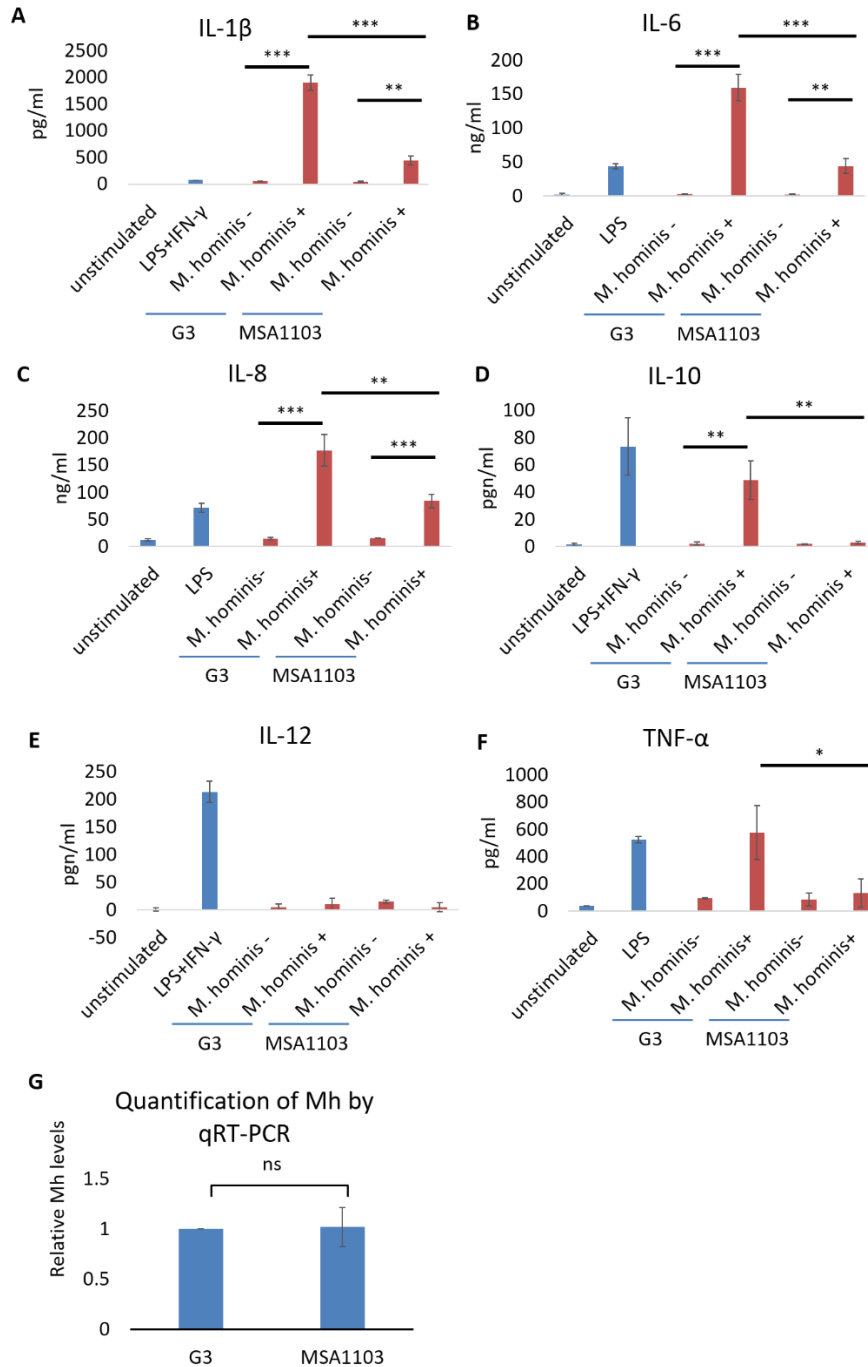


Figure 5-3: Cytokines IL-1 β , IL-6, IL-8, IL-10, IL-12 and TNF- α from MDM are induced by *M. hominis*-positive live *T. vaginalis* and significantly more in the laboratory adapted strain G3 than the clinical strain MSA1103. (A-F) Unstimulated is PBS-treated. LPS or LPS + IFN- γ are the positive controls. Live G3 or MSA1103 parasites were co-cultured with MDM at multiplicity of infection = 1 for 16 hours. (G) Comparison of *M. hominis* (Mh) quantity in each strain was quantified by qRT-PCR. The Mh rRNA-encoding gene was normalized to *T. vaginalis* housekeeping gene β -tubulin. The Mh levels are expressed as fold change (G3 = 1). ns = not significant * = $p \leq 0.05$, ** = $p \leq 0.01$, * = $p \leq 0.001$**

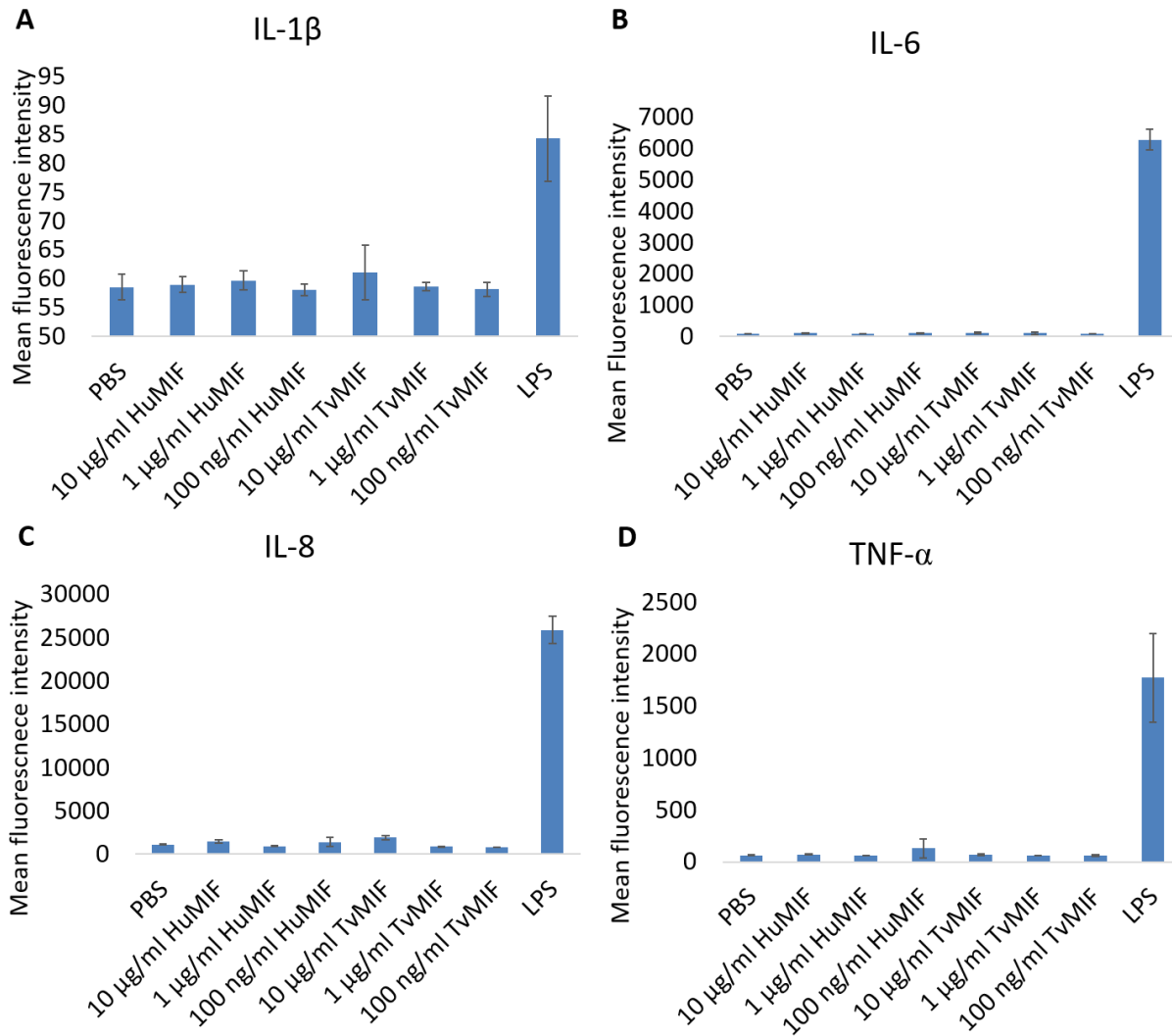


Figure 5-4: TvMIF does not induce significant amounts of pro-inflammatory cytokine responses from MDDC. (A-D) 100 ng/ml, 1 μ g/ml, 10 μ g/ml of rHuMIF or rTvMIF were added to the MDDC culture and the culture was then incubated for 16 hours. PBS-treated was the negative control and LPS-treated was the positive control.

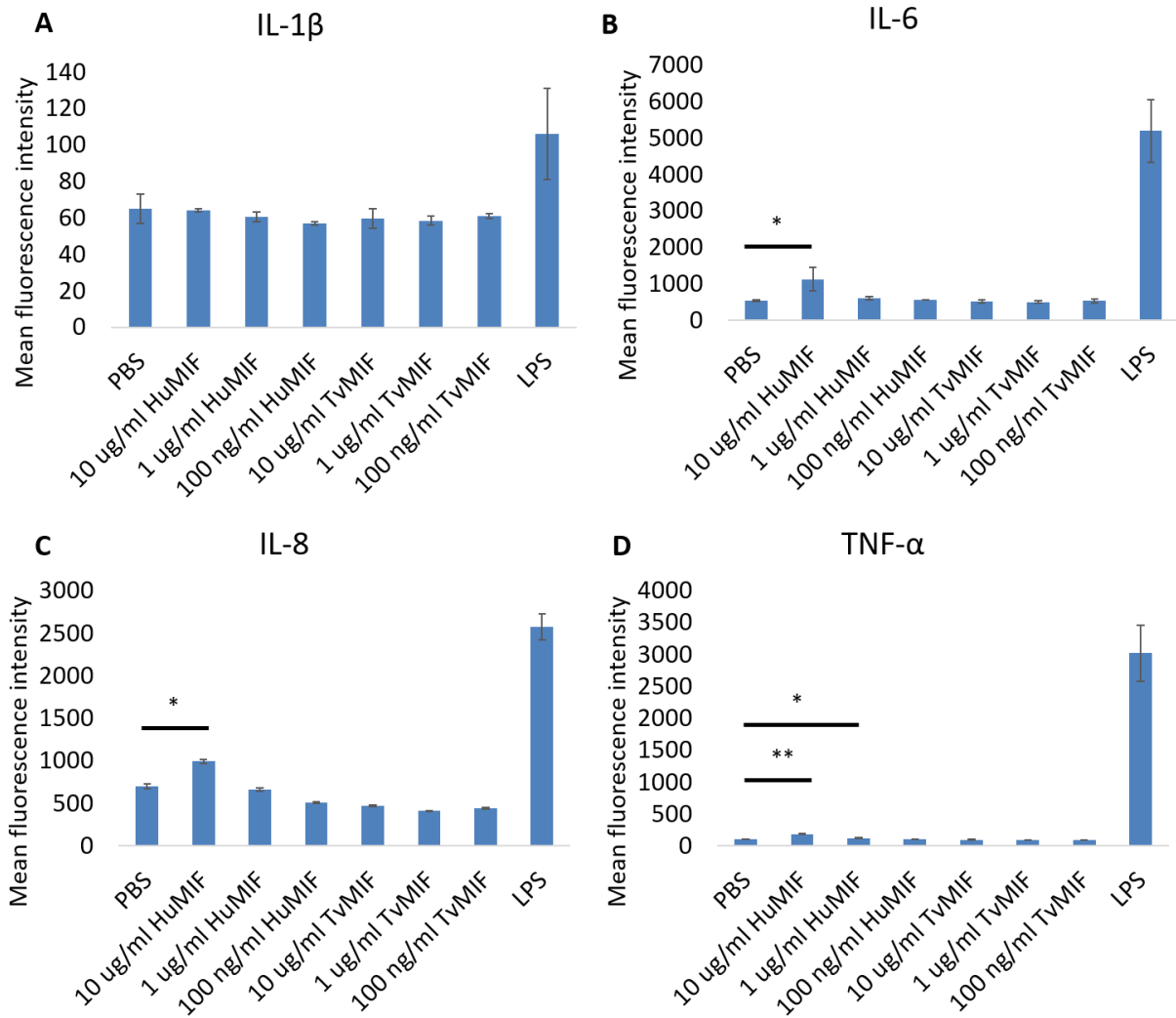


Figure 5-5: HuMIF but not TvMIF induces significant amounts of pro-inflammatory cytokine responses from MDM. (A-D) 100 ng/ml, 1 μ g/ml, 10 μ g/ml of rHuMIF or rTvMIF were added to MDM culture and the culture was then incubated for 16 hours. PBS-treated was the negative control and LPS-treated was the positive control. * = $p \leq 0.05$, ** = $p \leq 0.01$

References

- [1] Fichorova, R. N. (2009). Impact of *T. vaginalis* infection on innate immune responses and reproductive outcome. *J. Reprod. Immunol.* (83) 185–189.
- [2] Duque, G. A. & Descoteaux, A. (2014). Macrophage cytokines: Involvement in immunity and infectious diseases. *Front. Immunol.* (5) doi: 10.3389/fimmu.2014.00491.
- [3] Liu, K. & Nussenzweig, M. C. (2010). Origin and development of dendritic cells. *Immunol Rev* (234) 45–54.
- [4] Chapuis, F. *et al.* (1997). Differentiation of human dendritic cells from monocytes in vitro. *Eur. J. Immunol.* (27) 431–441.
- [5] Volcheck, G. W. (2001). How the Immune System Works. *Ann. Allergy, Asthma Immunol.* (86) 350.
- [6] Iijima, N., Linehan, M. M., Saeland, S. & Iwasaki, A. (2007). Vaginal epithelial dendritic cells renew from bone marrow precursors. *Proc. Natl. Acad. Sci.* (104) 19061–19066.
- [7] Fichorova, R. N. *et al.* (2006). *Trichomonas vaginalis* lipophosphoglycan triggers a selective upregulation of cytokines by human female reproductive tract epithelial cells. *Infect. Immun.* (74) 5773–5779.
- [8] Fichorova, R. N. *et al.* (2012). Endobiont Viruses Sensed by the Human Host - Beyond Conventional Antiparasitic Therapy. *PLoS One* (7) e48418.
- [9] Twu, O. *et al.* (2013). *Trichomonas vaginalis* Exosomes Deliver Cargo to Host Cells and Mediate Host:Parasite Interactions. *PLoS Pathog.* (9) e1003482.

- [10] Twu, O. *et al.* (2014). Trichomonas vaginalis homolog of macrophage migration inhibitory factor induces prostate cell growth, invasiveness, and inflammatory responses. *Proc. Natl. Acad. Sci.* (111) 8179–8184.
- [11] Song, M. J. *et al.* (2015). Modulation of dendritic cell function by trichomonas vaginalis-derived secretory products. *BMB Rep.* (48) 103–108.
- [12] Han, I.-H. *et al.* (2009). Proinflammatory cytokine and nitric oxide production by human macrophages stimulated with Trichomonas vaginalis. *Korean J. Parasitol.* (47) 205–12.
- [13] Chang, J.-H., Ryang, Y.-S., Morio, T., Lee, S.-K. & Chang, E.-J. (2004). Trichomonas vaginalis inhibits proinflammatory cytokine production in macrophages by suppressing NF-kappaB activation. *Mol. Cells* (18) 177–185.
- [14] Fichorova, R., Fraga, J., Rappelli, P. & Fiori, P. L. (2017). Trichomonas vaginalis infection in symbiosis with Trichomonasvirus and Mycoplasma. *Res. Microbiol.* (168) 882–891.
- [15] Mercer, F. *et al.* (2016). Leukocyte Lysis and Cytokine Induction by the Human Sexually Transmitted Parasite Trichomonas vaginalis. *PLoS Negl. Trop. Dis.* (10) e0004913.
- [16] Das, R. *et al.* (2013). Macrophage migration inhibitory factor (MIF) is a critical mediator of the innate immune response to Mycobacterium tuberculosis. *Proc. Natl. Acad. Sci. U. S. A.* (110) E2997-3006.
- [17] Roger, T., David, J., Glauser, M. P. & Calandra, T. (2001). MIF regulates innate immune responses through modulation of Toll-like receptor 4. *Nature* (414) 920–924.
- [18] Bozza, M. *et al.* (1999). Targeted disruption of migration inhibitory factor gene reveals its

- critical role in sepsis. *J. Exp. Med.* (189) 341–346.
- [19] Moonah, S. N., Abhyankar, M. M., Haque, R. & Petri, W. A. (2014). The macrophage migration inhibitory factor homolog of *Entamoeba histolytica* binds to and immunomodulates host macrophages. *Infect. Immun.* (82) 3523–3530.
- [20] Sommerville, C. *et al.* (2013). Biochemical and immunological characterization of *Toxoplasma gondii* macrophage migration inhibitory factor. *J. Biol. Chem.* (288) 12733–41.
- [21] Shao, D. *et al.* (2010). Structural and functional comparison of MIF ortholog from *Plasmodium yoelii* with MIF from its rodent host. *Mol. Immunol.* (47) 726–737.
- [22] Falcone, F. H. *et al.* (2001). A *Brugia malayi* Homolog of Macrophage Migration Inhibitory Factor Reveals an Important Link Between Macrophages and Eosinophil Recruitment During Nematode Infection. *J. Immunol.* (167) 5348–5354.
- [23] Cobo, E. R., Eckmann, L. & Corbeil, L. B. (2011). Murine models of vaginal trichomonad infections. *Am. J. Trop. Med. Hyg.* (85) 667–673.
- [24] Rey-Giraud, F., Hafner, M. & Ries, C. H. (2012). In vitro generation of monocyte-derived macrophages under serum-free conditions improves their tumor promoting functions. *PLoS One* (7) e42656.
- [25] Sandor, N. *et al.* (2016). CD11c/CD18 Dominates Adhesion of Human Monocytes, Macrophages and Dendritic Cells over CD11b/CD18. *PLoS One* (11) e0163120.
- [26] Cassol, E., Cassetta, L., Rizzi, C., Alfano, M. & Poli, G. (2009). M1 and M2a Polarization of Human Monocyte-Derived Macrophages Inhibits HIV-1 Replication by Distinct

- Mechanisms. *J. Immunol.* (182) 6237–6246.
- [27] Nair, S., Archer, G. E. & Tedder, T. F. (2012). *Isolation and generation of human dendritic cells. Current Protocols in Immunology* doi:10.1002/0471142735.im0732s99.
- [28] Chaudhry, H. *et al.* (2013). Role of cytokines as a double-edged sword in sepsis. *In Vivo* (27) 669–684.
- [29] Yang, C., Chalasani, G., Ng, Y. H. & Robbins, P. D. (2012). Exosomes released from mycoplasma infected tumor cells activate inhibitory B cells. *PLoS One* (7) e36138.
- [30] Bendrat, K. *et al.* (1997). Biochemical and mutational investigations of the enzymatic activity of macrophage migration inhibitory factor. *Biochemistry* (36) 15356–15362.
- [31] Fan, C. *et al.* (2013). MIF intersubunit disulfide mutant antagonist supports activation of CD74 by endogenous MIF trimer at physiologic concentrations. *Proc. Natl. Acad. Sci.* (110) 10994–10999.
- [32] Terrazas, C. A. *et al.* (2011). MIF synergizes with trypanosoma cruzi antigens to promote efficient dendritic cell maturation and IL-12 production via p38 MAPK. *Int. J. Biol. Sci.* (7) 1298–1310.
- [33] Seow, V. *et al.* (2013). Inflammatory Responses Induced by Lipopolysaccharide Are Amplified in Primary Human Monocytes but Suppressed in Macrophages by Complement Protein C5a. *J. Immunol.* (191) 4308–4316.
- [34] Daigneault, M., Preston, J. A., Marriott, H. M., Whyte, M. K. B. & Dockrell, D. H. (2010). The identification of markers of macrophage differentiation in PMA-stimulated THP-1 cells and monocyte-derived macrophages. *PLoS One* (5) e8668.

- [35] Netea, M. G. *et al.* (2009). Differential requirement for the activation of the inflammasome for processing and release of IL-1 β in monocytes and macrophages. *Blood* (113) 2324–2335.
- [36] Chen, Y., Olivia, T. & Johnson, P. J. (2018). *Trichomonas vaginalis* Macrophage Migration Inhibitory Factor Mediates Parasite Survival during Nutrient Stress. *MBio* (9) e00910-18.
- [37] Clark, C. G. & Diamond, L. S. (2002). Methods for cultivation of luminal parasitic protists of clinical importance. *Clinical Microbiology Reviews* (15) 329–341.
- [38] Pascual, A., Jatou, K., Ninet, B., Bille, J. & Greub, G. (2010). New diagnostic real-time PCR for specific detection of *Mycoplasma hominis* DNA. *Int. J. Microbiol.* doi:10.1155/2010/317512.
- [39] de Miguel, N. *et al.* (2010). Proteome analysis of the surface of *Trichomonas vaginalis* reveals novel proteins and strain-dependent differential expression. *Mol. Cell. Proteomics* (9) 1554–1566.

Chapter 6:

Summary and discussion

Summary

Trichomonas vaginalis is a human-infective protozoan that is highly prevalent yet commonly neglected [1]. With the development of molecular tools [2] and efforts from researchers in the field, understanding how the parasite establishes and maintains the infection has become possible. The goals of this dissertation are identification of survival factor of the parasite (Chapter 2), characterization of a *Tv* cadherin-like protein involved in host cell binding and killing (Chapter 3), efforts in adapting CRISPR-Cas9 to edit *T. vaginalis* genome (Chapter 4), and examination of immune responses to *Tv* and TvMIF from human macrophages and dendritic cells (Chapter 5). These studies reveal that the parasite depends on multiple factors to establish infection and the development of novel techniques is necessary to better understand the mechanisms underlying infection.

Insight into *Tv* survival factor and pathways

TvMIF is the first identified survival factor in *T. vaginalis* to our knowledge. The overexpression of TvMIF enhances the parasite survival more than 10-fold and knockout of the protein decreases their survival up to 16-fold under nutrient-poor conditions (Chapter 2). We show that TvMIF inhibits the apoptosis of the parasite by lowering reactive oxygen species in the parasite to enhance their survival (Chapter 2). Both TvMIF and huMIF are able to increase the parasite survival, suggesting the cross-talk between the parasite and its host (Chapter 2).

Identification of specific players involved in the survival pathway in *T. vaginalis* is laborious. Very few proteins that play a role in apoptosis in other eukaryotic systems are known in protozoan parasites. Metacaspases in yeast are believed to have the same function as mammalian caspases which are involved in apoptosis [3]. However, the specific roles of metacaspases in parasites are not entirely clear [4]. Other players in mammalian apoptotic

pathways such as pro-apoptotic factors/anti-apoptotic factors cannot be easily identified in the *T. vaginalis* genome based on primary sequence. As a result, to identify *T. vaginalis* survival pathways, transcriptomic and proteomic approaches that examine global differential expression are required. The lack of survival in TvMIF knockout (KO) cells suggests that comparison of wild-type (WT) cells and KO cells gene expression during serum starvation will provide information on unidentified factors involved in the survival pathway. In addition, *T. vaginalis* has conserved mitogen-activated protein kinases (MAPKs) and Akt that are known to be activated by phosphorylation downstream of huMIF activation. Phosphoproteome on WT versus TvMIF KO parasites under serum starvation may aid the process of identifying survival players.

HuMIF receptor CD74 is the key to huMIF downstream signaling including activating MAPK/Erk and Akt/PI3k pathways, and inhibiting apoptotic p53 [5][6][7]. We have made attempts to identify TvMIF receptor in *Tv* although unsuccessfully. Affinity chromatography using recombinant TvMIF and pulldown with tagged TvMIF expressed in *T. vaginalis* have not been able to reveal any promising candidates. For example, the adjusted p-values were not significant from 3 biological replicates or a candidate was not pulled down in independent experiments. Pulldown has always been challenging in *T. vaginalis* because commercially available tags used for pulldown lack specificity in the organism and the majority of the proteins in the genome are not annotated well. As a result, to identify a novel receptor in *T. vaginalis*, adaptation of new techniques is required. For example, proximity labeling which can label nearby proteins without strong interactions such as BioID used in *Toxoplasma gondii* [8][9] may assist in receptor identification. TurboID, an improved BioID that can label as quickly as 10 minutes and has stronger activity on cell surface may significantly speed up identification of surface receptors in *T. vaginalis* [10]. Alternatively, use of tandem affinity purification such as

PTP (ProtC-TEV-ProtA) tags employed in *Trypanosoma brucei* is likely to enhance the specificity of the identified products [11][12].

Characterization of a *Tv* cadherin-like protein in host adherence and killing

Previous surface proteome has allowed us to identify several adherent factors in *Tv* that mediate host binding [13]. As more and more *Tv* adherence factors such as the parasite exosomes and lipoglycan have been discovered, it became clear that host binding by *Tv* is mediated by a multifactorial process [13][14][15]. Cadherin-like protein (CLP) described in Chapter 3 was identified in the surface proteome comparing less adherent versus adherent parasite strains [13]. In addition, CLP was also found in the *Tv* exosomal proteome [16], indicating that the adherent factor on the parasite surface may mediate host binding by being delivered to another parasite or host via exosomal fusion. Using our CRISPR-Cas9 system in *Tv* to knock out the CLP gene to further characterize its role in host adherence and its role in exosome-mediated host adherence is currently underway and will provide insight to these questions.

A clumping phenotype was observed when CLP is overexpressed in the parasite. The behavior is reminiscent of *T. vaginalis* tetraspanin 8 (TvTSP8)-overexpressing parasites and highly adherent parasite strains [17]. The role of parasite aggregation in *T. vaginalis* infection is not entirely understood. Clumping increases the number of parasites in contact with the host and this behavior may enhance the chance of successful infection. In addition, when parasites aggregate, the outside parasites may be able to protect the parasites in the center from attack from host immune cells as a potential mechanism to increase parasite survival inside the host. These hypotheses are yet to be tested.

The interaction between human E-cadherin protein and tetraspanin Co-029 determines cell motility of colon cancer cell [18]. Several *T. vaginalis* TSP proteins have been found to be

localized to the parasite surface and re-localize during host contact [17][19]. The clumping phenotype of both TvTSP8-overexpressing and CLP-overexpressing parasites indicate that these two surface proteins may complement each other in host binding. Whether TvTSP8 or other parasite proteins act as CLP partners requires further investigation.

Optimization of CRISPR-Cas9 techniques in *T. vaginalis*

Adaptation of CRISPR-Cas9 system in *T. vaginalis* has significantly improved the ability to knock out (KO) genes in the parasite [20]. However, the need to use homology-directed repair CRISPR-Cas9 pathway in the parasite requires the researchers to build knockout (KO) cassette [20] and amplify the KO cassette by PCR which is extremely time-consuming and expensive. KO genes in a population also requires extensive PCR screening to obtain a parasite clone that has the gene replacement at the right locus. In addition, it is unfeasible to KO genes with multiple copies since that would require various selectable markers for multiple gene replacement and multiple rounds of screening. As a result, CRISPRi knockdown system using catalytically inactive Cas9 guided by guide RNAs to block transcription initiation or transcription elongation [21][22] is considered to be useful in *T. vaginalis*. For example, CRISPRi does not require cloning of KO cassettes and PCR screening for the right clone. Furthermore, targeting genes with multiple copies with CRISPRi is more feasible than CRISPR-Cas9 knockout as CRISPRi blocks the transcription of the same genes without the need to replace each of them with different drug selectable markers. For these reasons, repurposing CRISPR-Cas9 in *T. vaginalis* may provide a more efficient platform to control gene expression.

More information is yet to be explored on immune responses to *Tv*

From our data testing cytokine responses induced by live *T. vaginalis* in the presence or absence of *Mycoplasma hominis*, we found that *M. hominis* plays a significant role in inducing

cytokine releases from human macrophages and dendritic cells. In addition, the *M. hominis*-induced cytokine responses are remarkably higher in a laboratory adapted strain G3 than a clinical strain MSA1103 we tested. To draw a meaningful conclusion on whether clinical strains are less immunogenic than lab-adaptive strains, a significantly larger number of *Tv* strains will need to be tested.

An interesting follow-up question to our observation in Chapter 5 that a laboratory adapted strain G3 is significantly more immunogenic than a clinical strain MSA1103 is whether G3 is more susceptible to killing by host immune cells than MSA1103. For example, the induction of cytokines by G3 parasites may alert more immune cells to attack them than MSA1103 parasites. However, lacking a good animal model is likely to be an impediment to truly understanding host immune responses to *Tv*. As a result, our laboratory is now developing a male mouse model because female mice as *Tv* hosts have not been a successful model given that the infection often requires treatments of estrogens and/or immunosuppressants [23][24][25]. The existing data lack good quantification of the infection rates and evidence of long-term infection [23][24][25]. Treatment with immunosuppression resulted in disruption of host immune system that failed to reflect the immune responses during a natural infection. Once a mouse model is established, it will open doors to many hypotheses related to *T. vaginalis* infection such as how different each *Tv* strain is in terms of infectivity, how *Tv* regulates its gene expression during host contact, and how host immune cells respond to *Tv* infection *in vivo*. Efforts towards developing an animal model and other technologies for studying *T. vaginalis* are the keys to truly understanding how to prevent the infection.

References

- [1] Secor, W. E., Meites, E., Starr, M. C. & Workowski, K. a. (2014). Neglected parasitic infections in the United States: trichomoniasis. *Am. J. Trop. Med. Hyg.* (90) 800–804.
- [2] Conrad, M. D., Bradic, M., Warring, S. D., Gorman, A. W. & Carlton, J. M. (2013). Getting trichy: Tools and approaches to interrogating *Trichomonas vaginalis* in a post-genome world. *Trends in Parasitology* (29) 17–25.
- [3] Carmona-Gutierrez, D., Fröhlich, K. U., Kroemer, G. & Madeo, F. (2010). Editorial: Metacaspases are caspases. Doubt no more. *Cell Death and Differentiation* (17) 377–378.
- [4] Meslin, B., Zalila, H., Fasel, N., Picot, S. & Bienvenu, A. L. (2011). Are protozoan metacaspases potential parasite killers? *Parasites and Vectors* (4) doi: 10.1186/1756-3305-4-26.
- [5] Mitchell, R. a, Metz, C. N., Peng, T. & Bucala, R. (1999). Sustained mitogen-activated protein kinase (MAPK) and cytoplasmic phospholipase A2 activation by macrophage migration inhibitory factor (MIF). Regulatory role in cell proliferation and glucocorticoid action. *J. Biol. Chem.* (274) 18100–18106.
- [6] Lue, H. *et al.* (2007). Macrophage migration inhibitory factor (MIF) promotes cell survival by activation of the Akt pathway and role for CSN5/JAB1 in the control of autocrine MIF activity. *Oncogene* (26) 5046–5059.
- [7] Mitchell, R. A. *et al.* (2002). Macrophage migration inhibitory factor (MIF) sustains macrophage proinflammatory function by inhibiting p53: Regulatory role in the innate immune response. *Proc. Natl. Acad. Sci.* (99) 345–350.

- [8] Chen, A. L. *et al.* (2015). Novel components of the toxoplasma inner membrane complex revealed by BioID. *MBio* (6) e02357-14.
- [9] Nadipuram, S. M. *et al.* (2016). In Vivo biotinylation of the toxoplasma parasitophorous vacuole reveals novel dense granule proteins important for parasite growth and pathogenesis. *MBio* (7) e00808.
- [10] Branon, T. C. *et al.* (2017). Directed evolution of TurboID for efficient proximity labeling in living cells and organisms. *bioRxiv* doi:10.1101/196980.
- [11] Puig, O. *et al.* (2001). The tandem affinity purification (TAP) method: a general procedure of protein complex purification. *Methods* (24) 218–229.
- [12] Schimanski, B., Nguyen, T. N. & Günzl, A. (2005). Highly efficient tandem affinity purification of trypanosome protein complexes based on a novel epitope combination. *Eukaryot. Cell* doi:10.1128/EC.4.11.1942-1950.2005.
- [13] de Miguel, N. *et al.* (2010). Proteome analysis of the surface of *Trichomonas vaginalis* reveals novel proteins and strain-dependent differential expression. *Mol. Cell. Proteomics* (9) 1554–1566.
- [14] Singh, B. N. (1993). Lipophosphoglycan-like glycoconjugate of *Tritrichomonas foetus* and *Trichomonas vaginalis*. *Mol. Biochem. Parasitol.* (57) 281–294.
- [15] Bastida-Corcuera, F. D., Okumura, C. Y., Colocoussi, A. & Johnson, P. J. (2005). *Trichomonas vaginalis* lipophosphoglycan mutants have reduced adherence and cytotoxicity to human ectocervical cells. *Eukaryot. Cell* (4) 1951–1958.

- [16] Olmos-Ortiz, L. M. *et al.* (2017). Trichomonas vaginalis exosome-like vesicles modify the cytokine profile and reduce inflammation in parasite-infected mice. *Parasite Immunol.* (39) doi: 10.1111/pim.12426.
- [17] Coceres, V. M. *et al.* (2015). The C-terminal tail of tetraspanin proteins regulates their intracellular distribution in the parasite Trichomonas vaginalis. *Cell. Microbiol.* (17) 1217–1229.
- [18] Greco, C. *et al.* (2010). E-cadherin/p120-catenin and tetraspanin Co-029 cooperate for cell motility control in human colon carcinoma. *Cancer Res.* (70) 7674–7683.
- [19] de Miguel, N., Riestra, A. & Johnson, P. J. (2012). Reversible association of tetraspanin with Trichomonas vaginalis flagella upon adherence to host cells. *Cell. Microbiol.* (14) 1797–1807.
- [20] Janssen, B. D. *et al.* (2018). CRISPR/Cas9-mediated gene modification and gene knock out in the human-infective parasite Trichomonas vaginalis. *Sci. Rep.* (8) doi: 10.1038/s41598-017-18442-3.
- [21] Qi, L. S. *et al.* (2013). Repurposing CRISPR as an RNA-guided platform for sequence-specific control of gene expression. *Cell* doi:10.1016/j.cell.2013.02.022.
- [22] Larson, M. H. *et al.* (2013). CRISPR interference (CRISPRi) for sequence-specific control of gene expression. *Nat. Protoc.* doi:10.1038/nprot.2013.132.
- [23] McGrory, T. & Garber, G. E. (1992). Mouse intravaginal infection with Trichomonas vaginalis and role of Lactobacillus acidophilus in sustaining infection. *Infect. Immun.* (60) 2375–2379.

- [24] Cobo, E. R., Eckmann, L. & Corbeil, L. B. (2011). Murine models of vaginal trichomonad infections. *Am. J. Trop. Med. Hyg.* (85) 667–673.
- [25] Escario, A., Gómez Barrio, A., Simons Diez, B. & Escario, J. A. (2010). Immunohistochemical study of the vaginal inflammatory response in experimental trichomoniasis. *Acta Trop.* (114) 22–30.